



Stability Issues in Thermal Barrier Coatings

Carlos G. Levi

Materials Department, University of California, Santa Barbara

with many thanks to:

R.M. Leckie, F.M. Pitek, T.A. Schaedler, M. Novak, K.M. Grant, S.G. Terry, N.R. Rebollo,
S. Krämer, A.S. Gandhi, J. Cho, J.Y. Yang, J.P.A. Löfvander, D. Stave (UCSB)
A.G. Evans, S. Faulhaber, C. Mercer, T.D. Bennett, D.R. Clarke, V. Lughì (UCSB),
U. Schulz (DLR), J. Cairney (UNSW/MPI), O. Fabrichnaya and M. Rühle (MPI-MF)
R. Darolia, D. Wortman (GE-A), C. Johnson (GE-GRC), M. Maloney (P&W)

Research Sponsored by

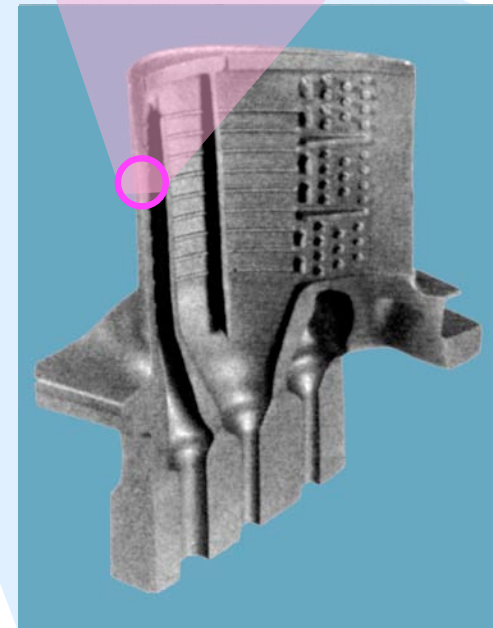
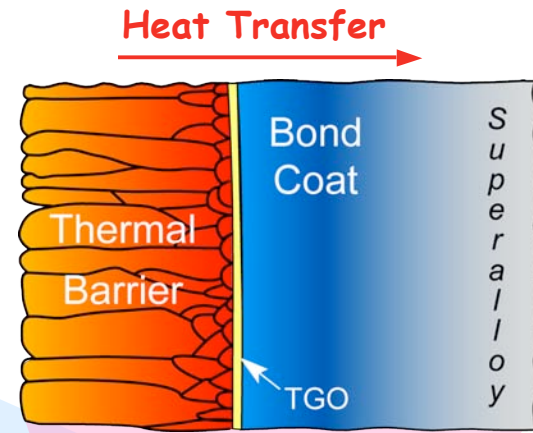
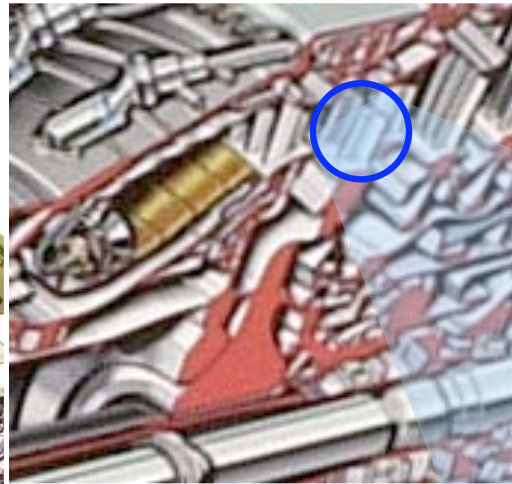
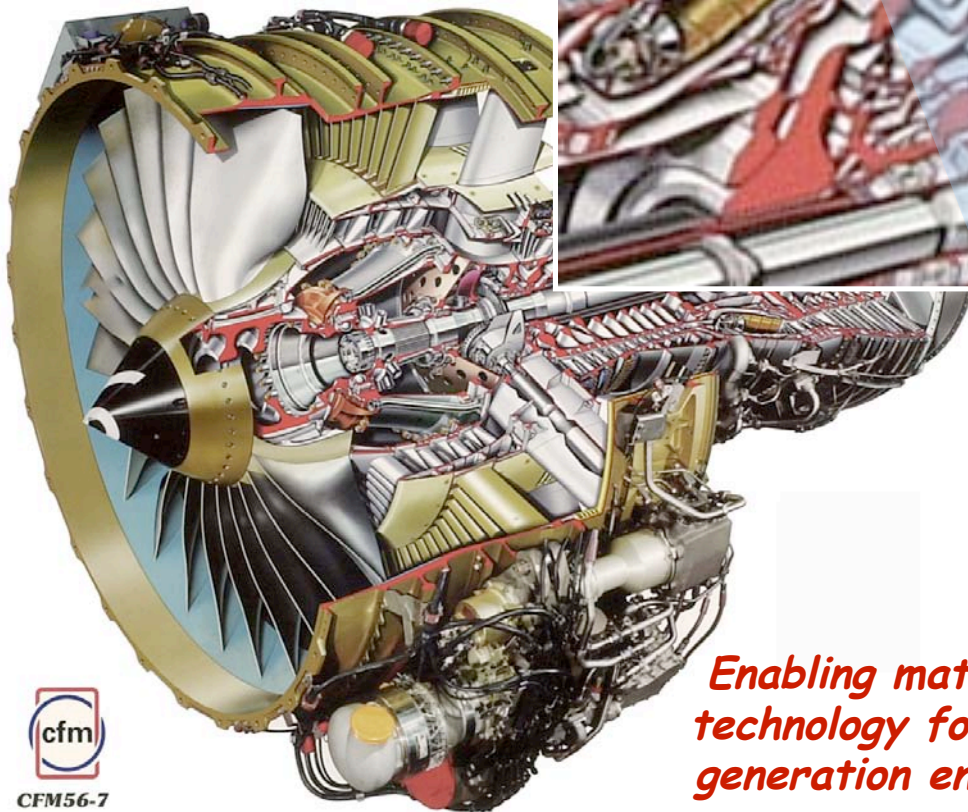
National Science Foundation and Office of Naval Research

Santa Barbara, CA, August 18, 2006



Thermal Barrier Coatings

Extend the limits and durability of high performance alloys in gas turbines



Enabling materials technology for next generation engines.

Mechanisms Limiting Durability in TBCs

Adapted from A.G. Evans

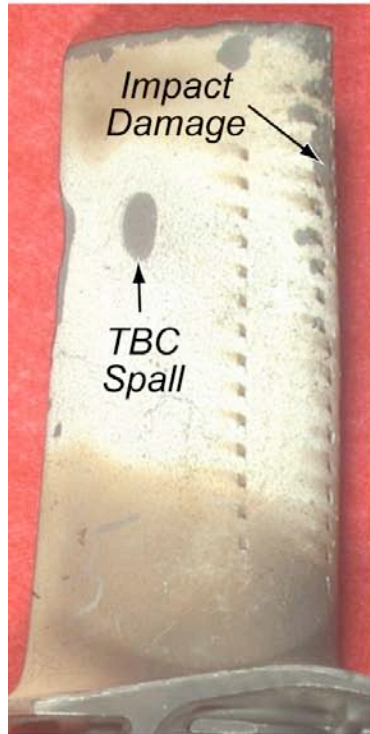
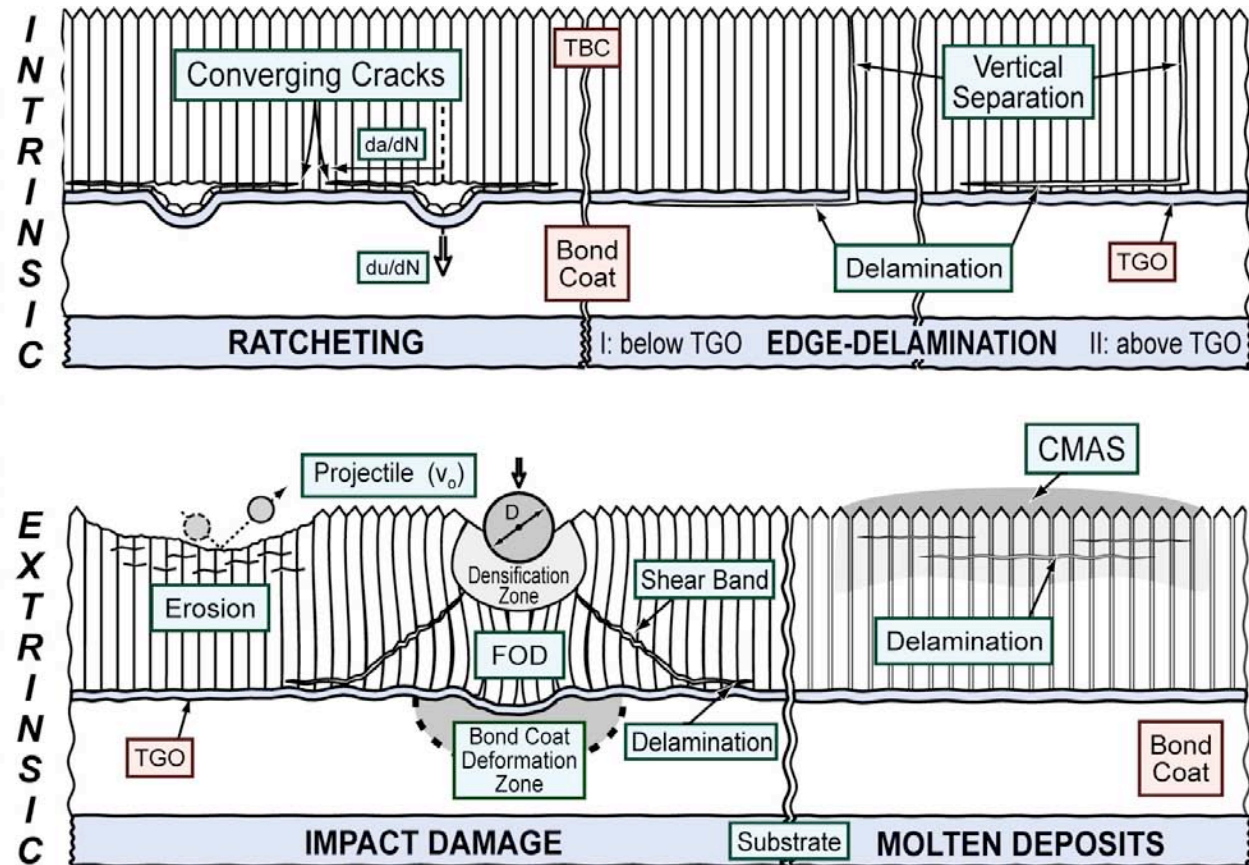


Image courtesy of R. Darolia (GE)



TBCs are "live" systems, whose structure evolves over time. Predictive models must incorporate effects of evolution dynamics on damage/failure mechanisms

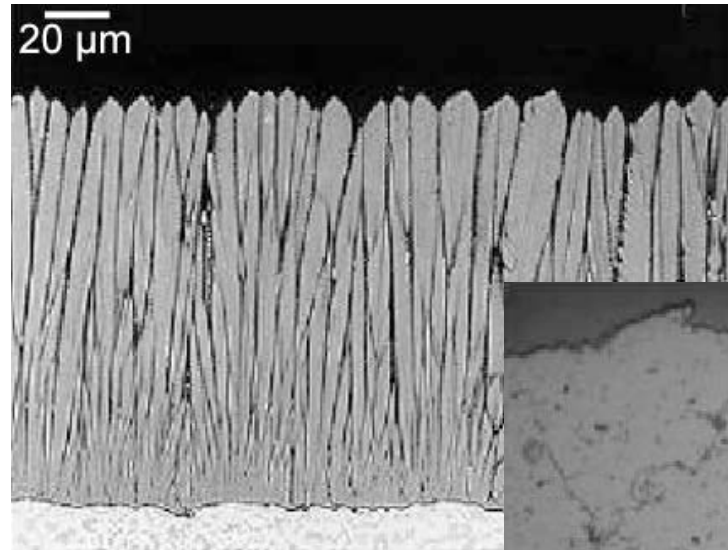
Historical Evolution of Thermal Barrier Coatings

Adapted from C. Johnson
GE Global Research Center

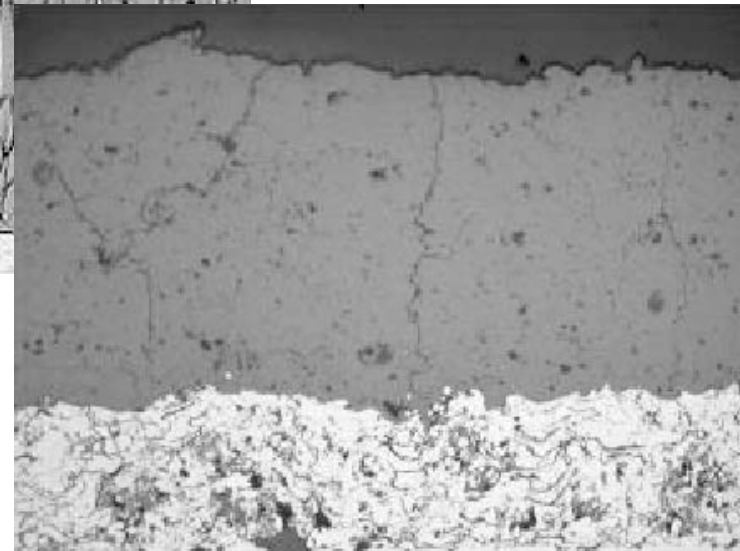
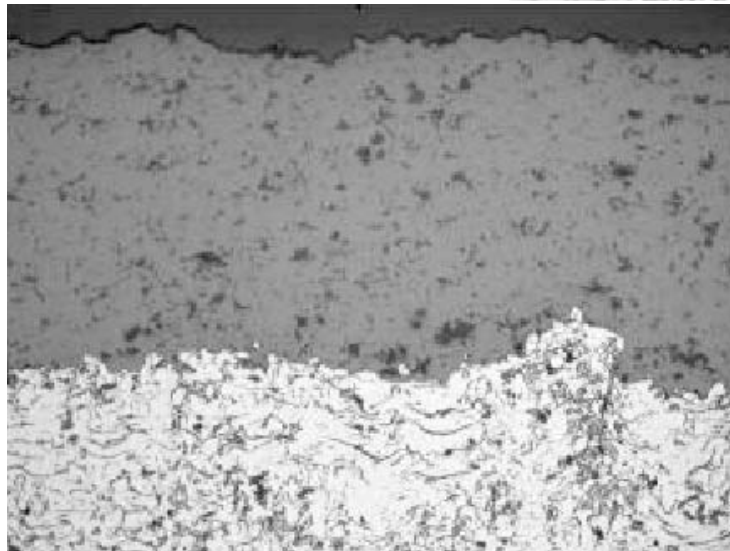
Performance



Air Plasma Spray
250-750 μm
Limited Performance
Combustors



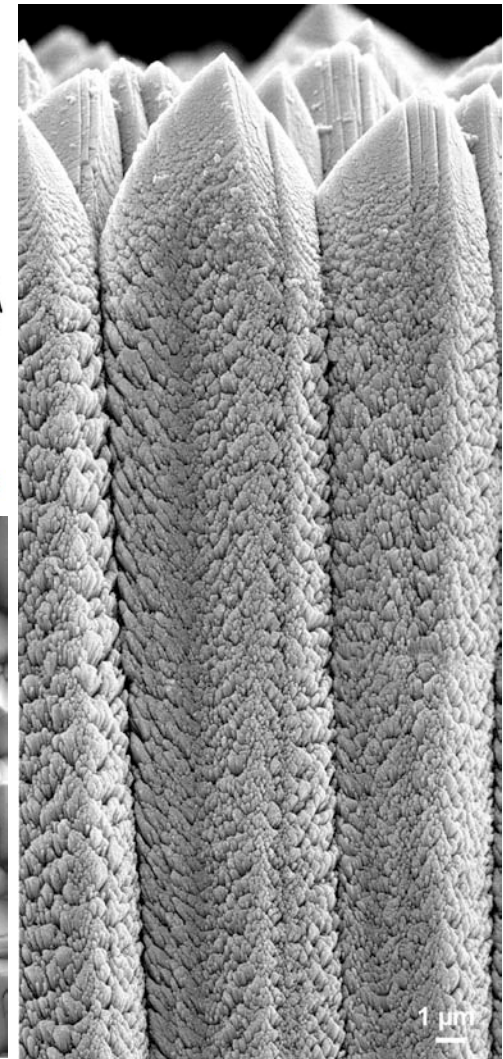
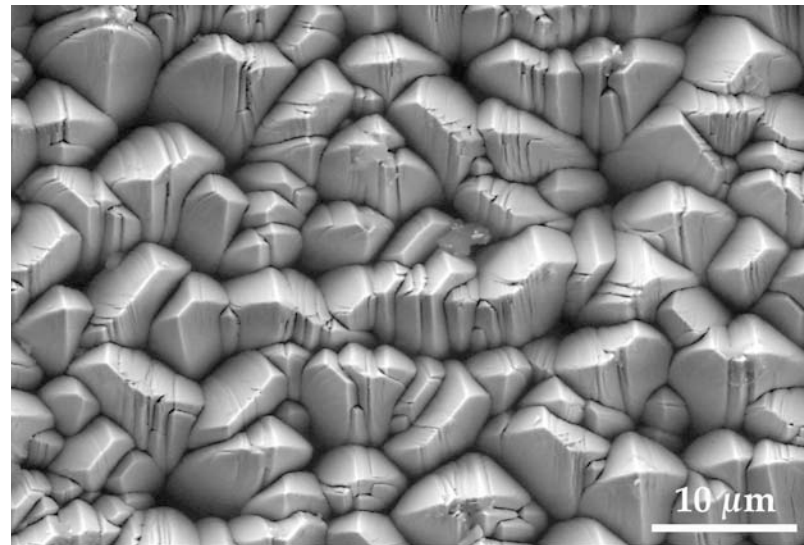
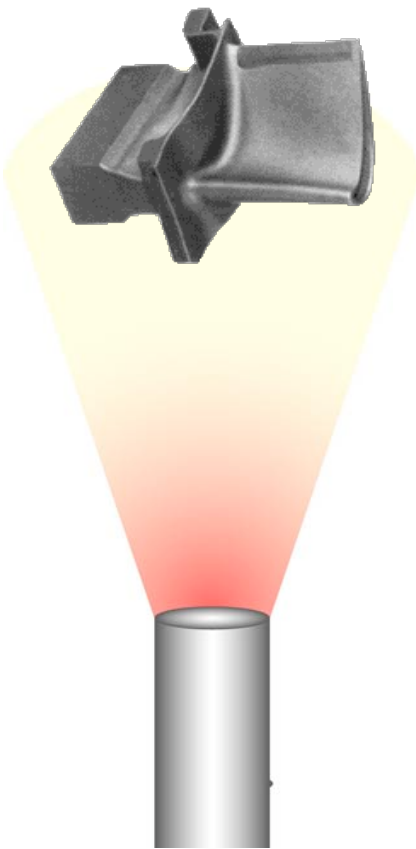
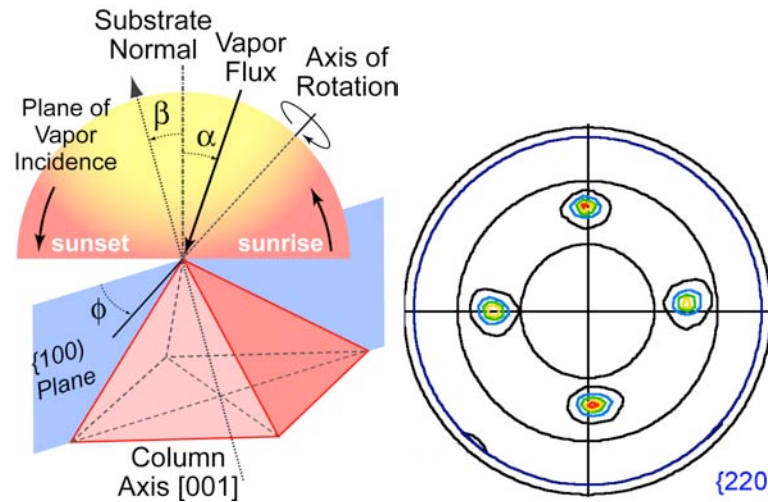
Electron Beam PVD
125-250 μm
High Performance
Aeroengine Airfoils



Dense Vertically Cracked APS
May be > 500 μm
Power Generation Turbine Airfoils

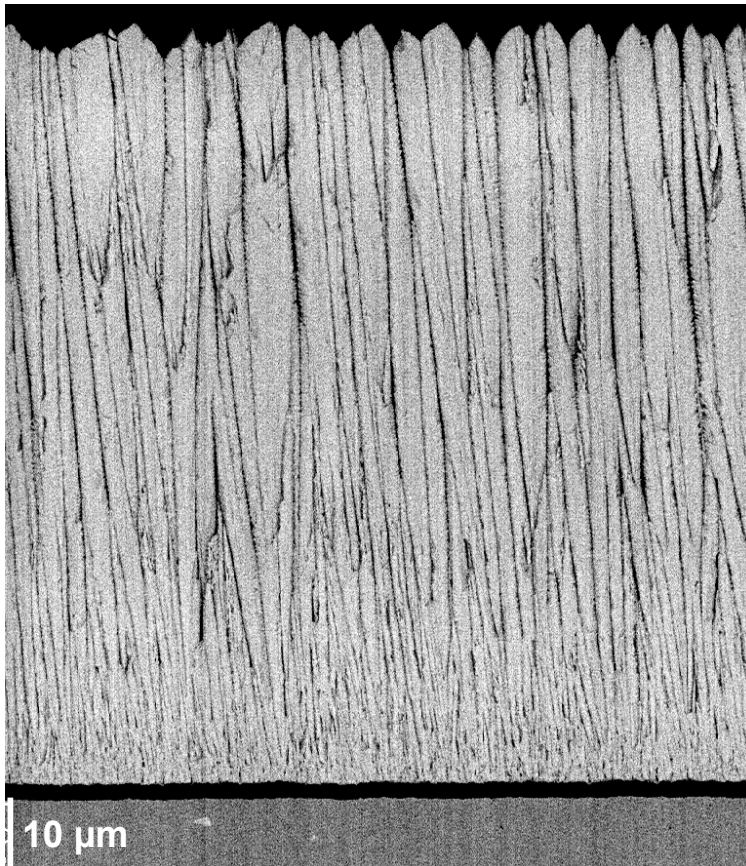
Time of introduction

EB-PVD Growth of TBCs

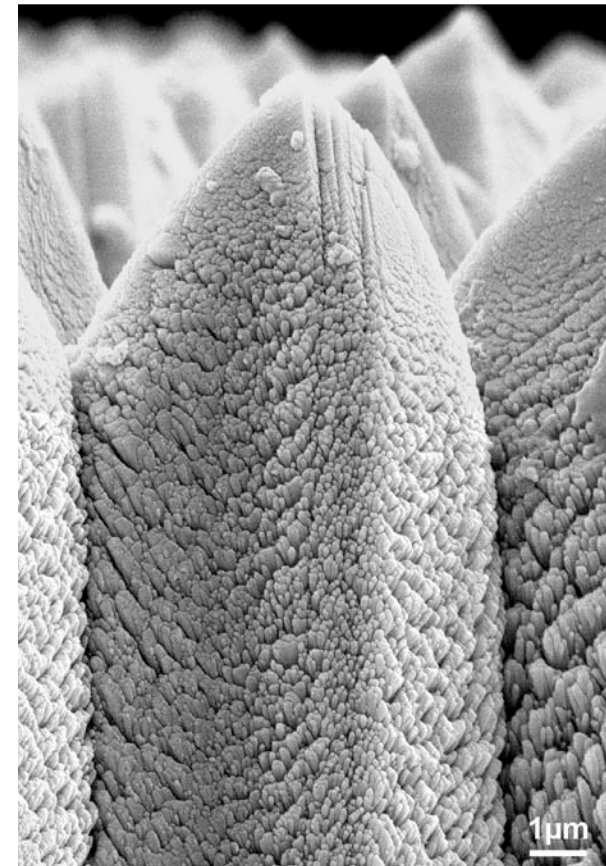


- Columnar structure with strong biaxial texture:
 - ⇒ [100] out of plane
 - ⇒ [001] in plane, \perp to rotation axis

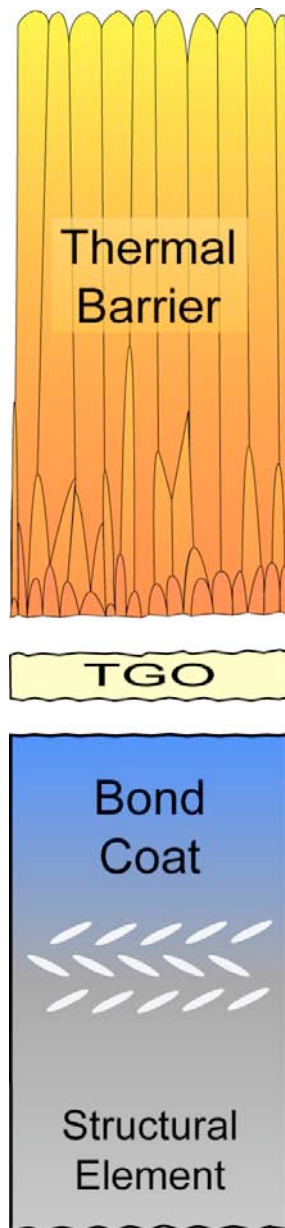
Porosity: A key to Performance and Durability



- *Through thickness segmentation enables accommodation of CTE mismatch during thermal cycling.*



- *Intra-columnar porosity further reduces intrinsically low thermal conductivity.*



Thermal Barrier Stability Issues

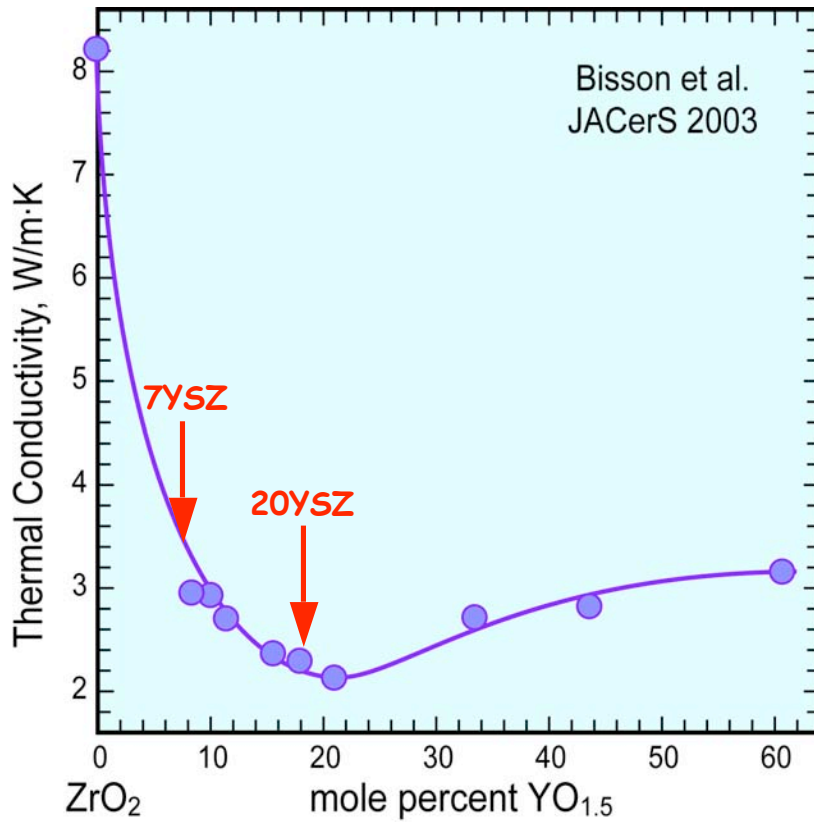
- *Evolution of pore architecture*
 - ↳ *Degradation of insulating efficiency*
 - ↳ *Degradation of strain tolerance/erosion resistance (may be accelerated by molten deposit penetration)*
- *Evolution of phase constitution*
 - ↳ *t' (non-transformable) \rightarrow t (transformable) + c*
 - ↳ *Accelerated by molten deposits (CMAS, S/V)*
- *Thermochemical interactions with TGO*

Two Broad Concerns:

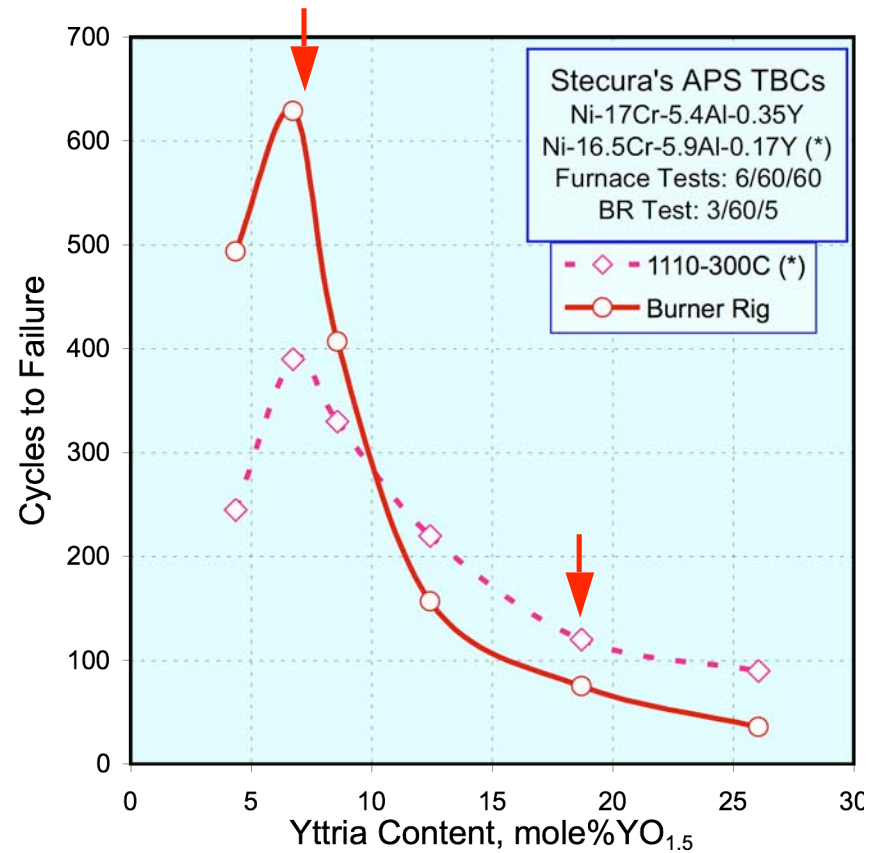
- *Problems are exacerbated by demands for operation at higher T or in more aggressive environments*
- *Uncertainty about the effects of novel TBC compositions on the stability of the system*

Chemistry and Phase Constitution

TBC Chemistry: Why "7"YSZ?

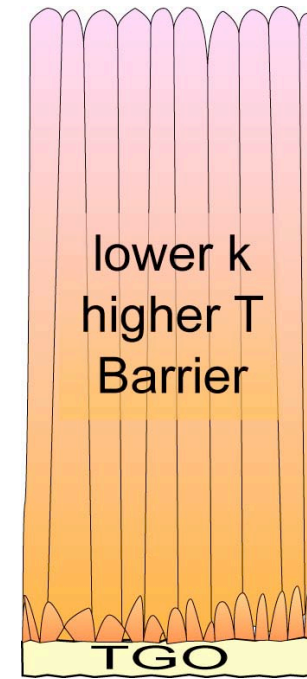
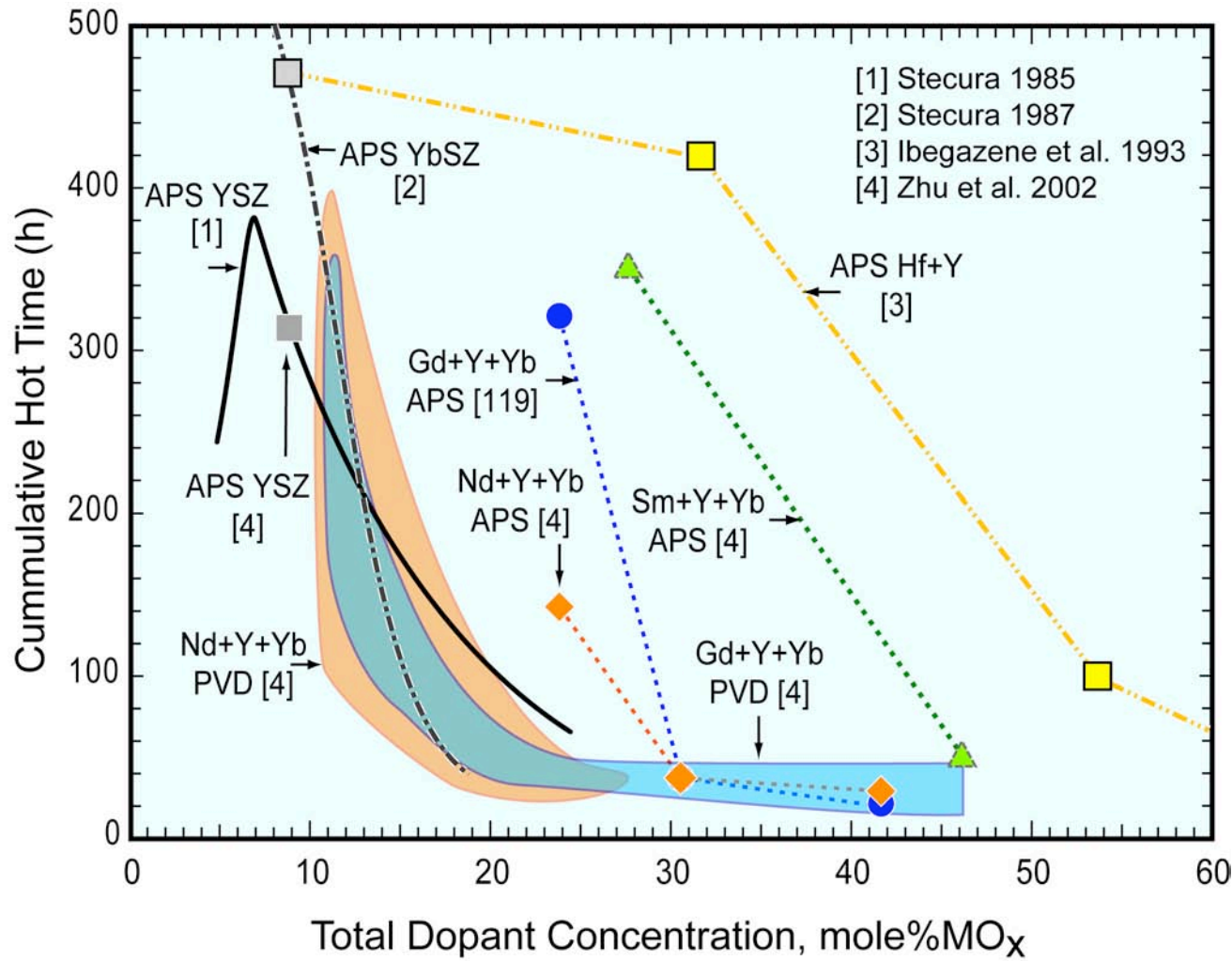


- *Not optimum in terms of thermal insulation efficiency*



- *Selection motivated by durability in cyclic tests*

Cyclic Life v. Stabilizer Content

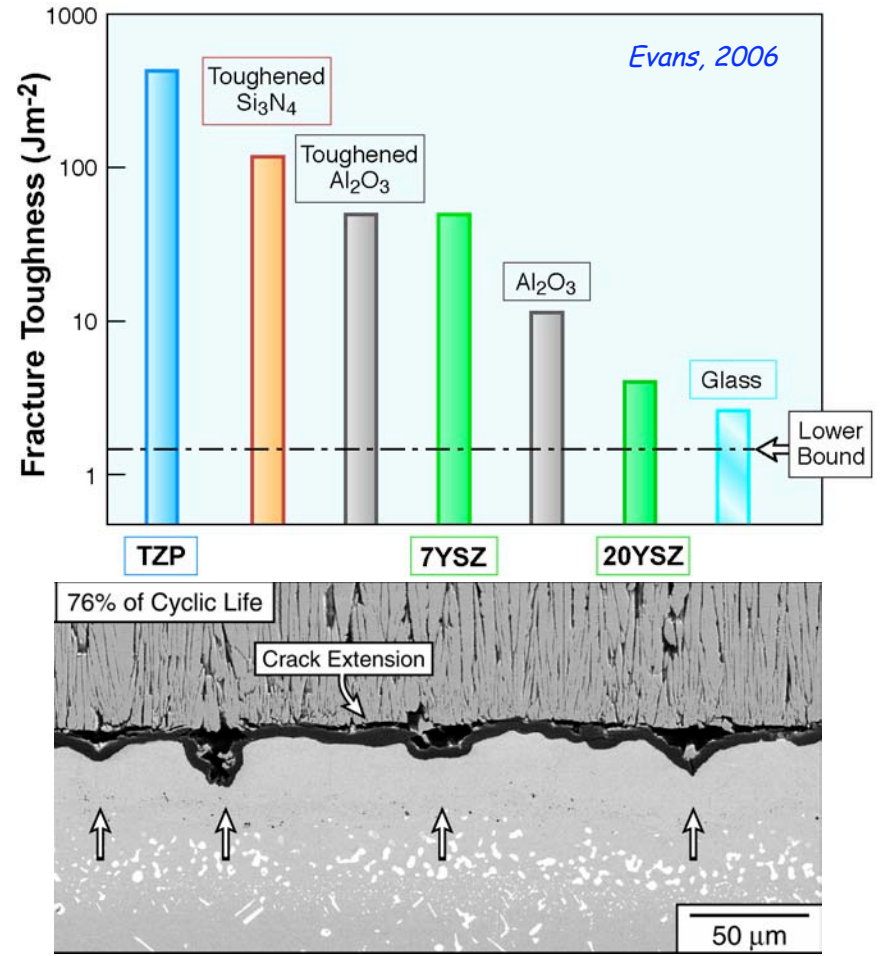
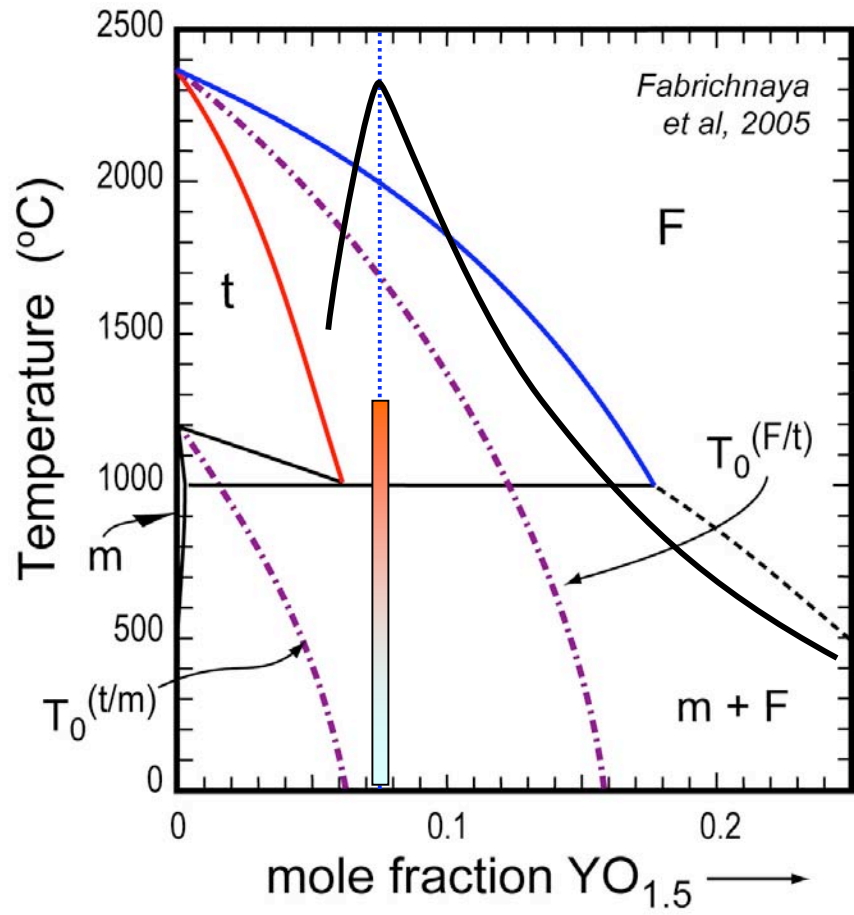


- *Cyclic life is compromised with increasing stabilizer content for singly- as well as co-doped ZrO₂.*

Levi, C.G.: *Current Opinion in Solid State and Materials Science*, 8 (2004) 77-91.

Phase Constitution and Implications

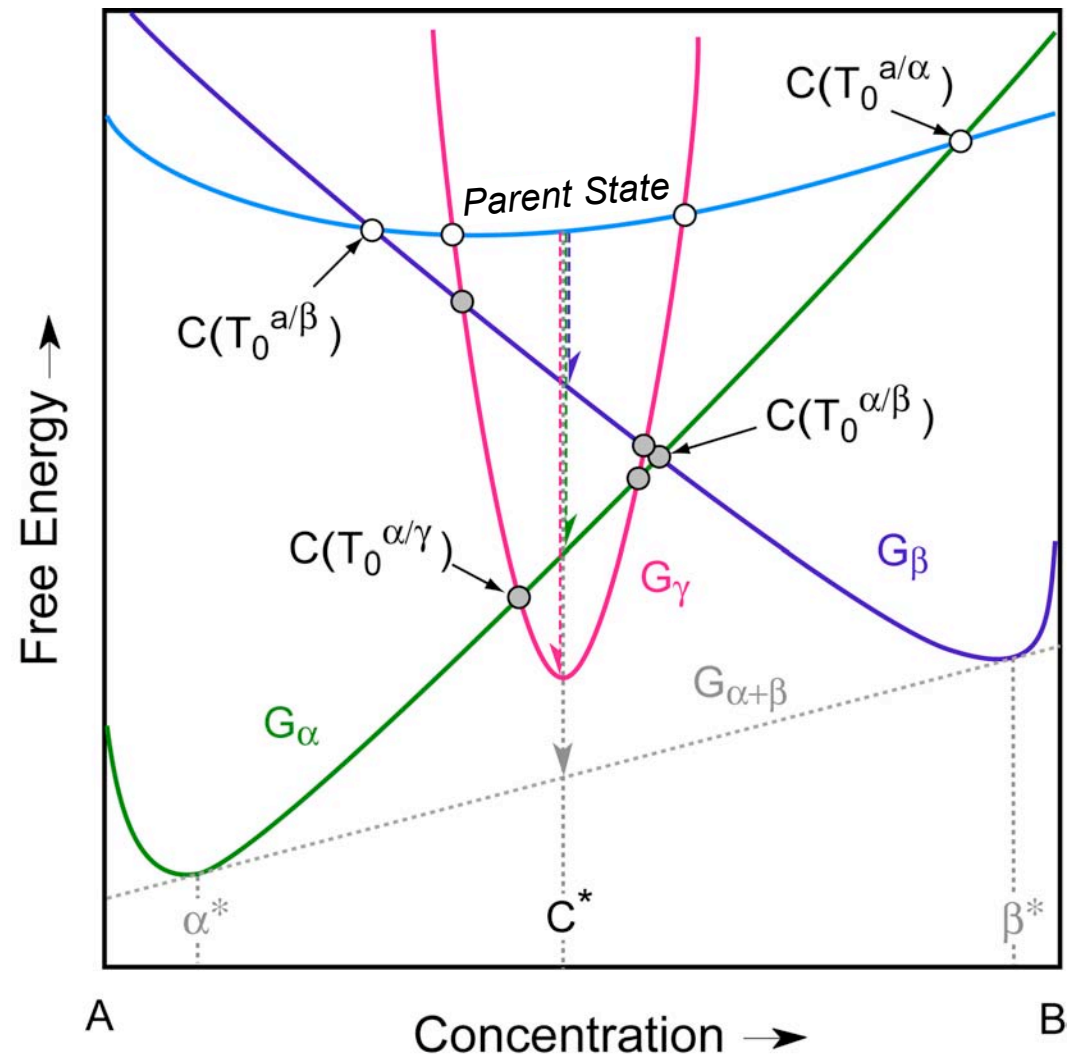
Image from Mumm & Evans



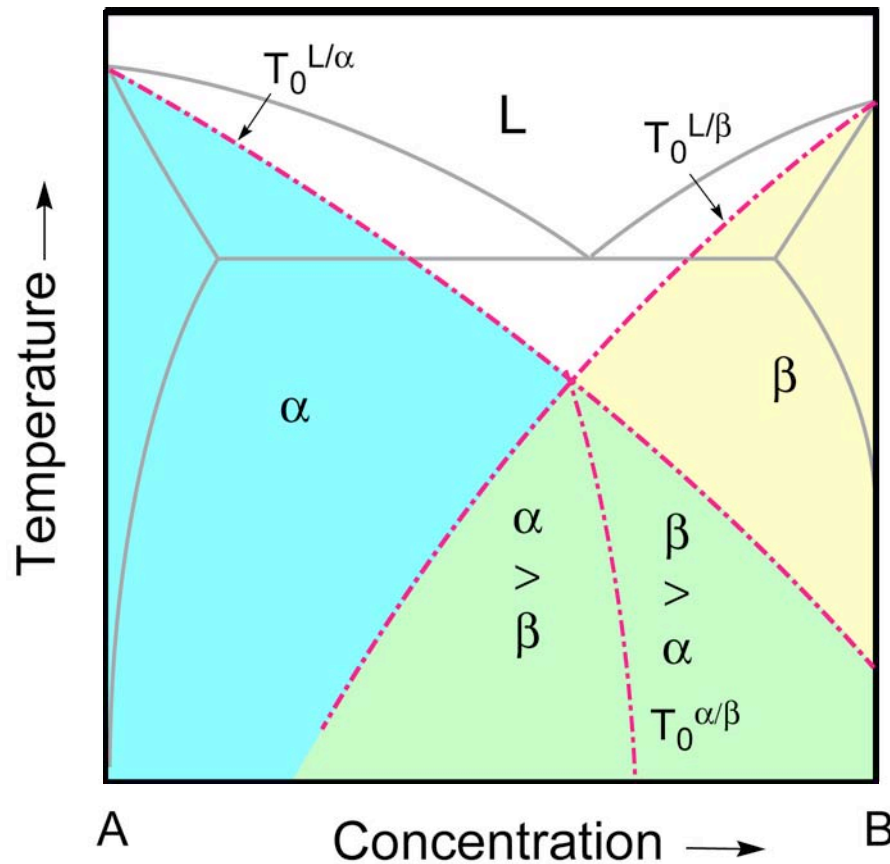
Durability limited by crack propagation through TBC: expected to depend on toughness, which depends on Y content, but why a peak?

Diffusionally Constrained Phase Selection

- How does one generate a tetragonal single phase beyond the solubility limit?
- Transformations requiring long range diffusion are constrained at low T/T_M . However, any single phase that yields a decrease in free energy relative to the parent phase can form.
- At any given T - X there is a menu of phases and a thermodynamic hierarchy.
- Menu and hierarchy change at intersection of the G - X curves (" T_0 " points).



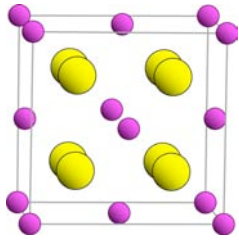
Mapping the Thermodynamic Possibilities



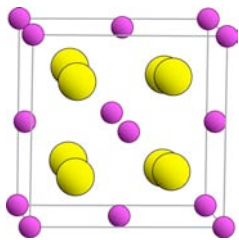
- When all other solid phases are kinetically suppressed, the stability limit for a crystalline phase of a given composition is set by onset of partitionless melting (low kinetic barrier) i.e. $T_0^{L/s}$
- Phase fields and hierarchies are determined by the position of the relevant T_0 curves.

Levi, C.G. : *Acta Materialia*
46 (3) 787-800, 1998.

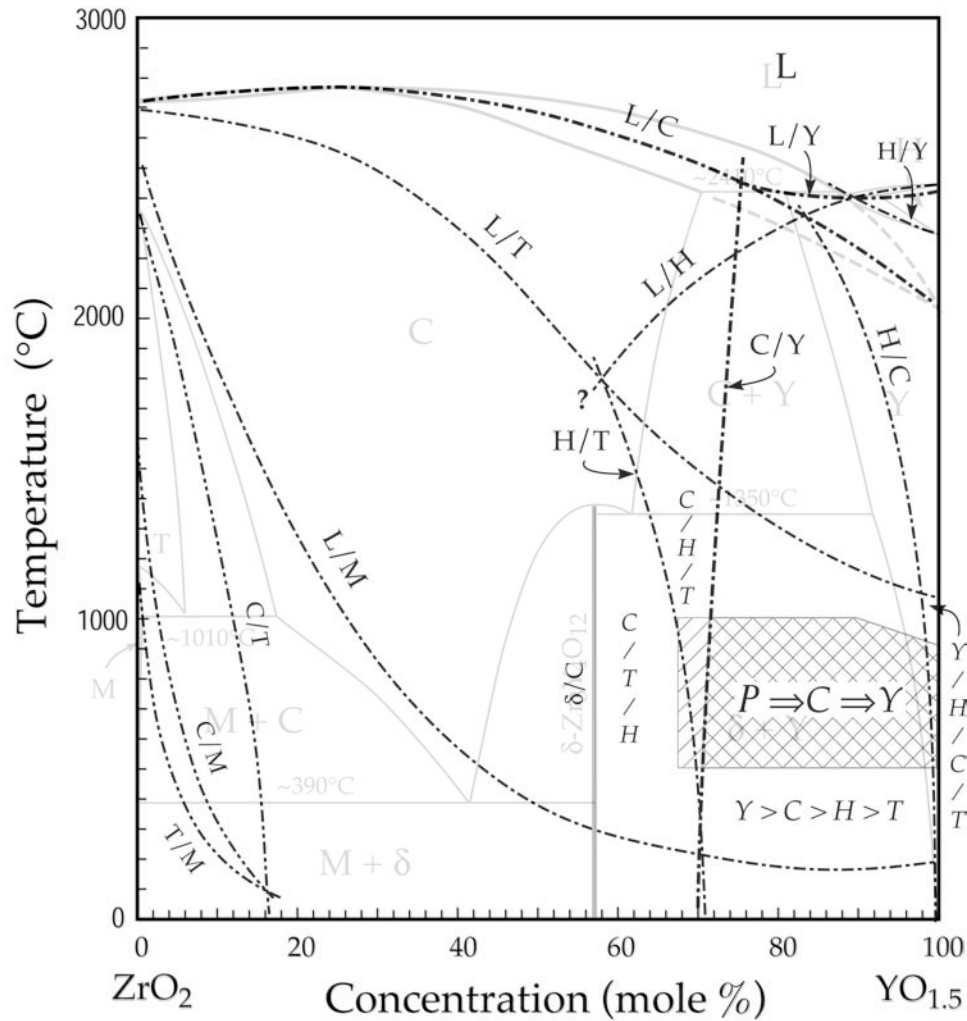
Phase Hierarchies in $ZrO_2-YO_{1.5}$



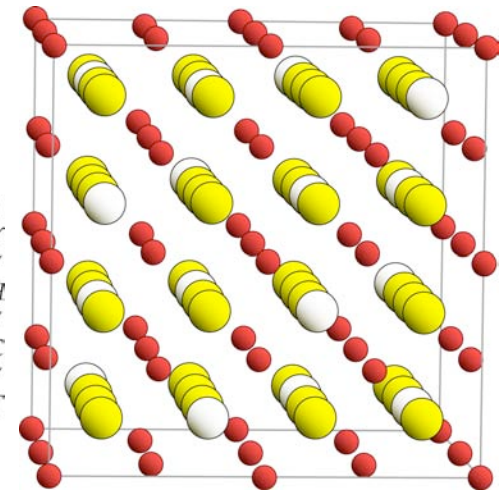
Fluorite (C)



Tetragonal Zirconia (t)

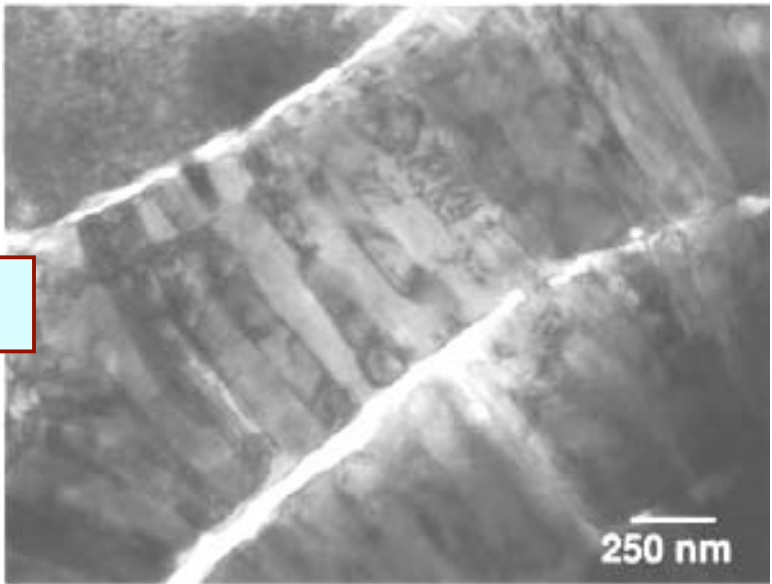


Levi, C.G. : *Acta Materialia*
46 (3) 787-800, 1998.

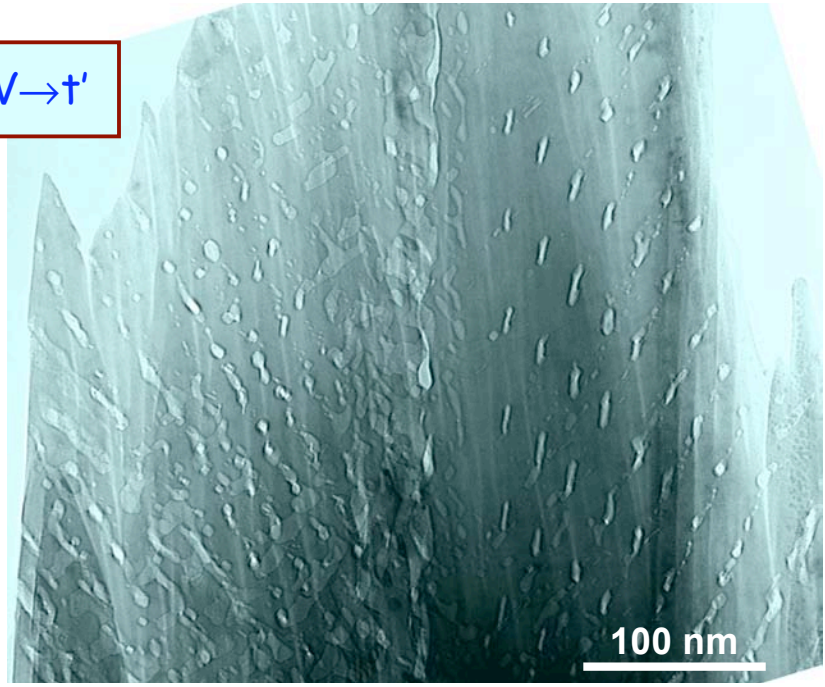
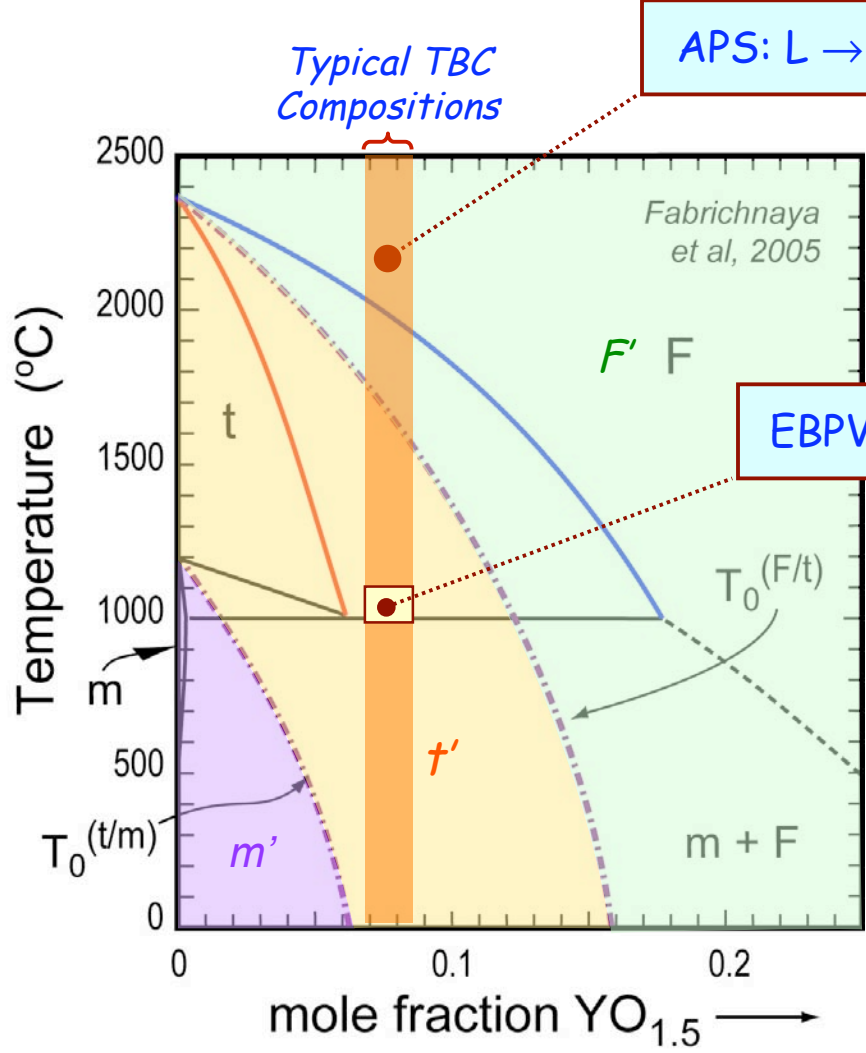


Bixbyite (Y)

Processing effects on t' microstructure

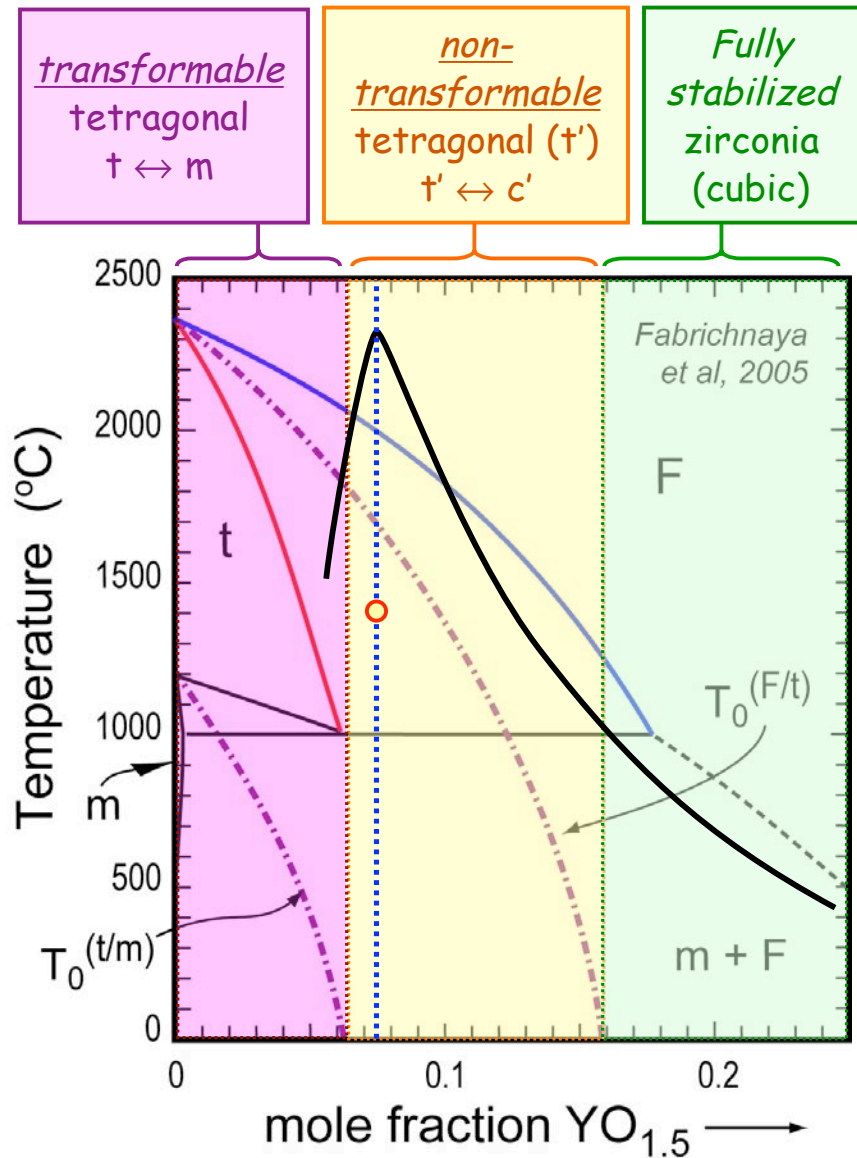


APS: L → F → t'



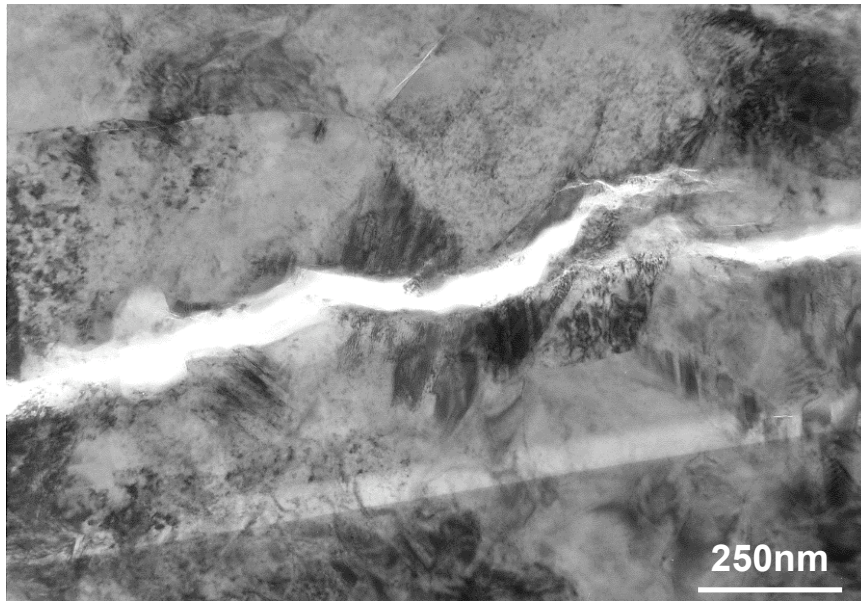
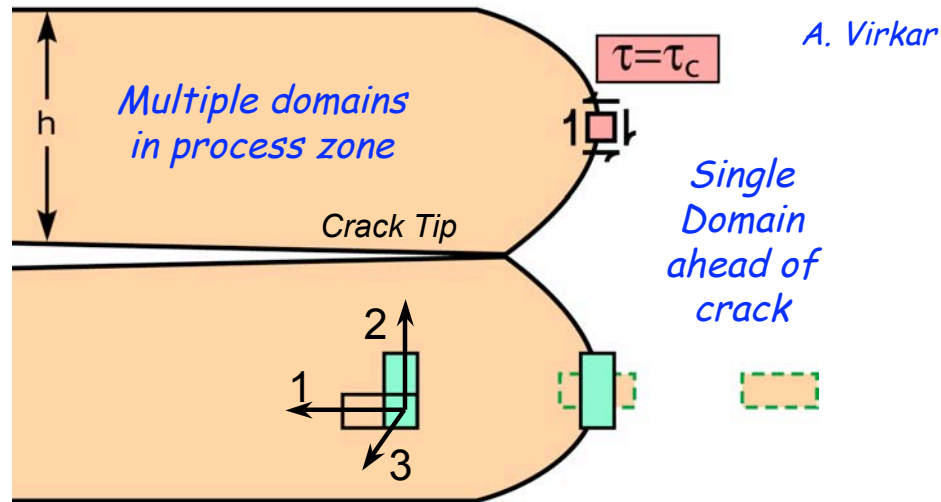
EBPVD: V → t'

Toughness dependence on composition



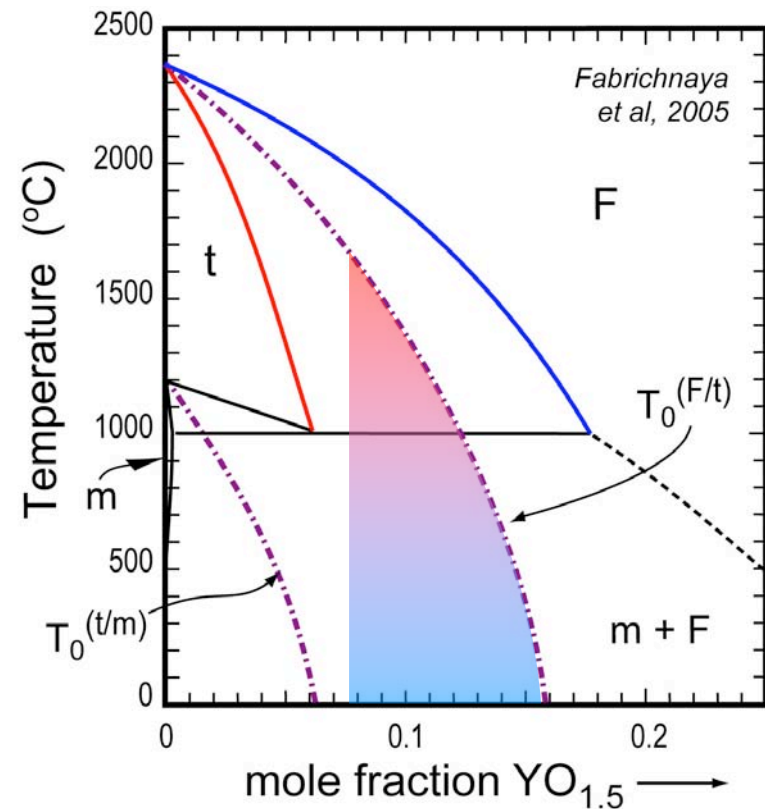
- Cubic zirconia (and pyrochlore) structures have generally low toughness. No significant toughening mechanisms available.
- Tetragonal compositions are much tougher. Substantial toughness available via controlled $t \rightarrow m$ transformation.
- Transformation toughening not operational at high temperature. "Transformability" not desirable under thermal cyclic conditions.
- Optimum TBC composition is tetragonal, single-phase, non-transformable $\Rightarrow t'$.

Ferroelastic Switching



Mercer et al. 2005

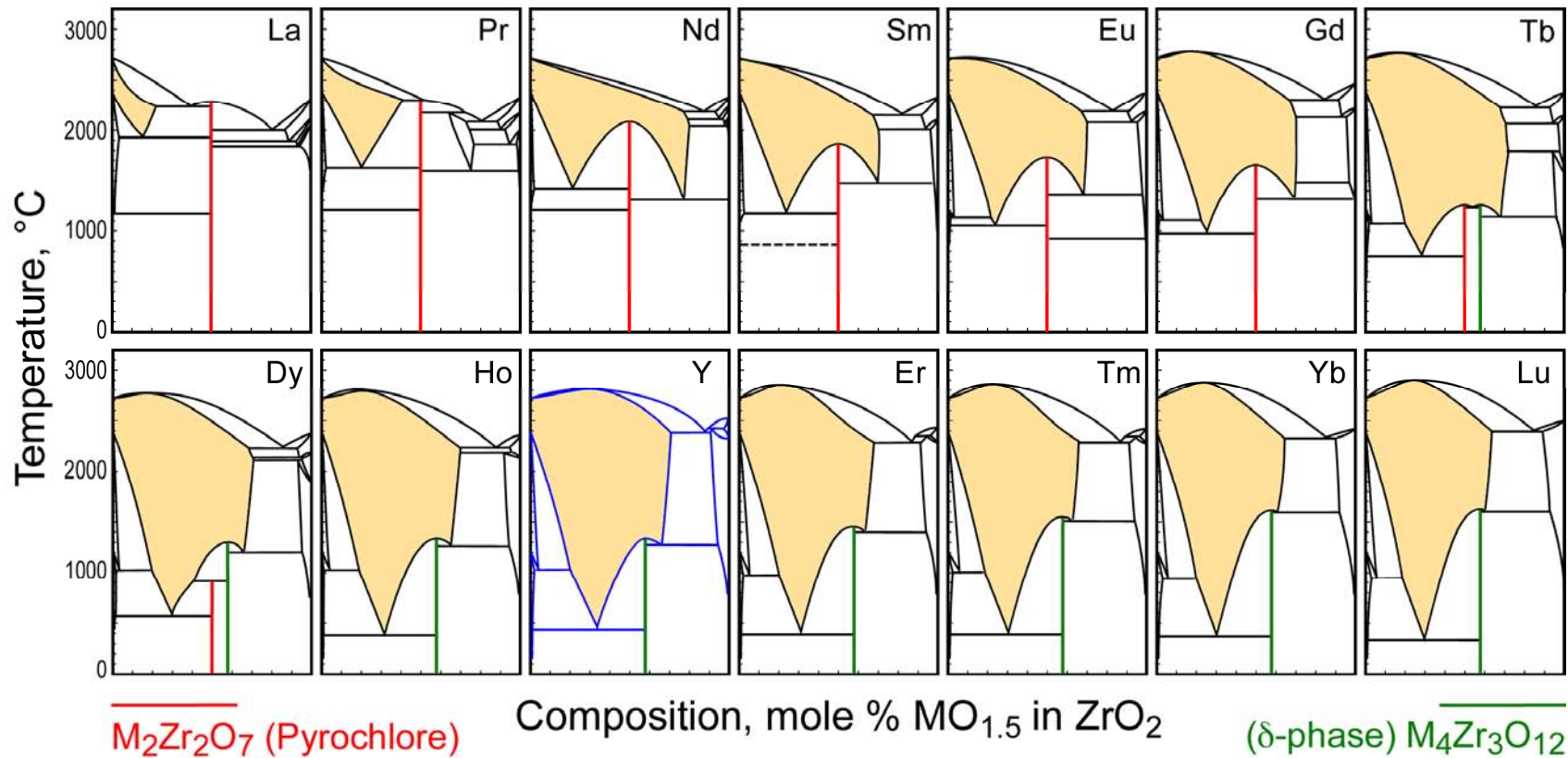
- Proposed toughening mechanism relies on tetragonality, which vanishes as $(c, T) \rightarrow T_0(F/t)$.



Dopants of Interest in ZrO₂-based TBCs

Well behaved phase equilibria with increasing ionic size

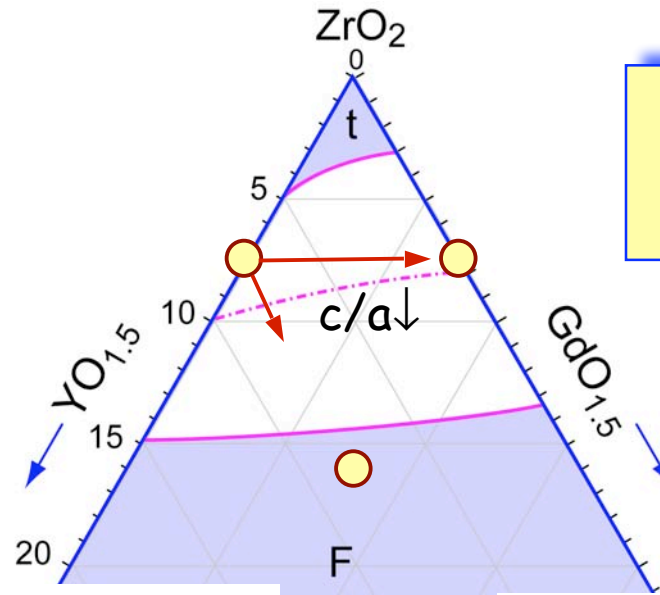
Pyrochlore stability decreasing ⇒



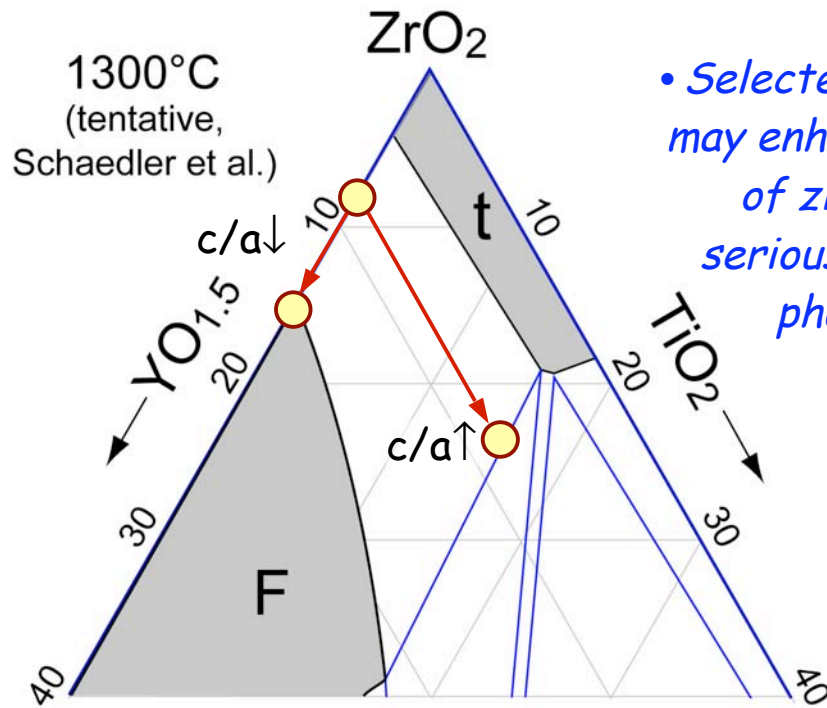
δ -phase stability increasing ⇒

Calculated diagrams,
after Yokokawa et al.

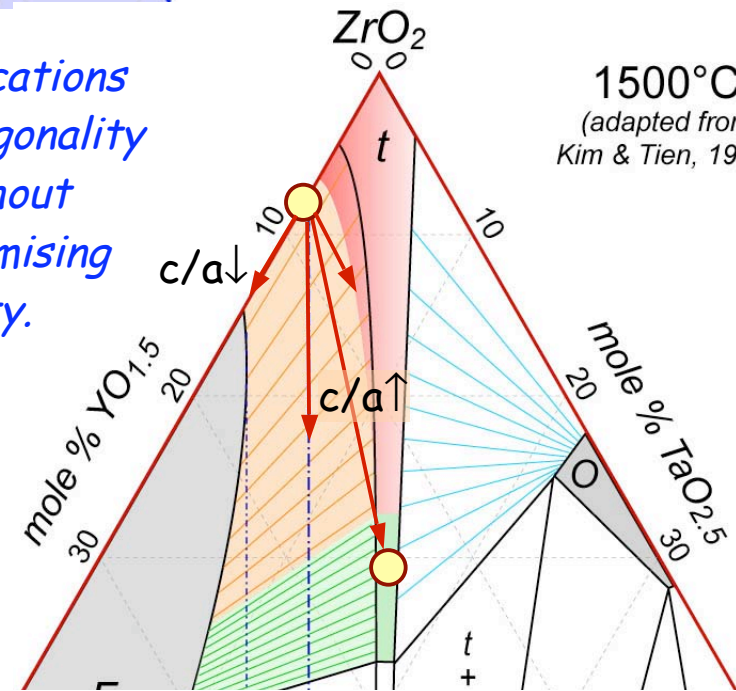
- Co-doping TYSZ with large RE cations decreases the tetragonality of the structure



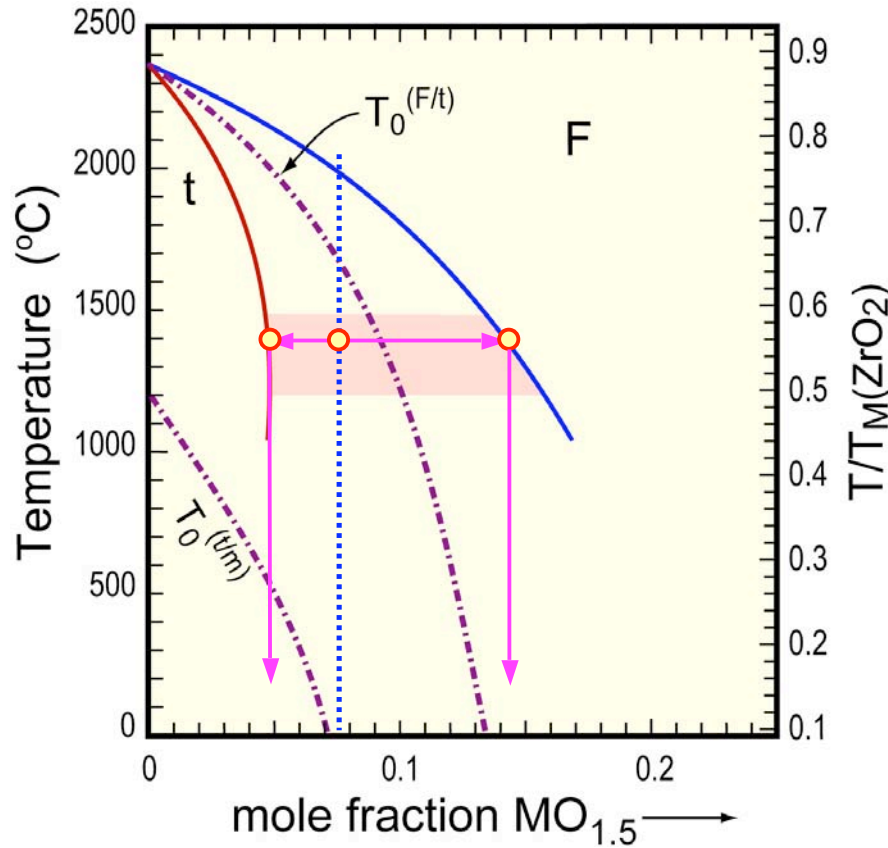
Looking for the right dopants



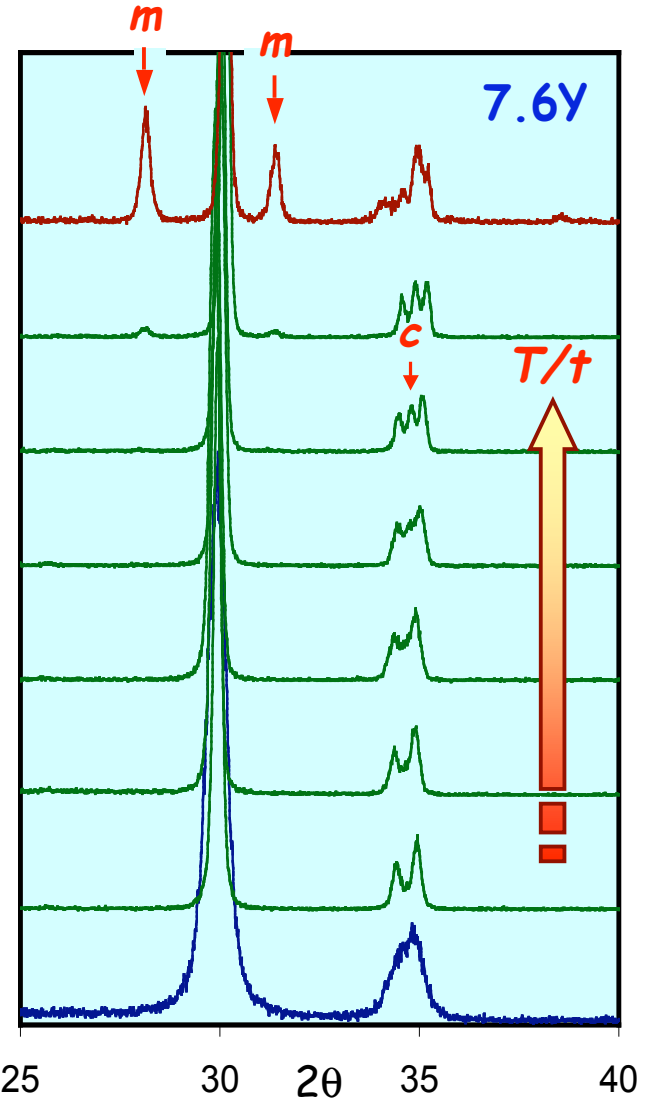
- Selected smaller cations may enhance tetragonality of zirconia without seriously compromising phase stability.



Phase Stability: Thermal Decomposition

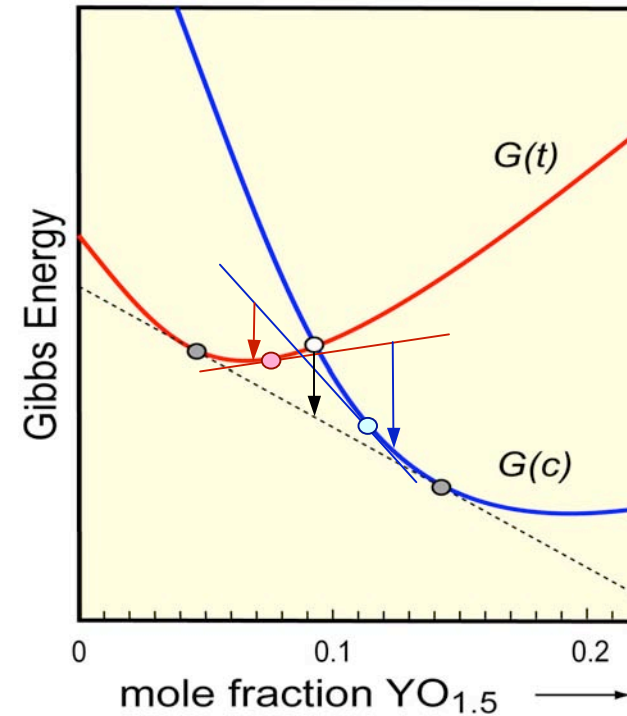
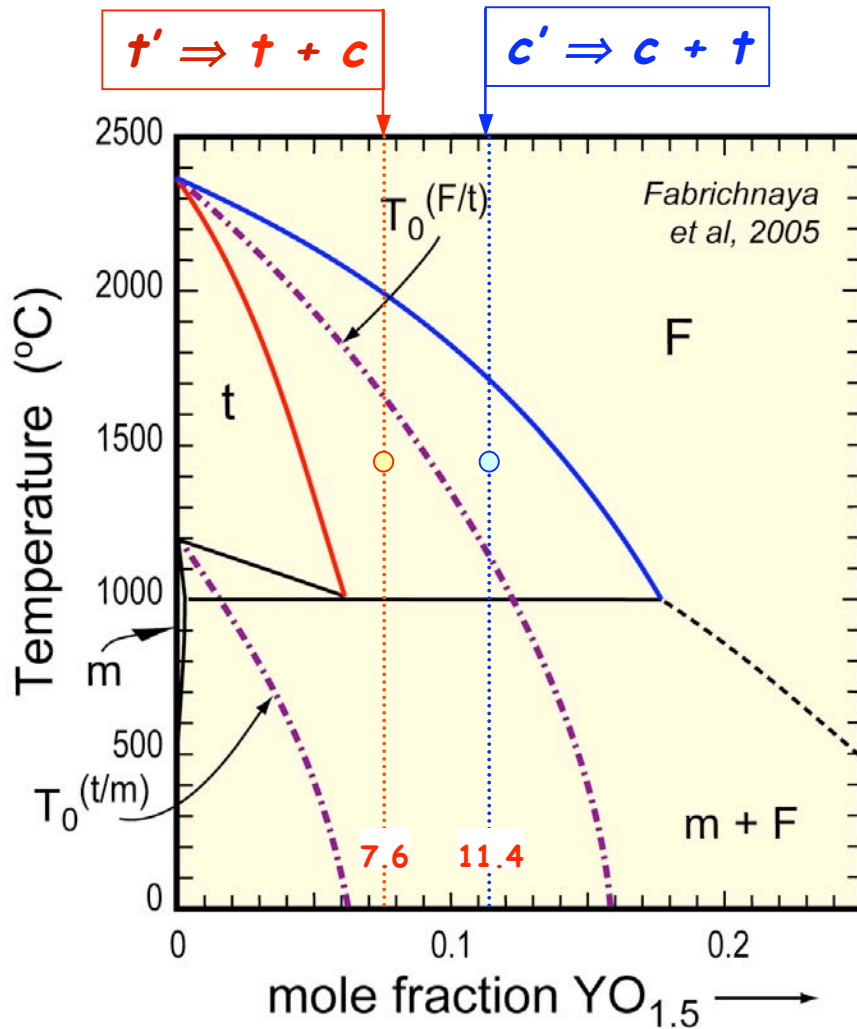


Phase (In)stability:
the operating limit to t'



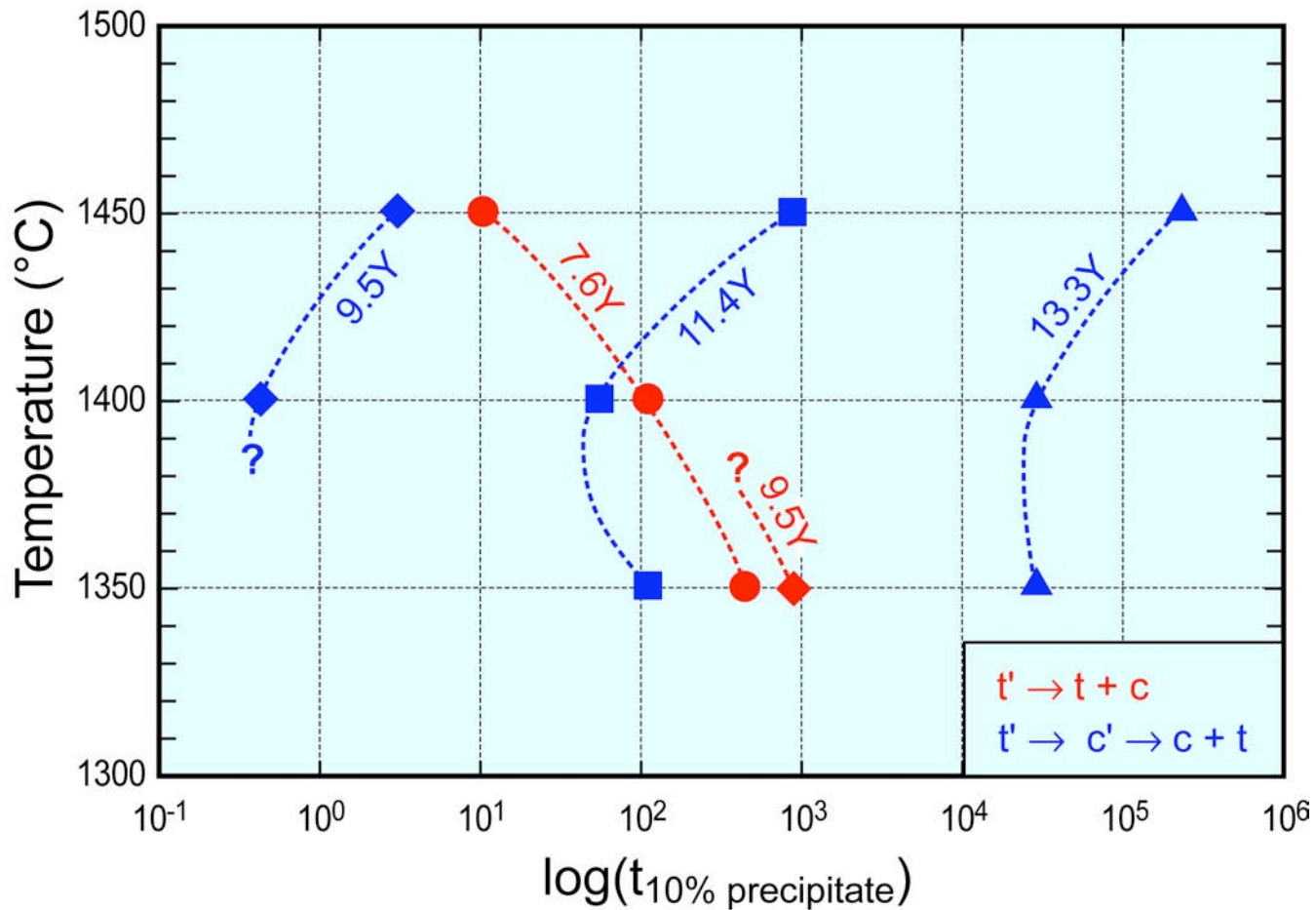
- *t'*-7YSZ falls in the equilibrium *t* + *c* field ⇨ inherently metastable
- Increasing *T* activates partitioning kinetics: *t'* → *t* + *c*
- depleted *t* → *m* upon cooling

Effect of Composition on De-stabilization Path

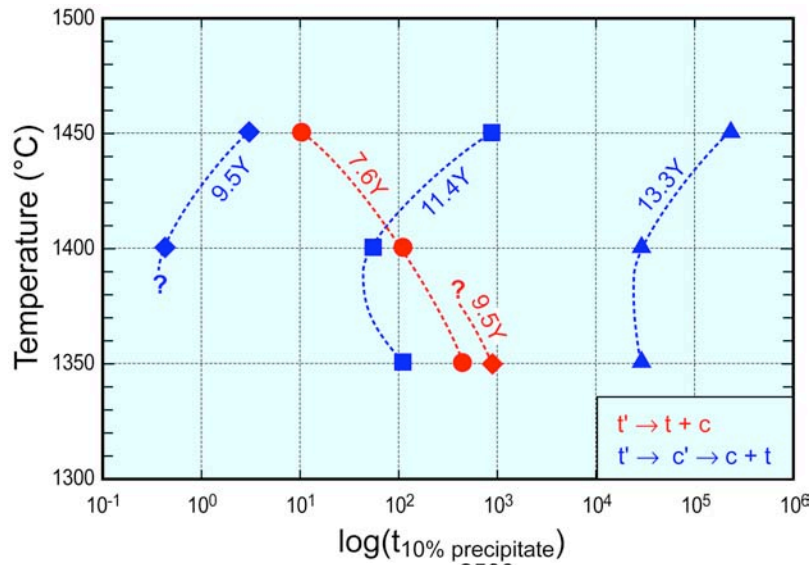


- Parent and precipitate phase switch with increasing %Y.
- Driving force scales with distance from equilibrium boundaries, peaks at $T_0(F/t)$

Effect of γ content on Kinetics



Precipitation follows approximately AJMK kinetics but significant differences observed depending on the decomposition path

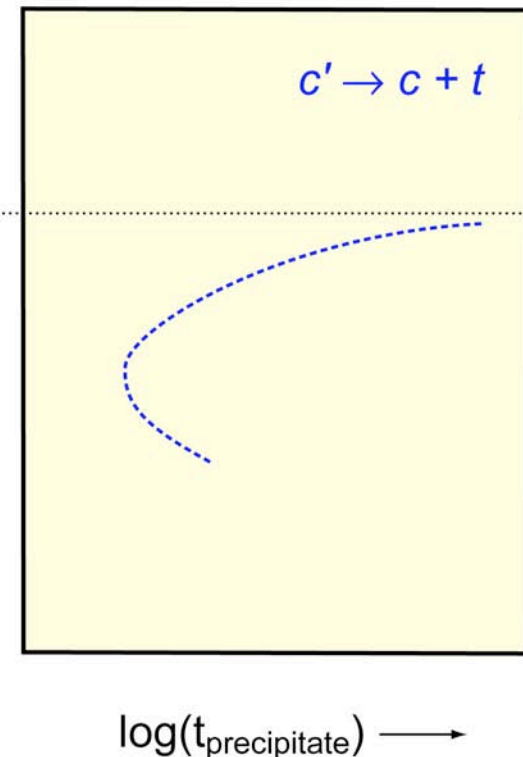
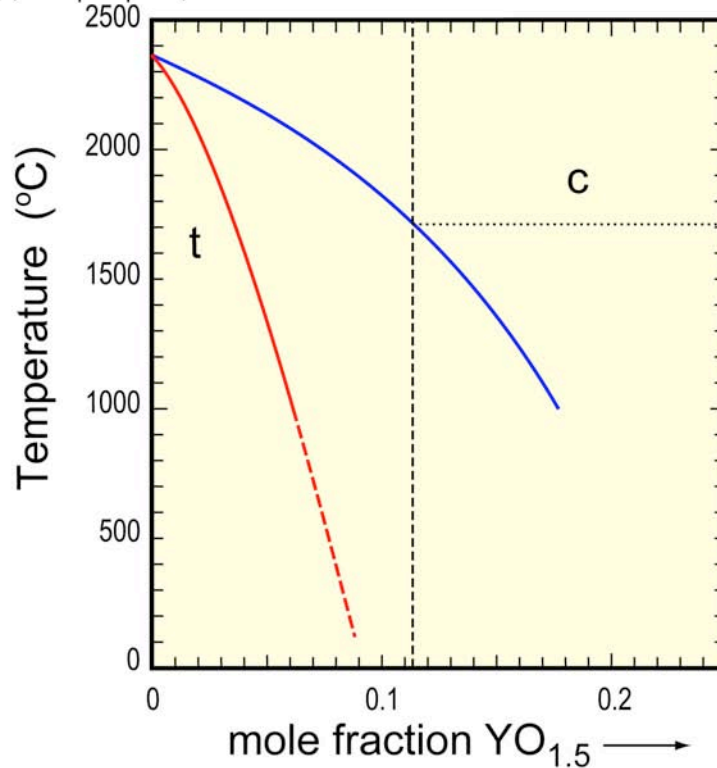


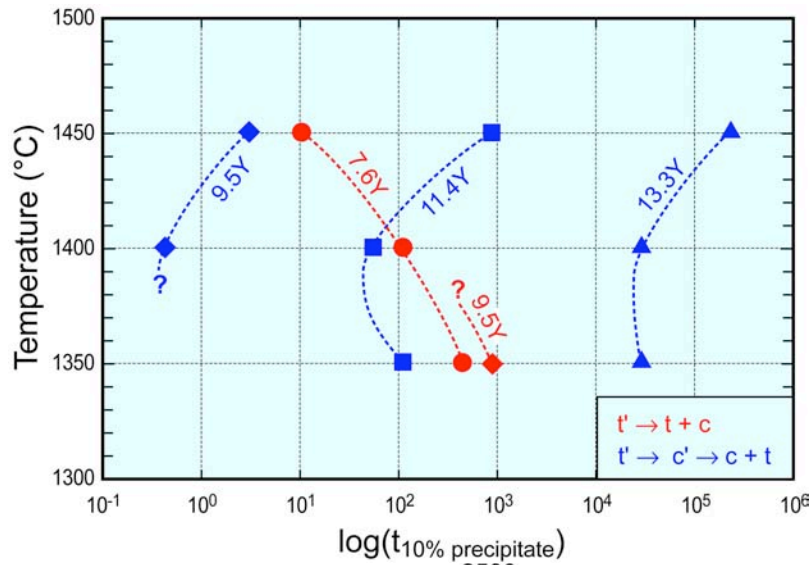
Understanding Partitioning Kinetics

The classical case: driving force increases with decreasing temperature but diffusion becomes more sluggish, giving rise to "knee" in the TTT curve.

Compositions with "High" Y content: 11- and 13-YSZ

t' at ambient, transform diffusionlessly to c' at the heat treating temperature.



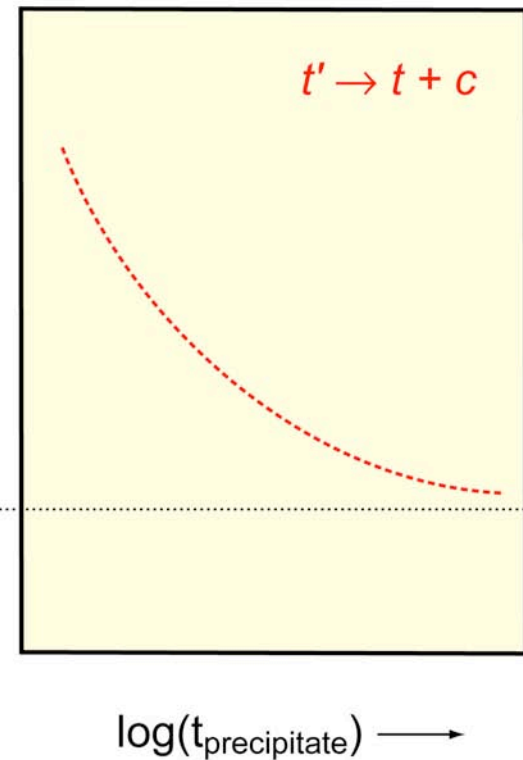
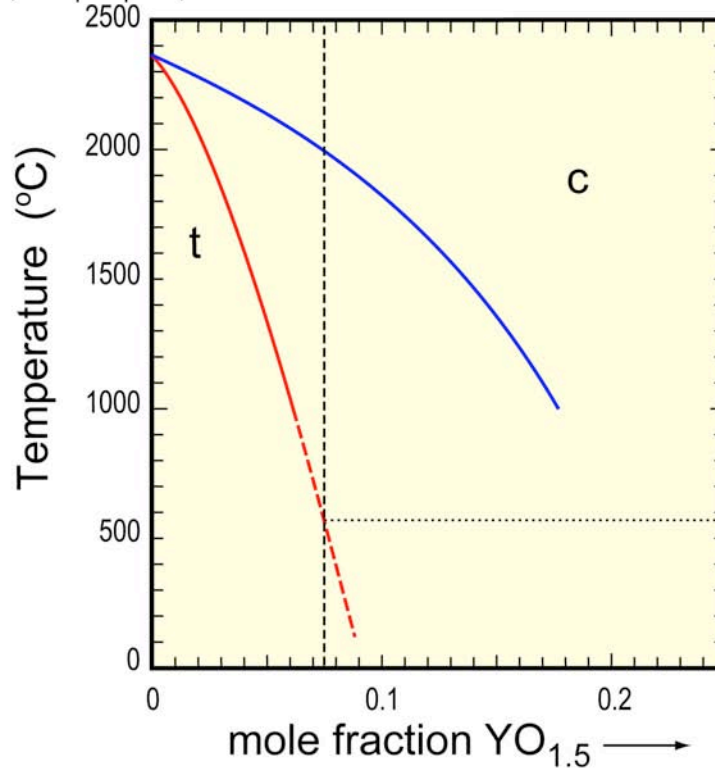


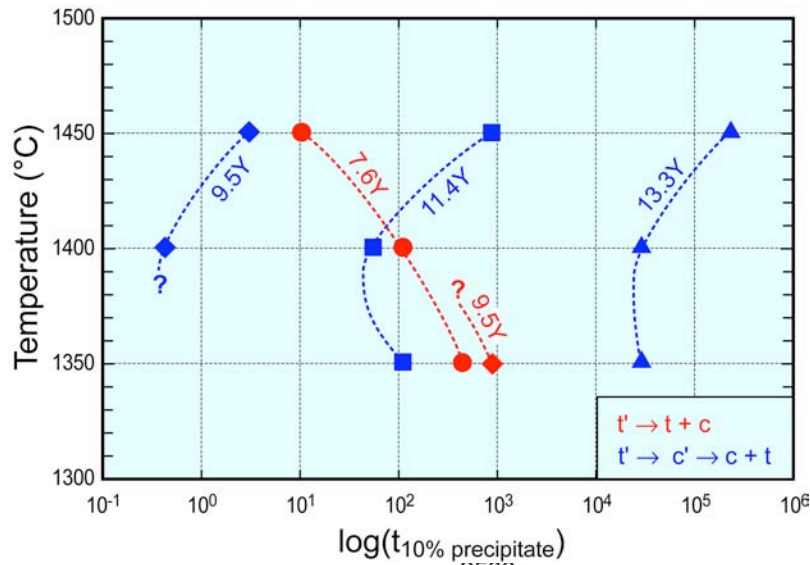
Understanding Partitioning Kinetics

The non-classical case: both driving force and diffusion kinetics increase with increasing temperature - no "knee".

Composition with "Low" Y content: 7YSZ

t' at ambient as well as at the heat treating temperature.



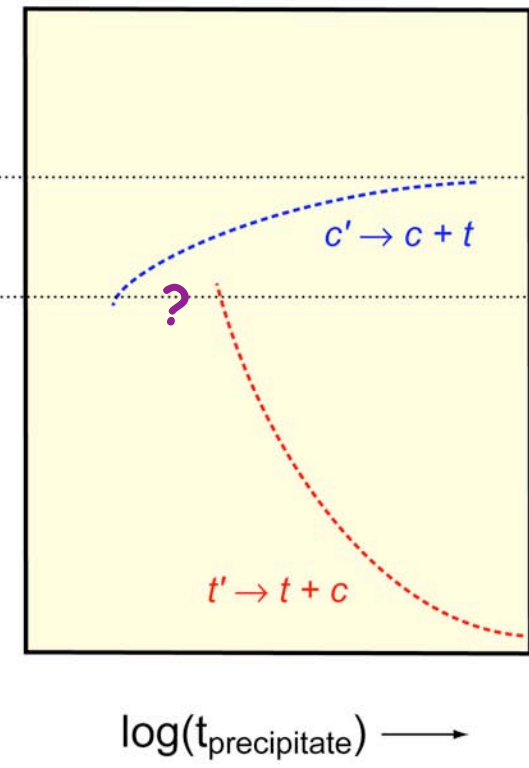
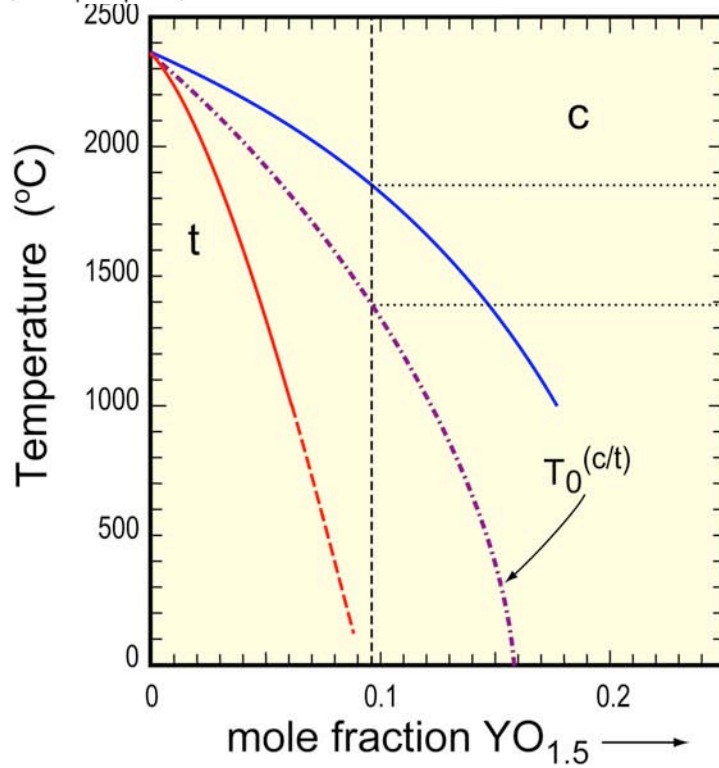


Understanding Partitioning Kinetics

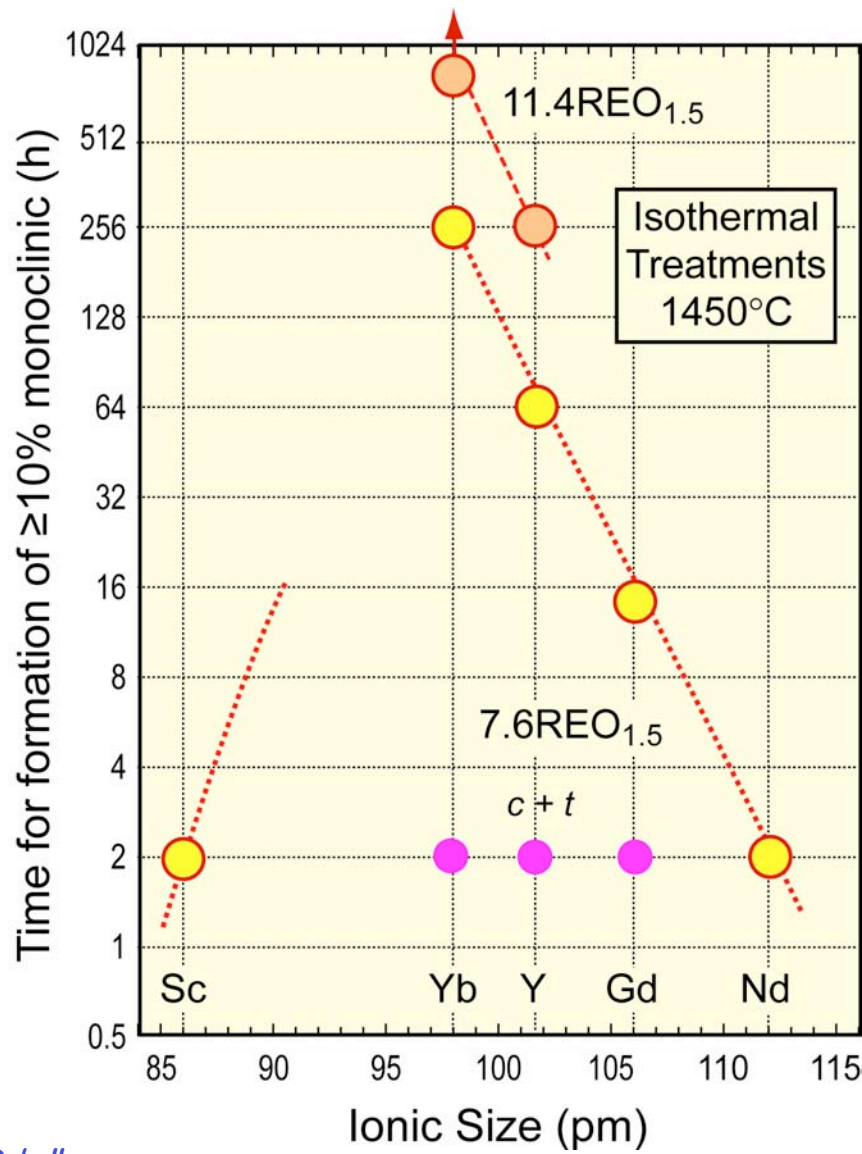
The special case: $T_0(c/t)$ is within range of heat treatment. It follows the "classical" case at $T > T_0(c/t)$ and the "non-classical" at $T < T_0(c/t)$.

Composition with "Intermediate" γ content: 9YSZ

*t' below $T_0(c/t)$
 c' above $T_0(c/t)$
 Possibility that both mechanisms operate in the vicinity of $T_0(c/t)$*



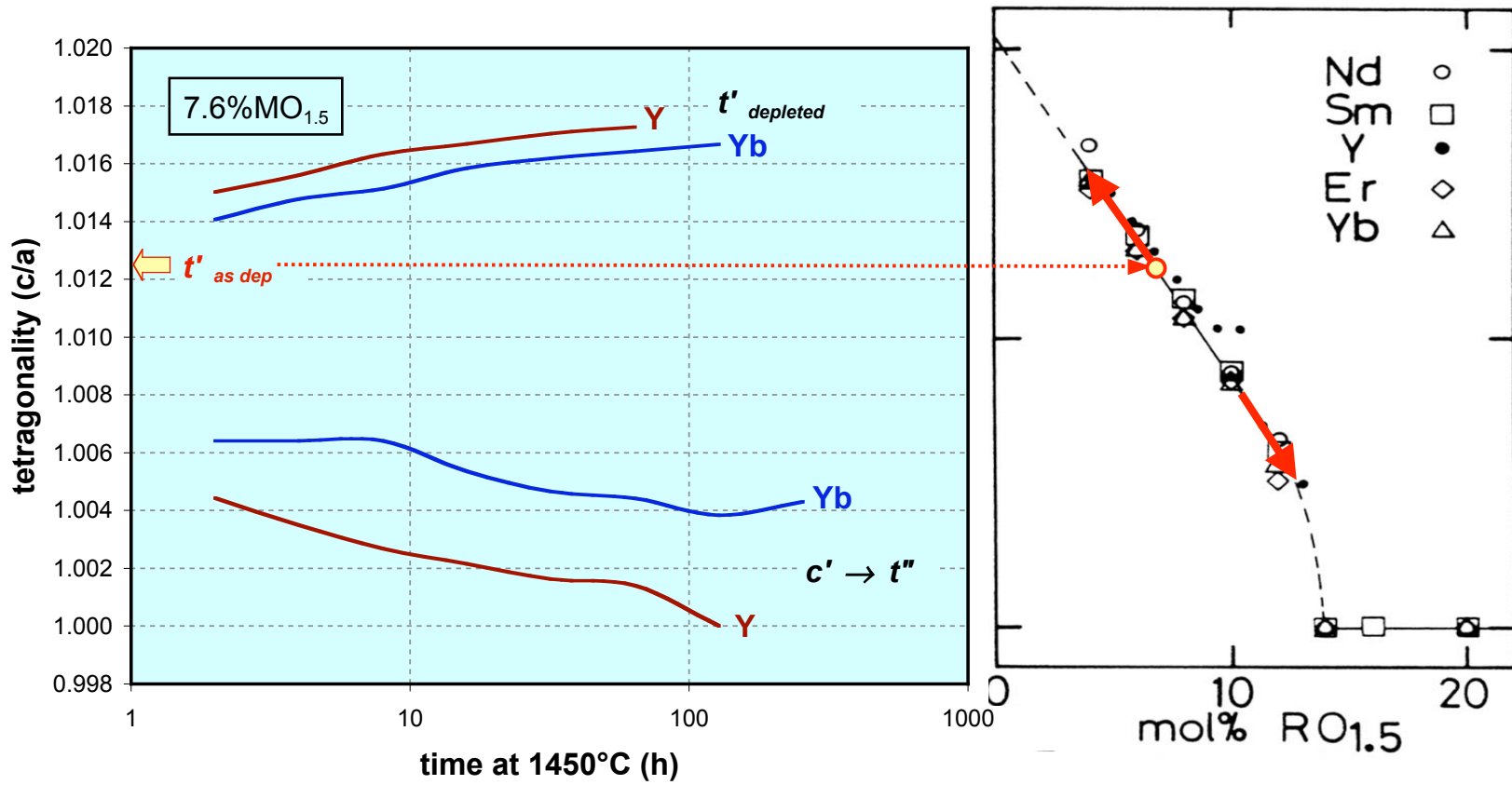
Effect of Cation Substitution

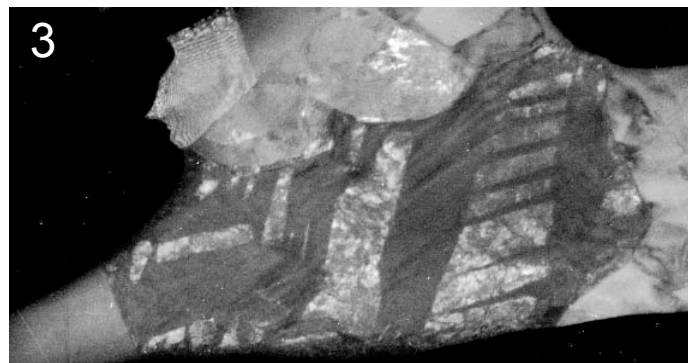
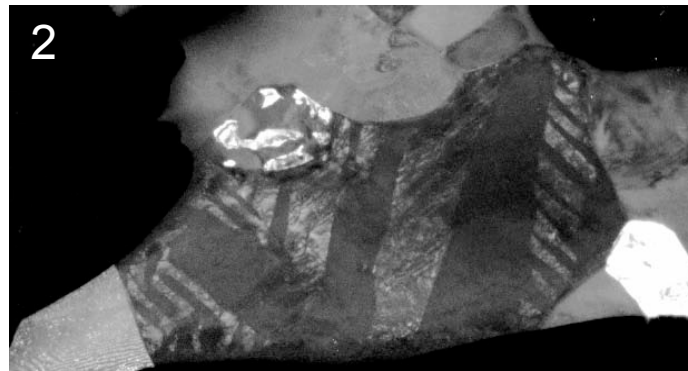
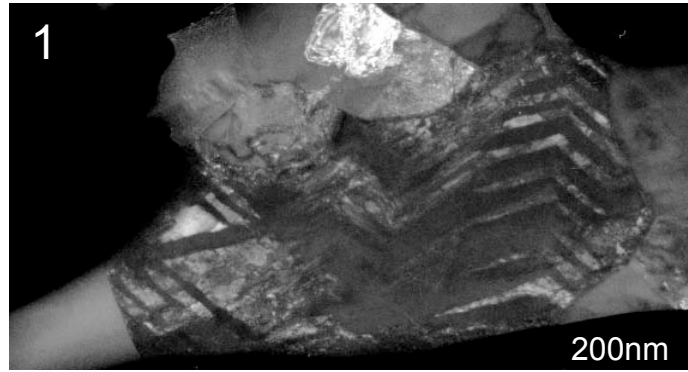


- Comparative kinetic study using isothermal treatments at 1350, 1400 and 1450°C.
- Well behaved trend showing substantial effects of ionic size and concentration.
- t' can exhibit early partial decomposition but remain "non-transformable" for much longer periods of time.
- Monoclinic can further evolve isothermally at ambient temperature (cf. Lughì and Clarke).

Evolution of Phase Compositions

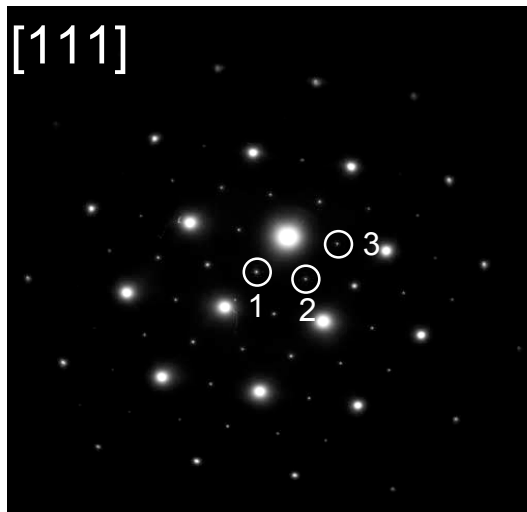
- Gradual depletion from t' or c'
- Precipitate composition evolves over time



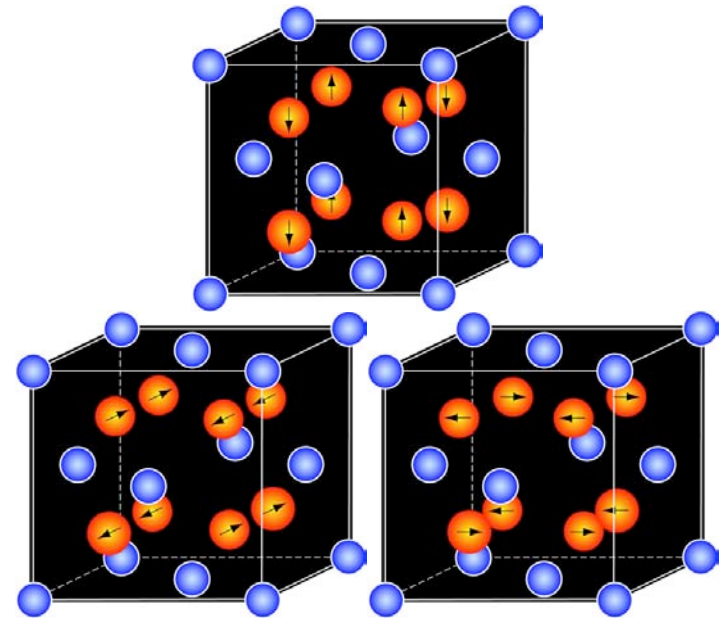
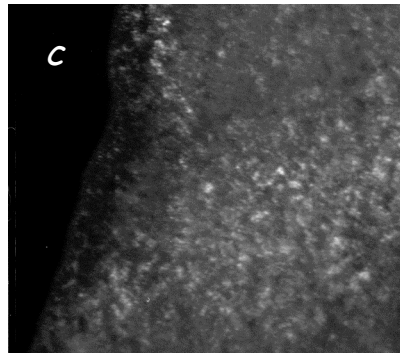
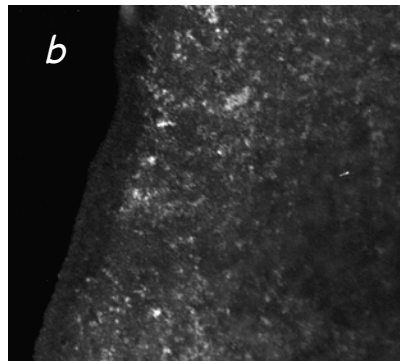
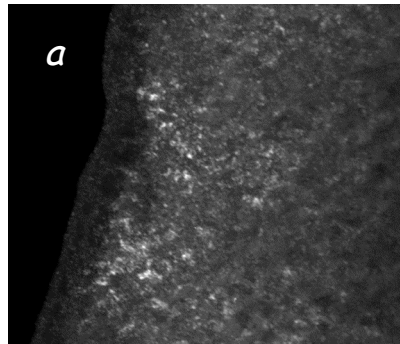
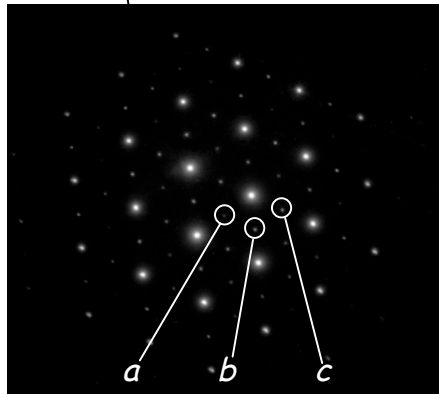
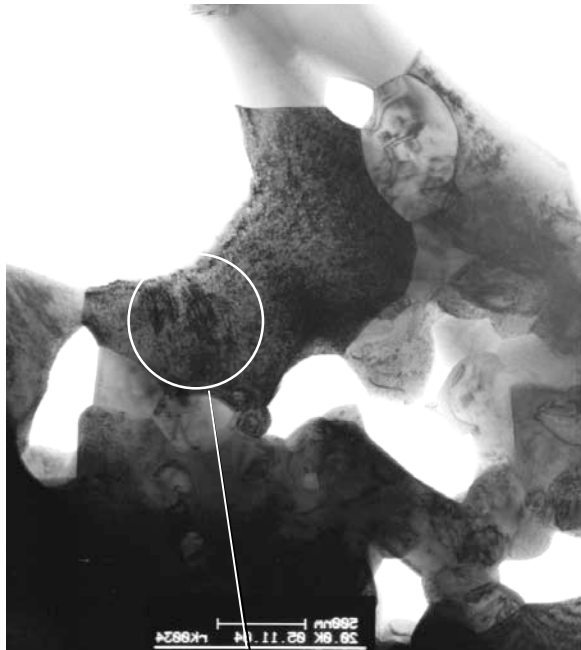


Displacive Transformation in 7YbSZ after 32h at 1450°C

Tetragonal variants result from shear transformation along equivalent crystallographic planes in the parent cubic structure



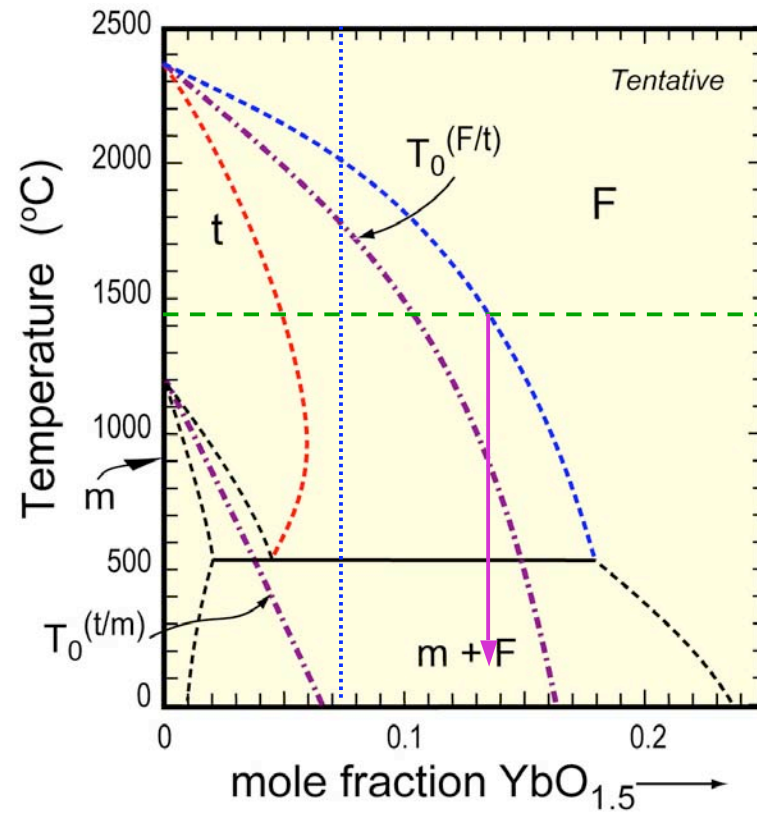
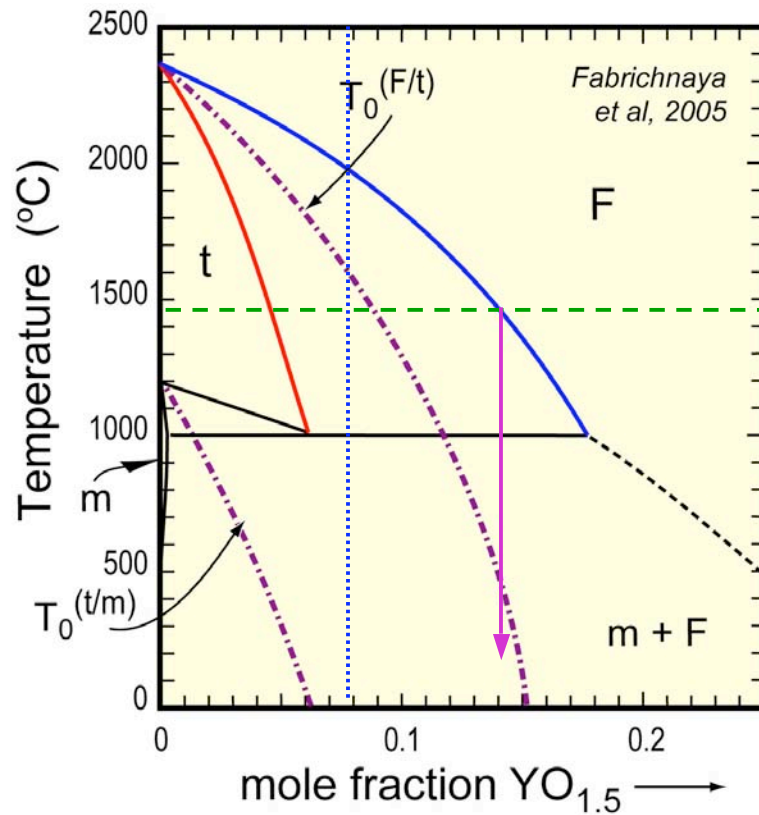
**7.6Y after
16h at 1450°C**



Postulate: Variants result from ordering of anion displacements in the characteristic tetragonal pattern along each of the 3 cubic directions $\Rightarrow t''$

Transformation of grains that are cubic (Y-rich) at high temperature yields 3 tetragonal variants

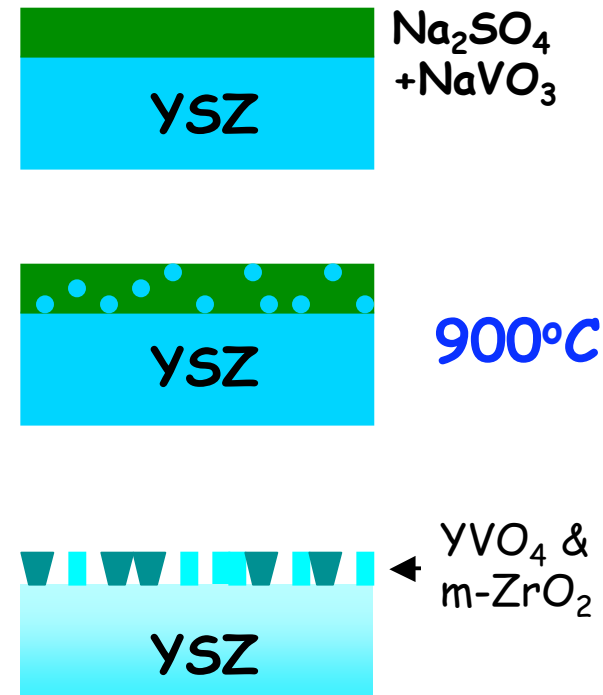
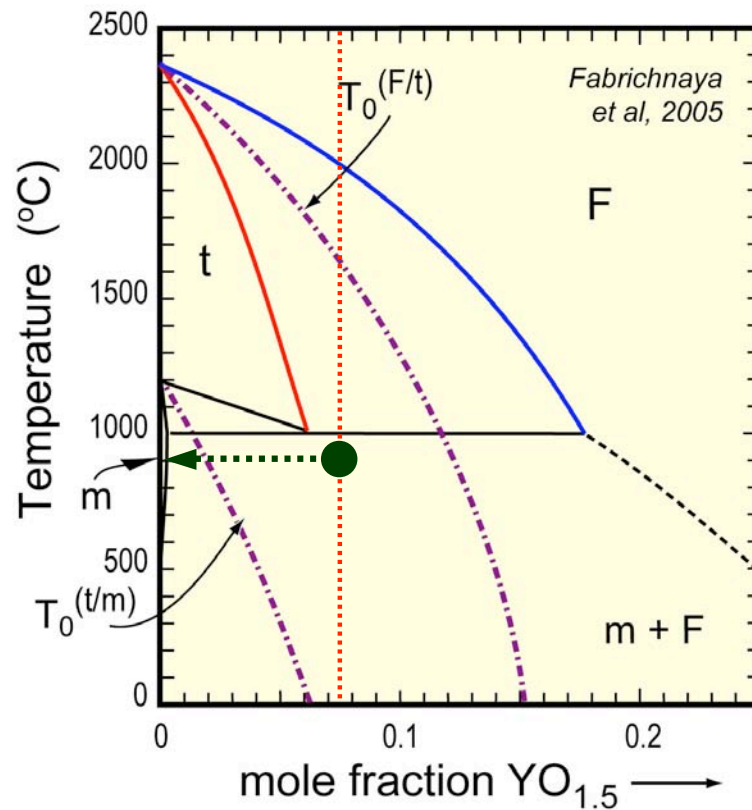
Thermodynamic Effects: Y v. Yb



- Evolution of twinned t' microstructures in Yb but not in Y
 ↳ suggests higher $T_0(T/F)$ for Yb compared with Y.

Chemically assisted de-stabilization of t'

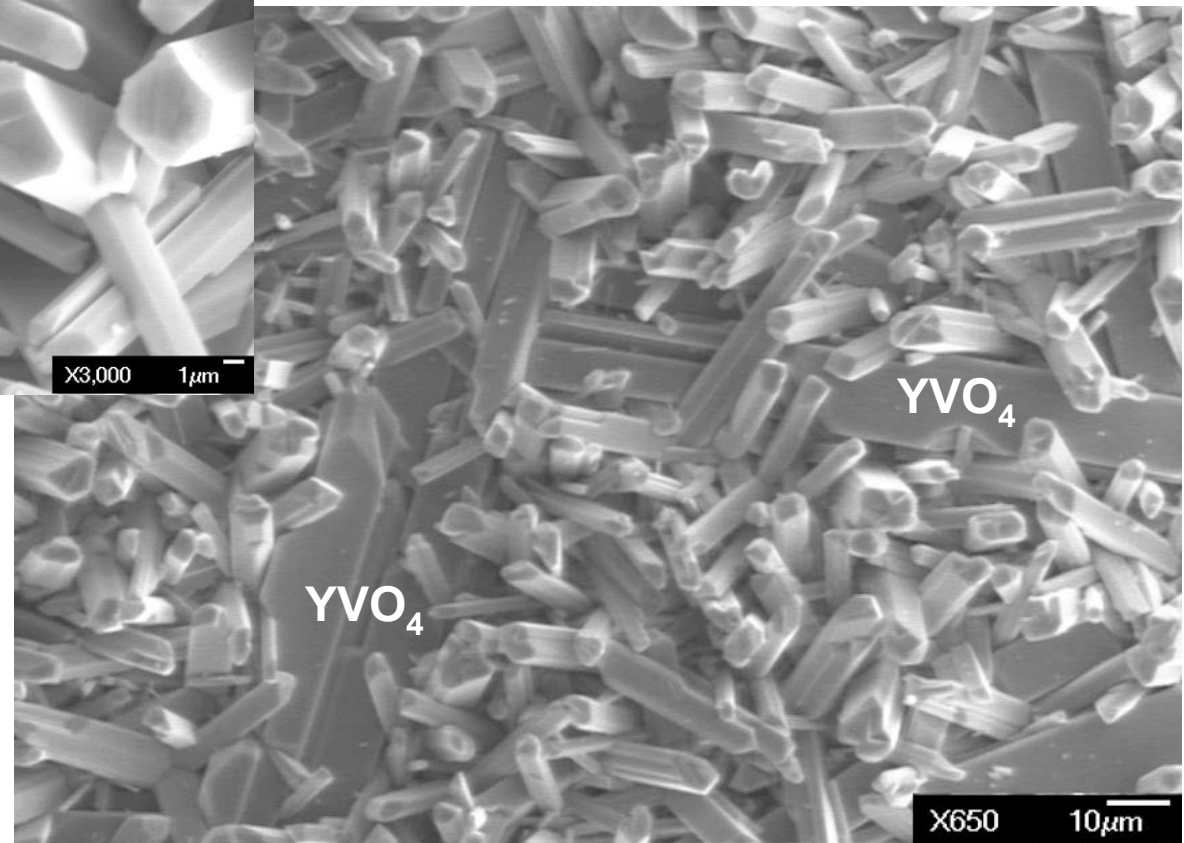
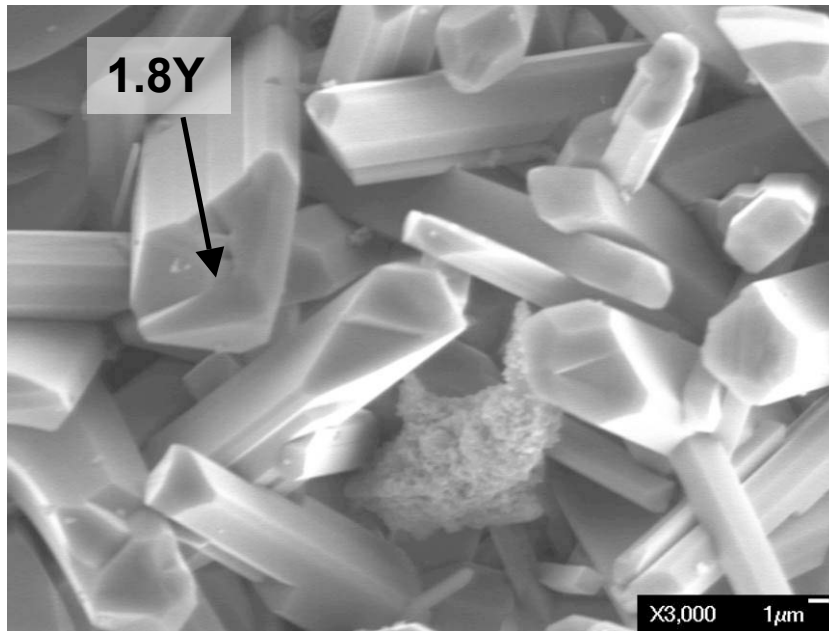
Low Temperature De-stabilization of t' by S/V



YVO_4 and monoclinic ZrO_2 precipitate directly from the melt.

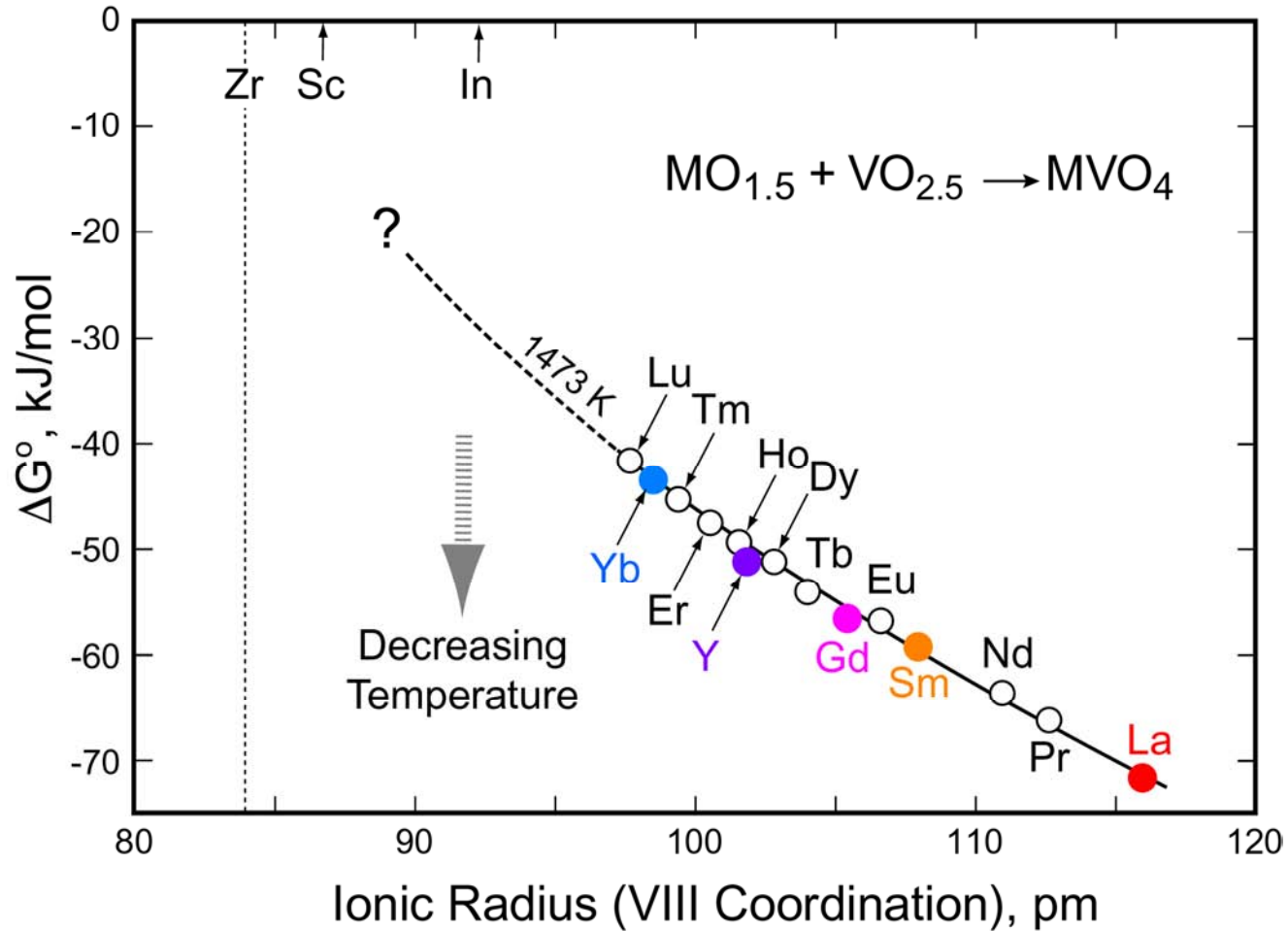
Vanadate attack on TYSZ

Molten 70:30 Sulfate:Vanadate
 25-35mg/cm², 100 h at 900°C in Air
 25 h cycles with salt replenishment



- *Precipitation of YVO_4 and $m-ZrO_2$ crystals on the surface.*
- *Extensive spallation after 100 h.*

Vanadate formation with REOs

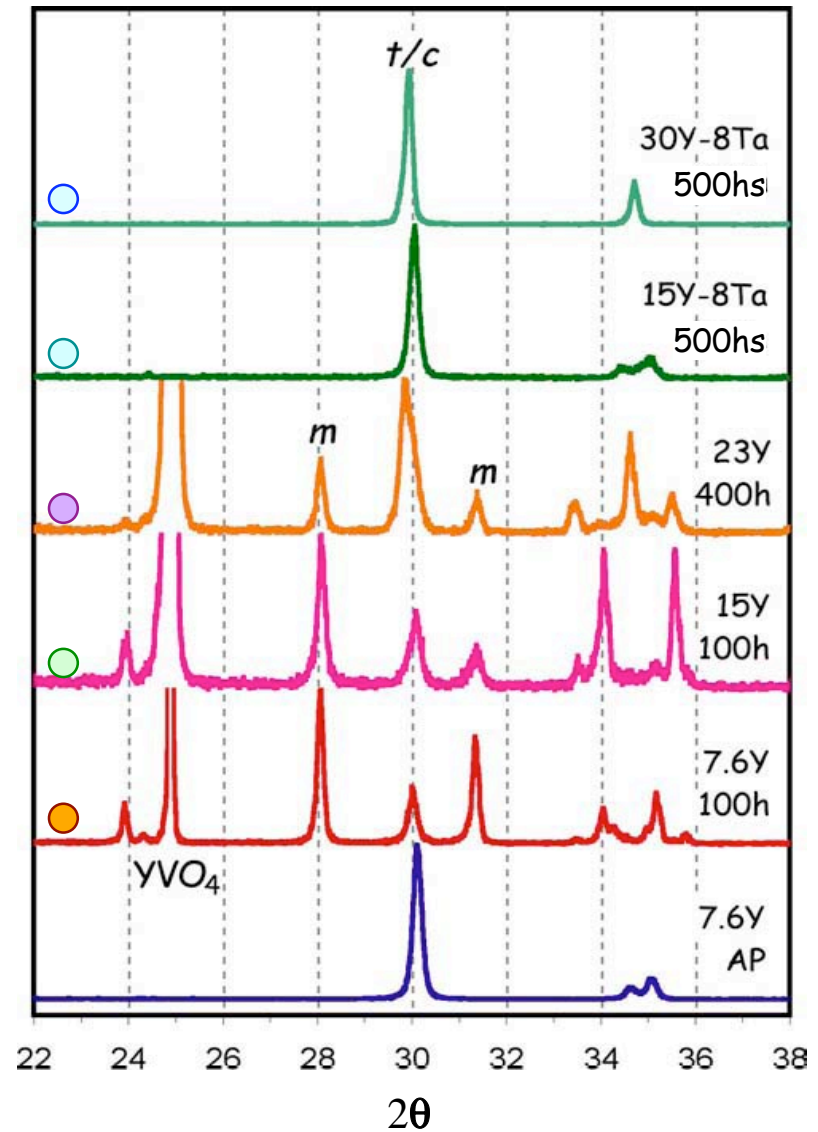
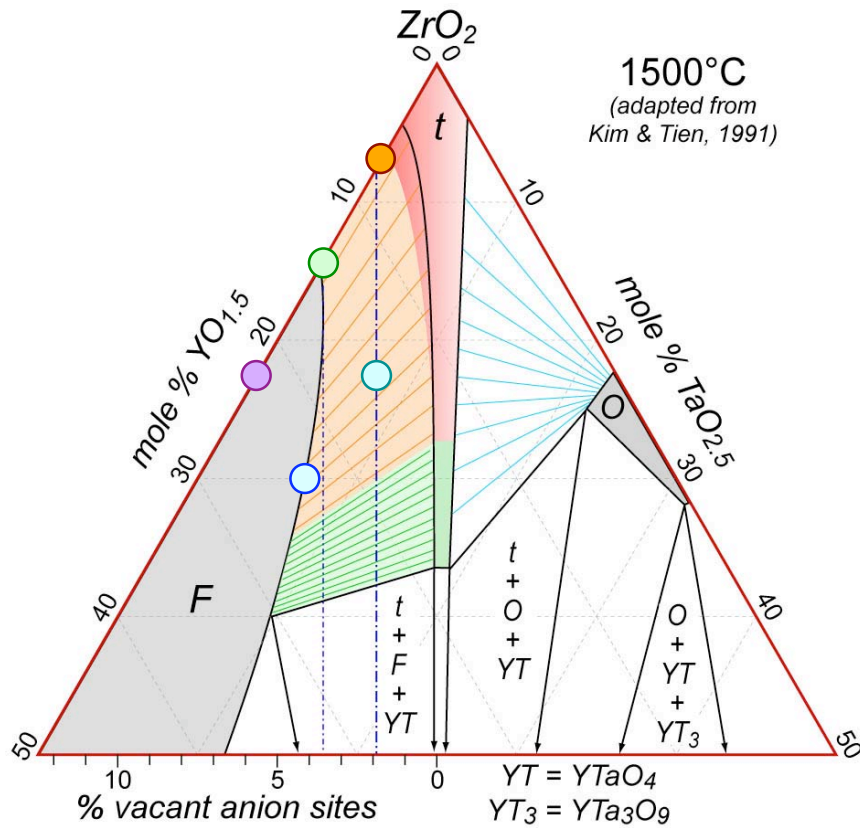


- All rare earth oxides of interest as dopants/stabilizers in novel TBCs susceptible to attack by vanadate-bearing molten deposits.

Corrosion Studies

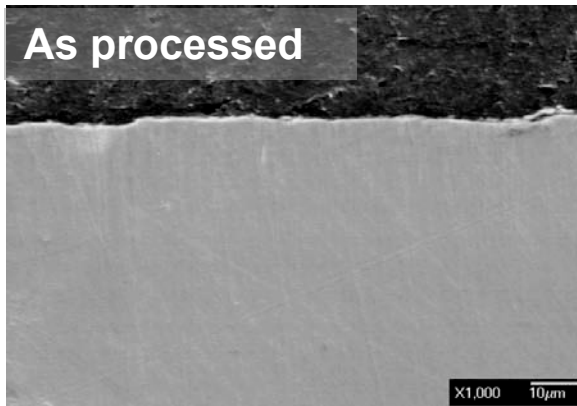
900C, 70S:30V
30±5 mg/cm²

- All Y compositions showed sign of de-stabilization, whereas the Ta co-doped materials revealed no evidence of attack.

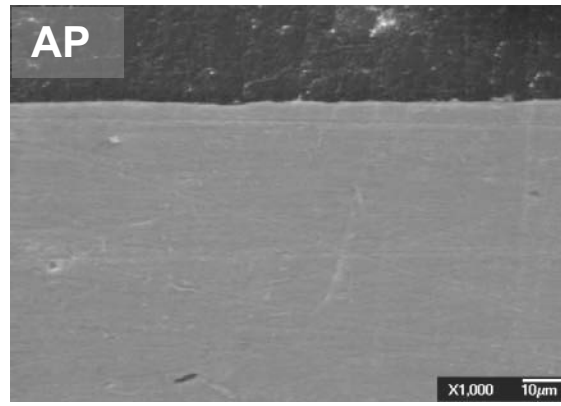


Comparison of Cross Sections

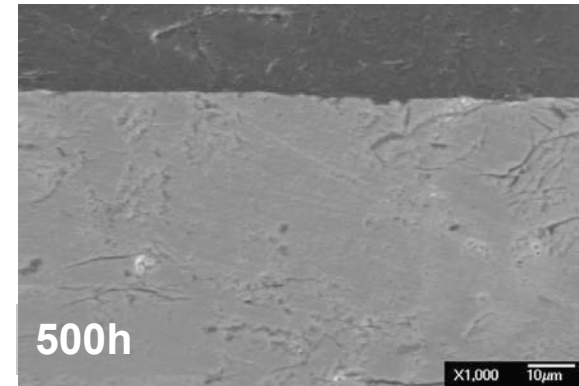
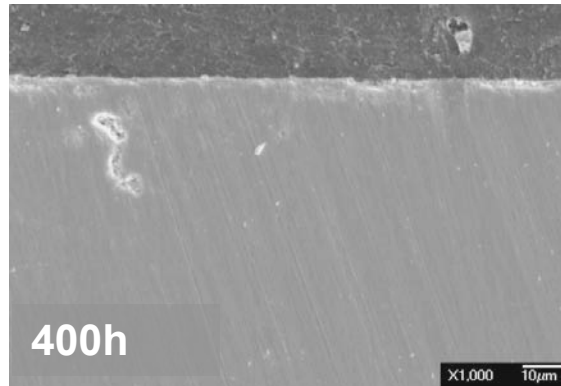
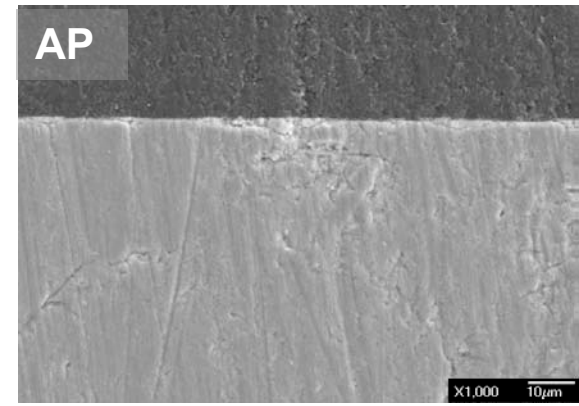
7.6Y



15.2Y+7.6Ta



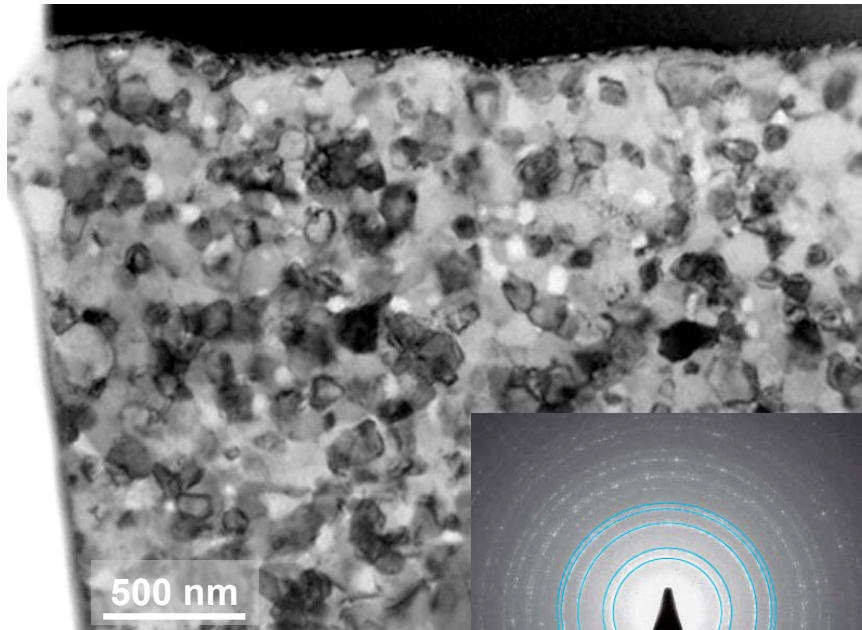
30Y+7.6Ta



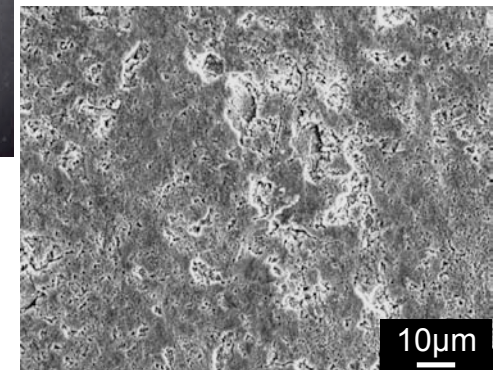
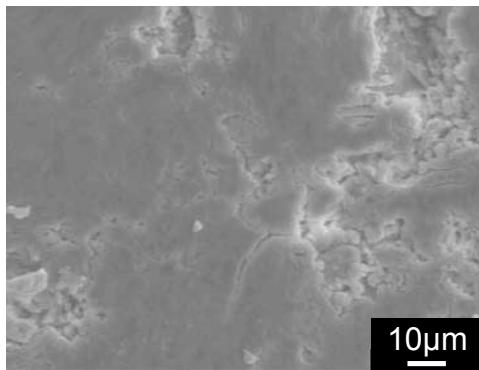
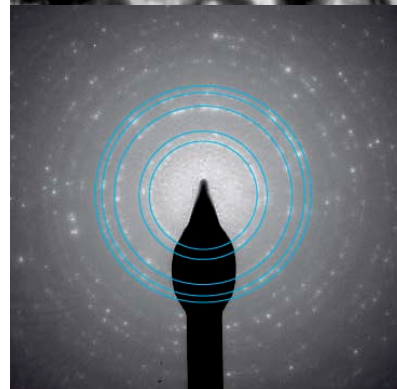
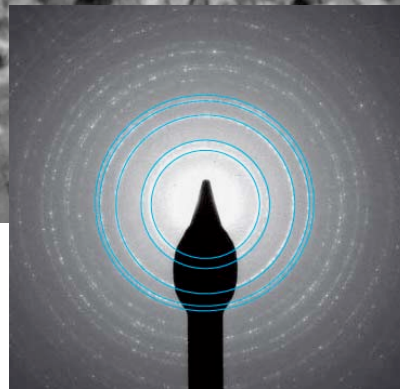
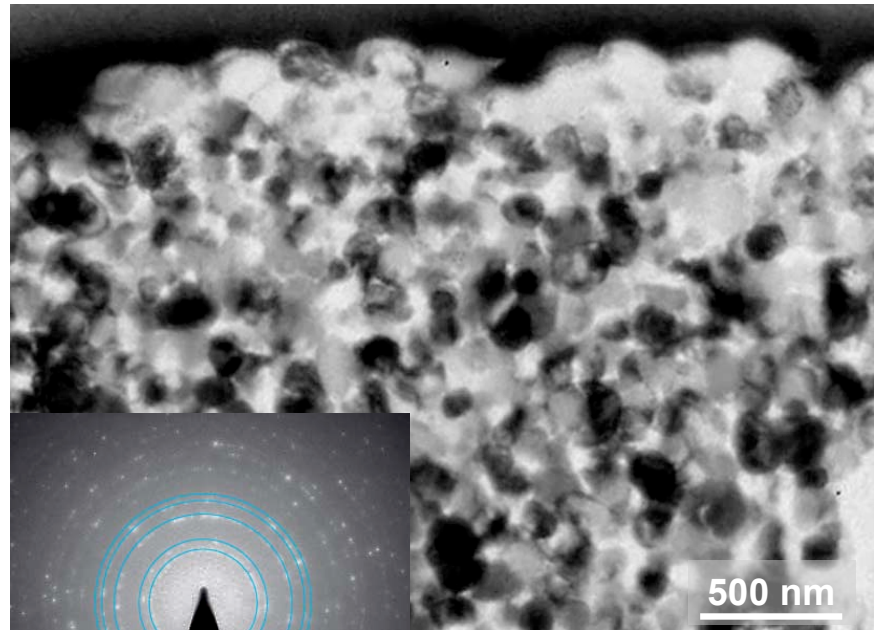
40µm

TEM Analysis of 30Y-7.6Ta Surfaces

As processed (cubic)



After 500h/900C, 30±5 mg/cm² 70S:30V



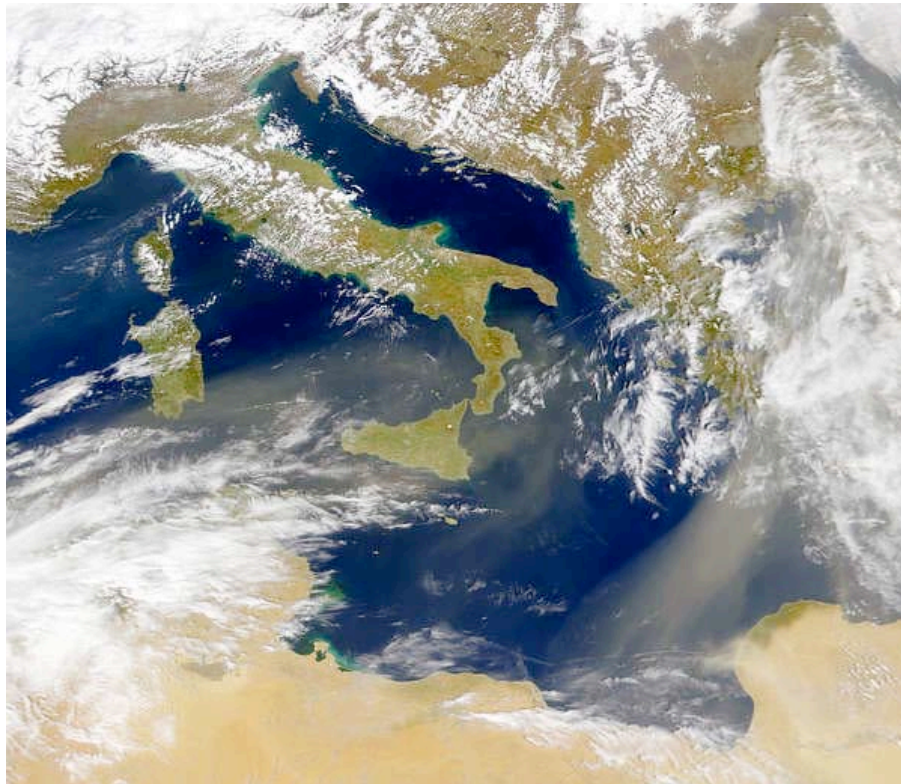
No detectable structural changes on surface after 500 h exposure, only small depletion of Y.

CMAS Degradation of TBCs: The Price Paid for Higher Temperature Operation



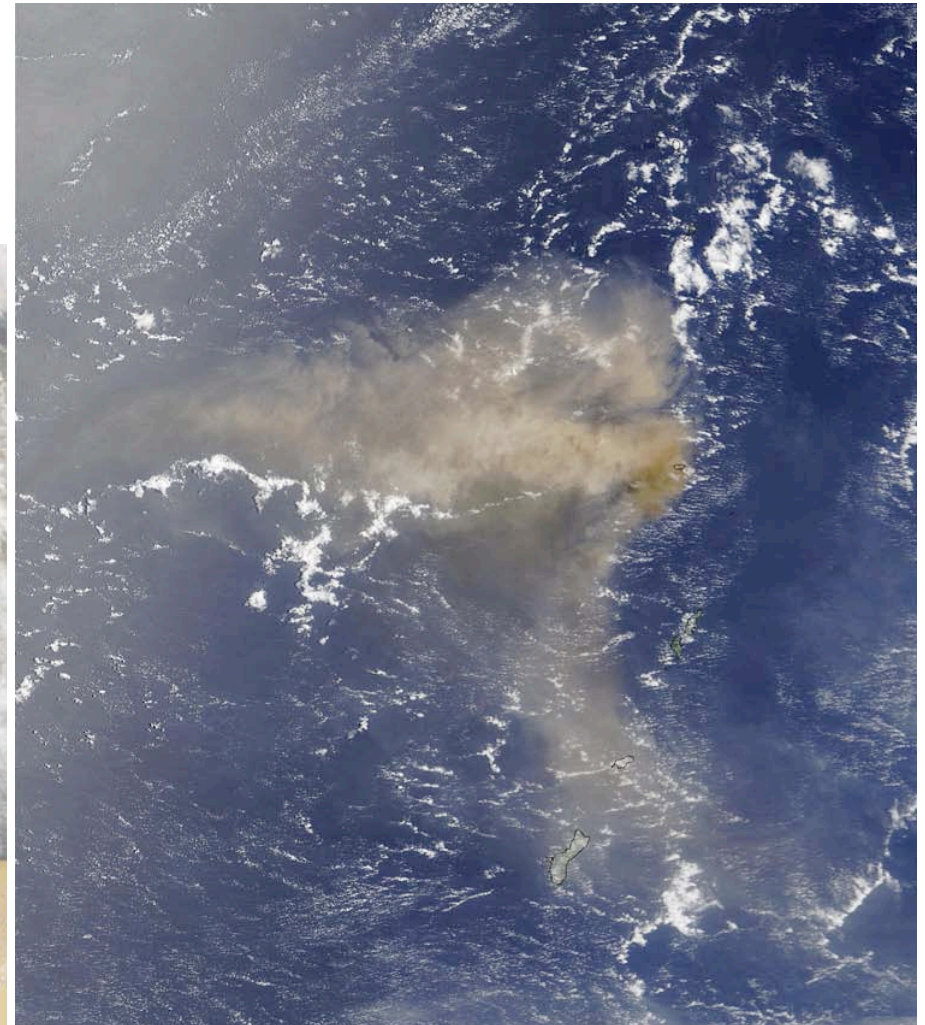
Photo Courtesy of R. Kowalik, US Navy

Sources of Airborne Siliceous Debris



*Saharan dust blowing
over the Mediterranean*

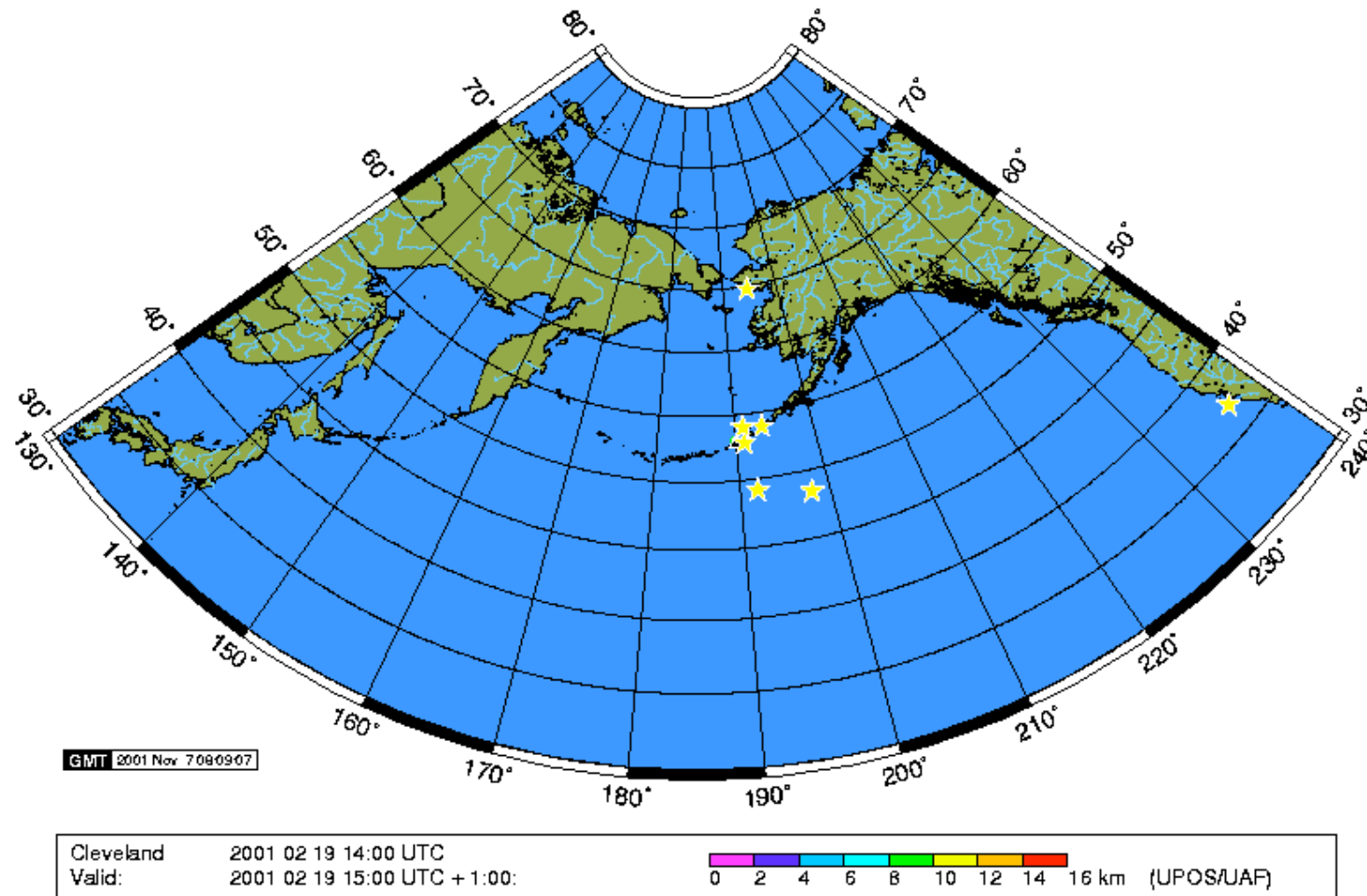
http://visibleearth.nasa.gov/view_rec.php?id=2197



*Eruption of Anatahan Volcano
Northern Mariana Islands*

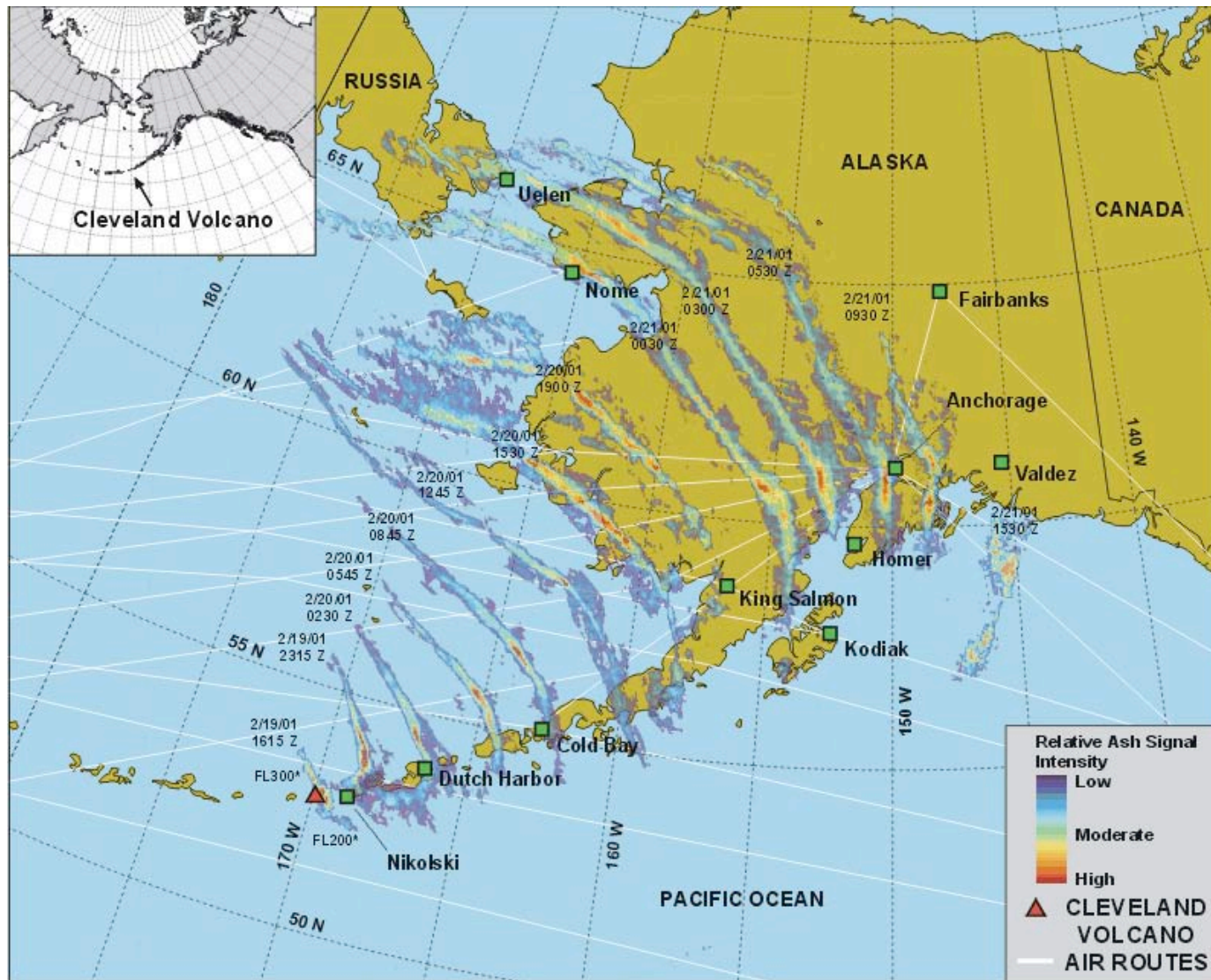
http://visibleearth.nasa.gov/view_rec.php?id=5257

Spread of Volcanic Ash Cloud



<http://puff.images.alaska.edu/satimg.shtml>

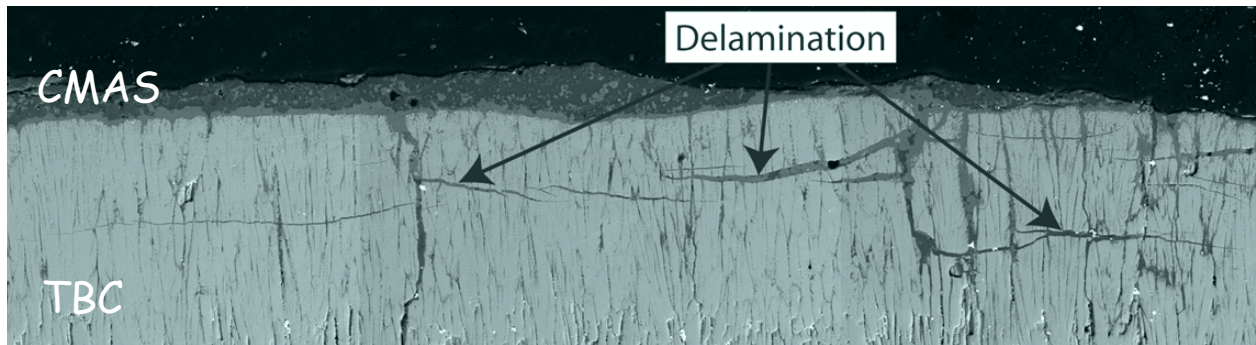
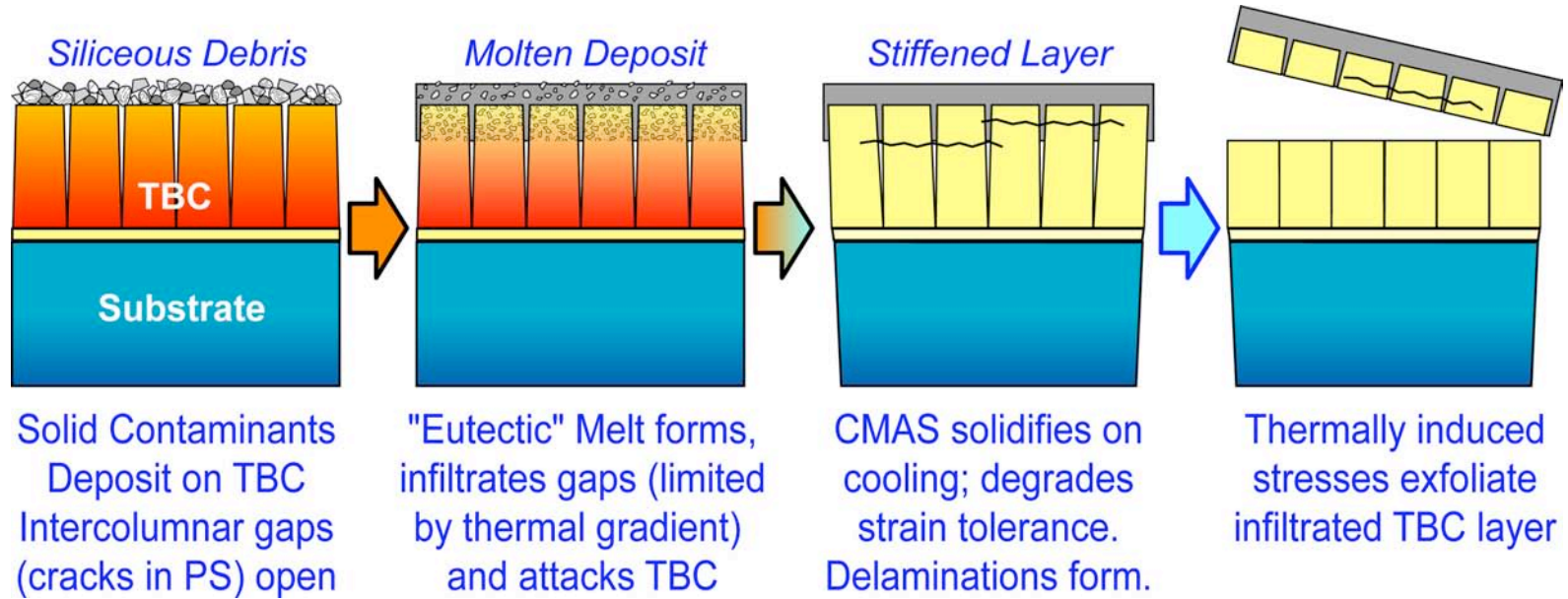
Spread of Volcanic Ash Cloud



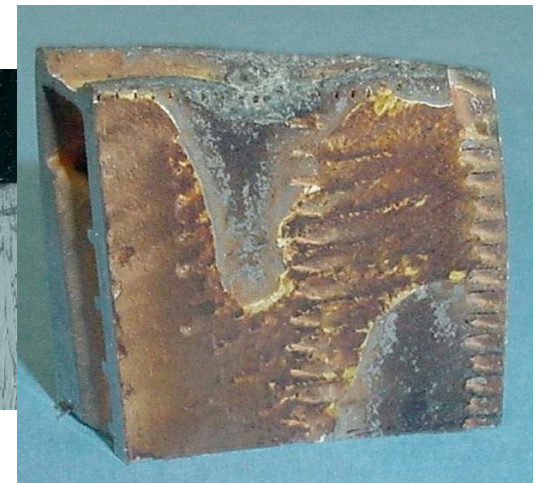
<http://puff.images.alaska.edu/satimg.shtml>

CMAS Induced Damage in TBCs

Adapted from
C. Johnson (GE-GRC)



Mercer, Faulhaber, Evans, Darolia, 2005



Isothermal Infiltration into EB-PVD TBCs

Model CMAS: 33Ca-9Mg-13Al-45Si ($T_M \sim 1235^\circ\text{C}$)
10mg/7mm diam.x200 μm thick pellet, 1300 $^\circ\text{C}$ Treatment

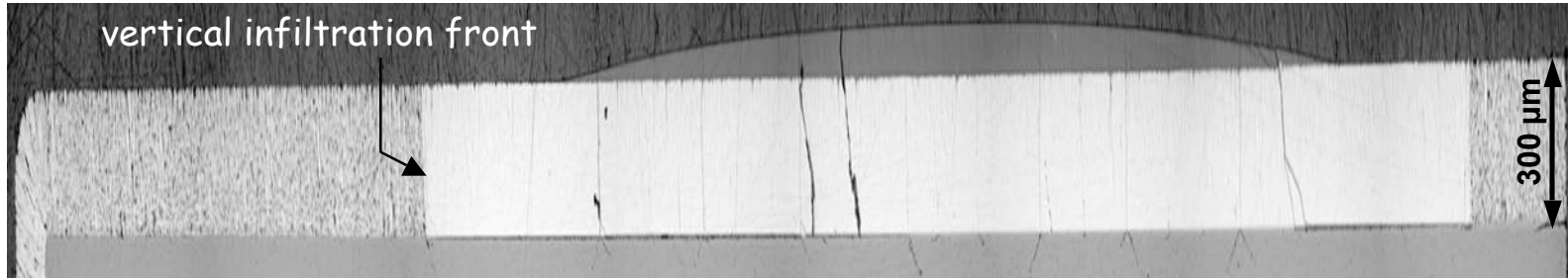
⊙ rotation axis

15 min

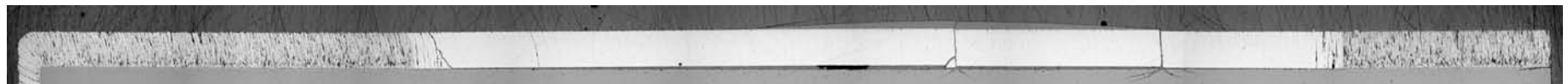


vertical infiltration front

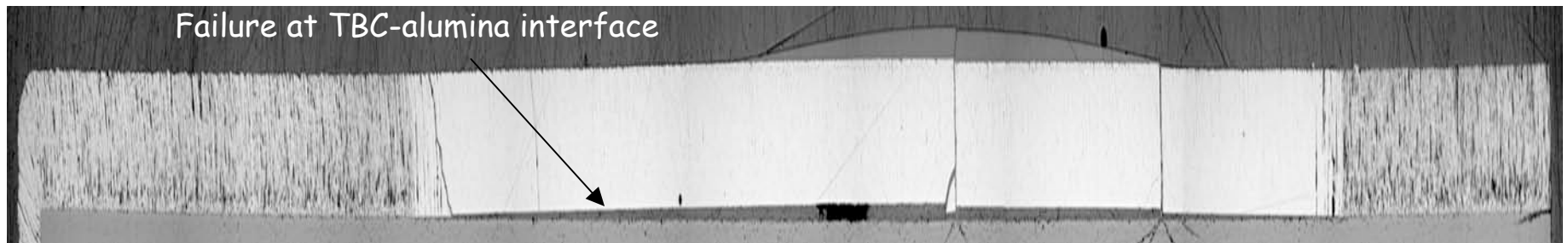
◆ x4
OM



4h



Failure at TBC-alumina interface



-1 | 0 | 1 | mm

Infiltration into Capillary Channels

$$\frac{dL}{dt} \approx \underbrace{\frac{4}{k_t} \left(\frac{\omega}{1-\omega} \right)^2 \left[\frac{D_c}{L} \right]}_{\text{Microstructure (porosity)}} \frac{\sigma_{LV} \cos \theta}{\eta}$$

Driving force ← $\sigma_{LV} \cos \theta$
Kinetic hindrance ← η

$$\sigma_{LV} \left(\text{mJ/m}^2 \right) = 271.2 + 1.96 [\text{MgO}] + 3.34 [\text{CaO}] + 2.68 [\text{FeO}] + 3.47 [\text{Al}_2\text{O}_3]$$

dL/dt = rate of infiltration into small channel under capillary pressure alone

k_t = tortuosity factor (~2-5)

ω = volume fraction porosity (~0.1 for intercolumnar gaps)

D_c = diameter of capillary (~0.1-1 μm)

L = length of penetration (0-250 μm)

σ_{LV} = liquid surface tension (~0.5J/m²)

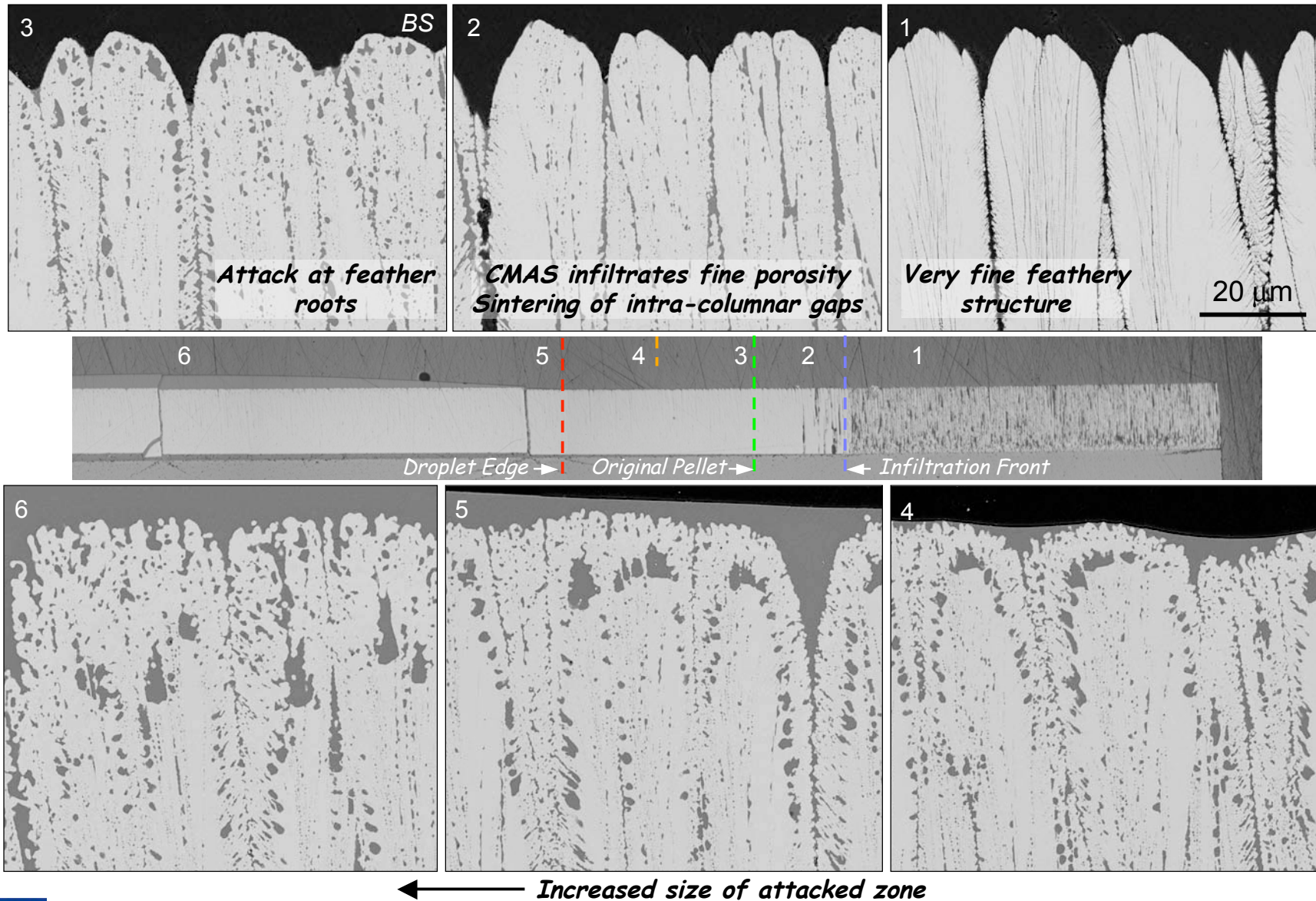
θ = contact angle ($\rightarrow 0$ for highly wetting liquids)

η = viscosity ([O]10p at 1400°C for model CMAS)

Estimated infiltration times are of the order of 1 min

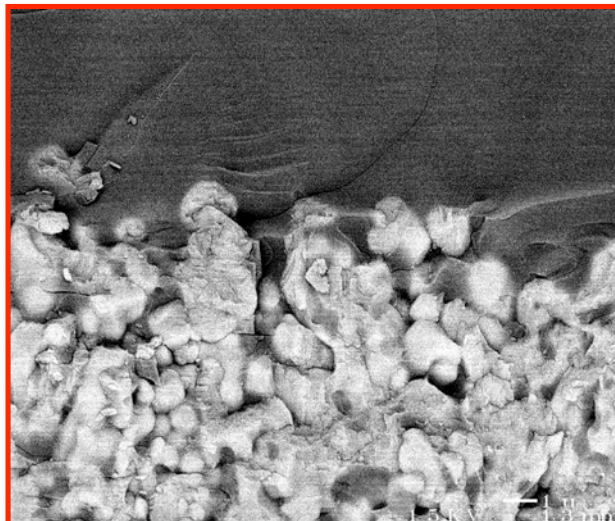
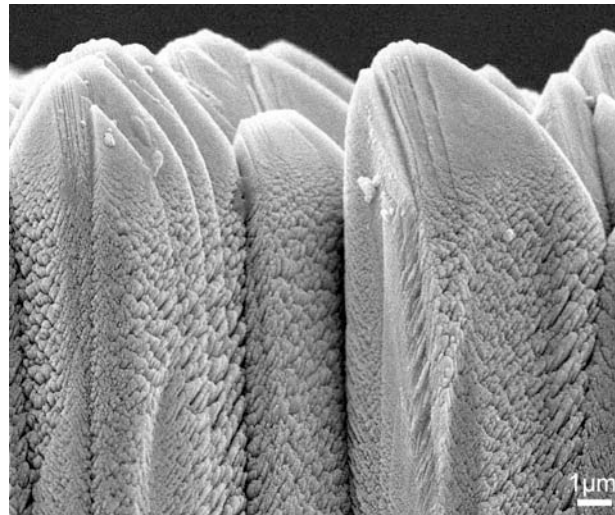
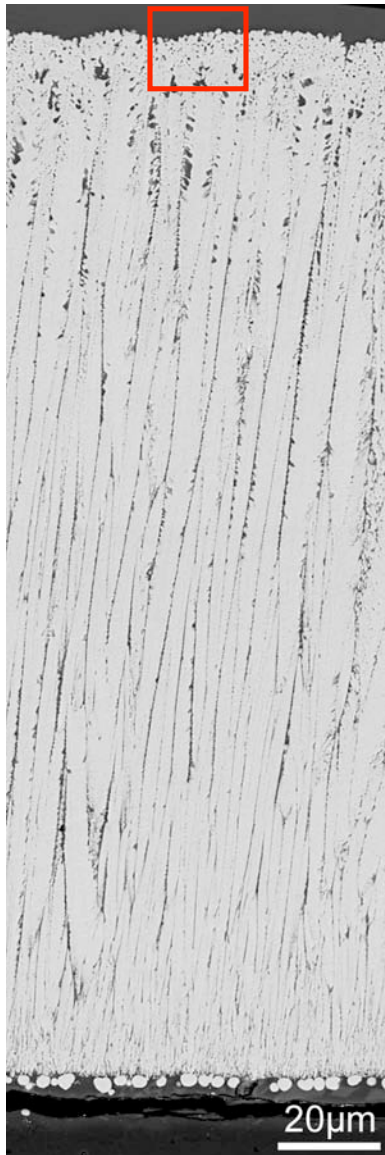
Progress of CMAS Attack on Column Tips

Krämer

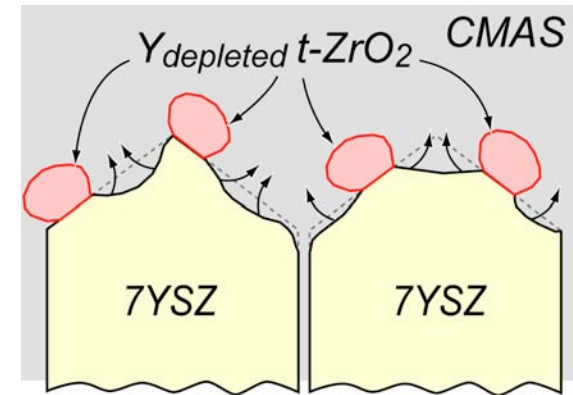


Si	45	Ca	33
Al	13	Mg	9

Corrosion Mechanism at Column Tips



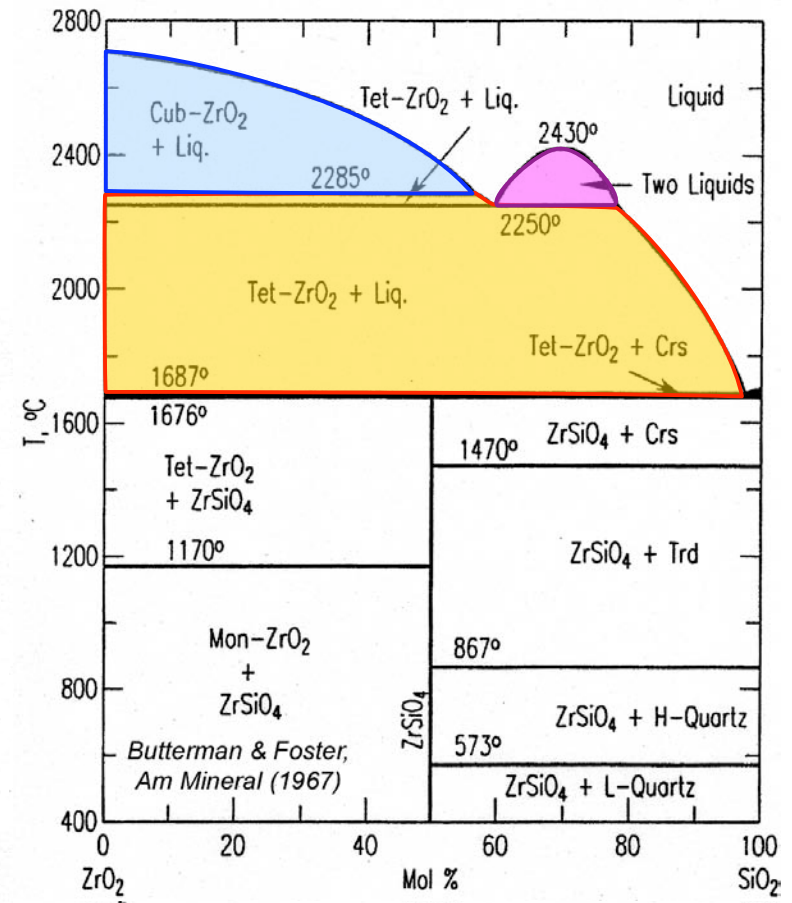
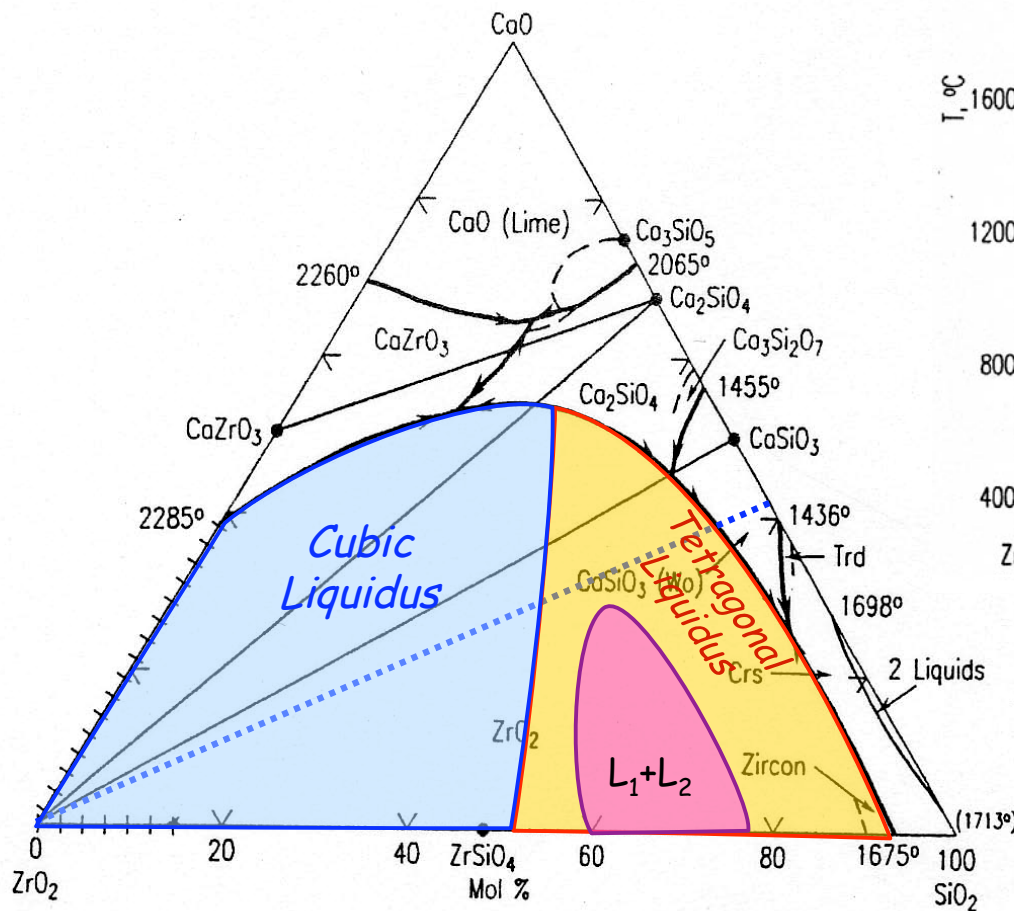
- *t'*-YSZ dissolves in CMAS and reprecipitates with a different Y concentration that depends on the local melt environment.
- Y-depleted Z at top ⇨ unstable *t* ⇨ monoclinic.



- Column tip morphology completely obliterated.

ZrO₂-CS: A Model

- Why does transformable tetragonal precipitate upon dissolution of t'?

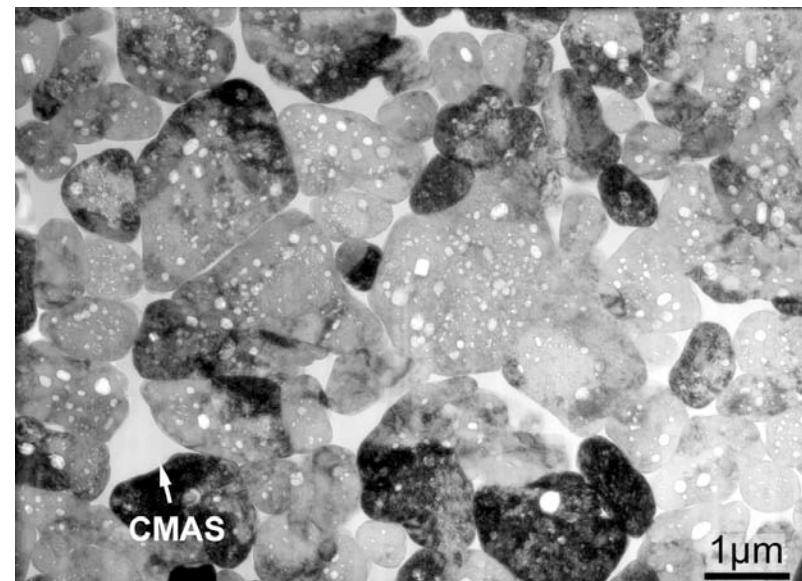
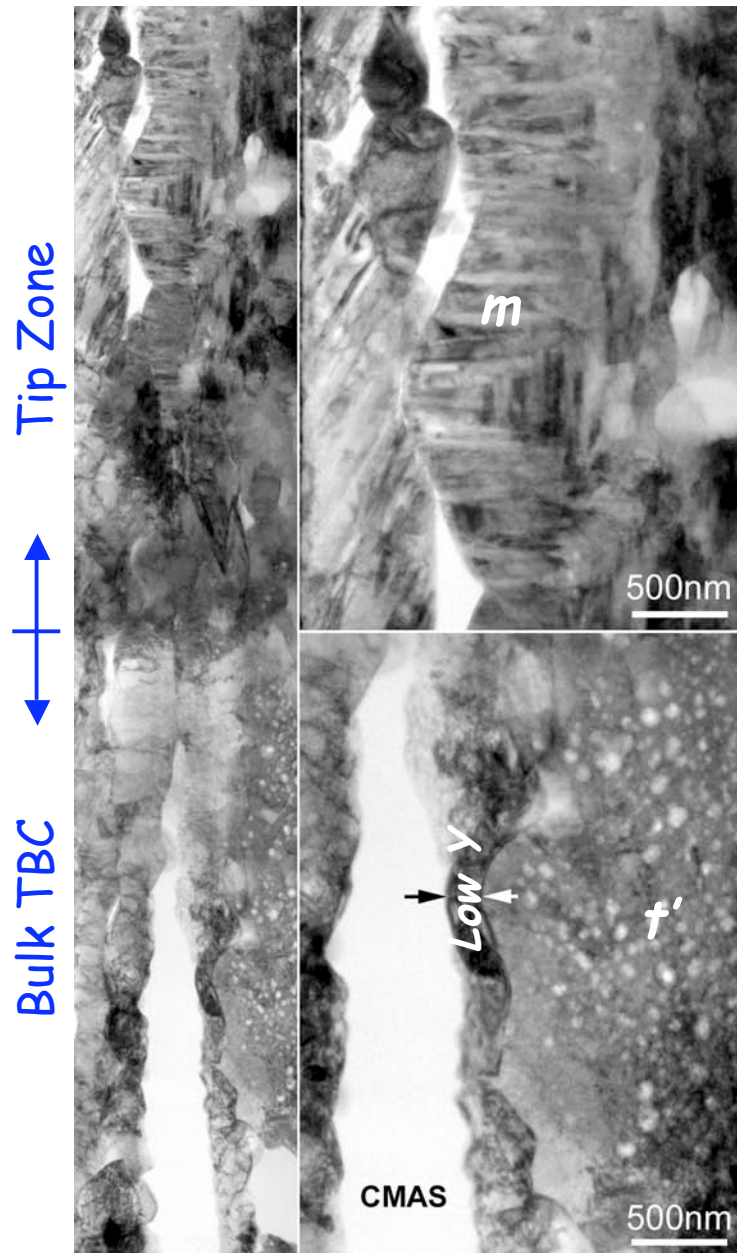


- "Current" phase diagram (1957) ignores tetragonal liquidus and miscibility gap emanating from Z-S binary.

Interaction within TBC bulk

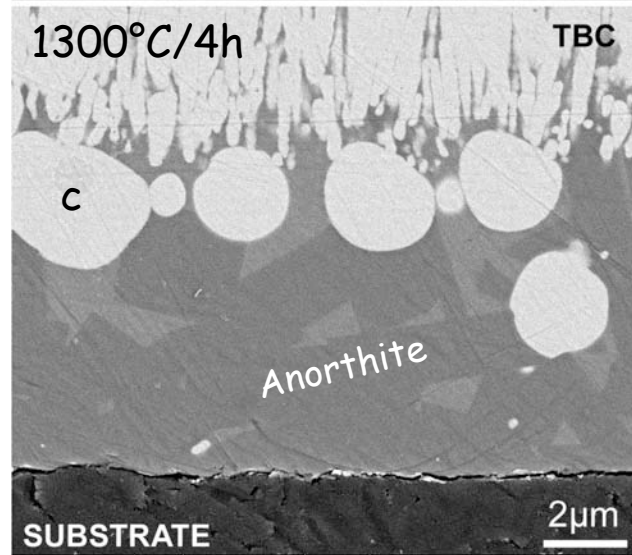
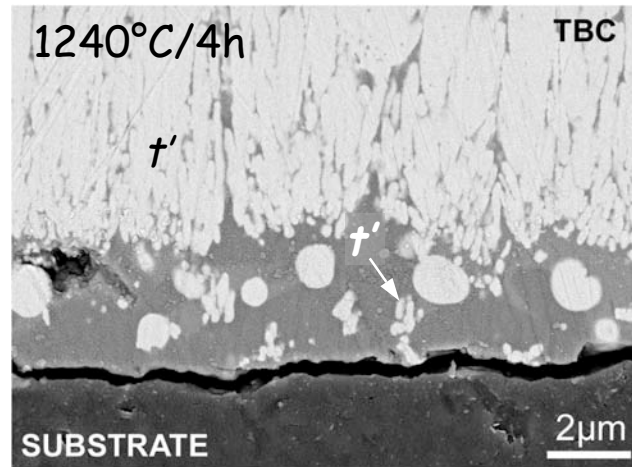
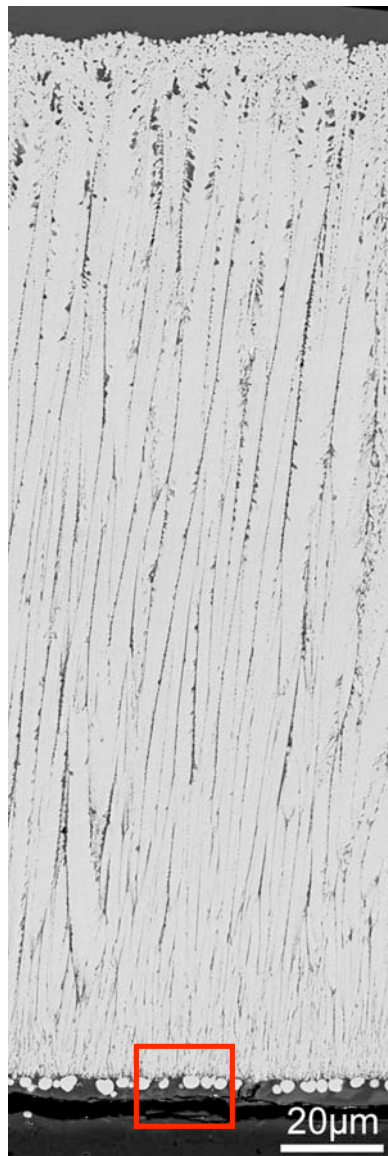
Krämer

- *Except for near-tip zone, no evidence of reprecipitated phases and only minimal dissolution of YSZ within bulk of the TBC*
 - ▶ *Rapid saturation of CMAS melt (small CMAS:YSZ volume ratio).*



Transverse view of columns near bottom

Mechanism at TBC/"TGO" Interface



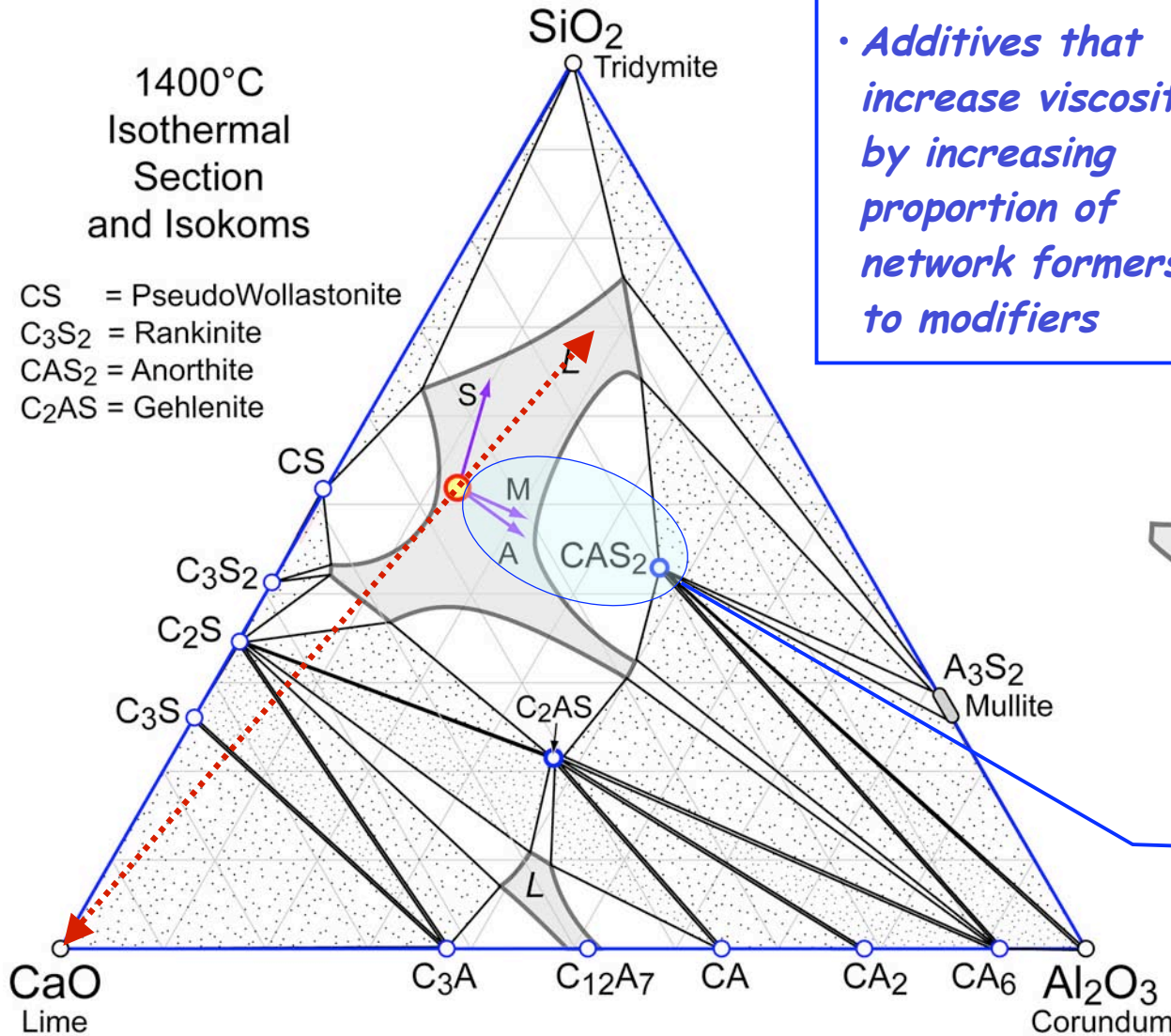
- If CMAS reaches substrate (TGO) Al_2O_3 dissolves concurrently with ZrO_2
 - Reprecipitated ZrO_2 is now Y-enriched (cubic).
 - Al_2O_3 also reprecipitates as crystalline silicate, $\sim CA_2S_2$ (Anorthite)
- Fine grains in "nucleation layer" detach from column roots and detach to feed growth of cubic globules.
- Extent of t' dissolution much smaller than in the column tip region.

Krämer and Yang

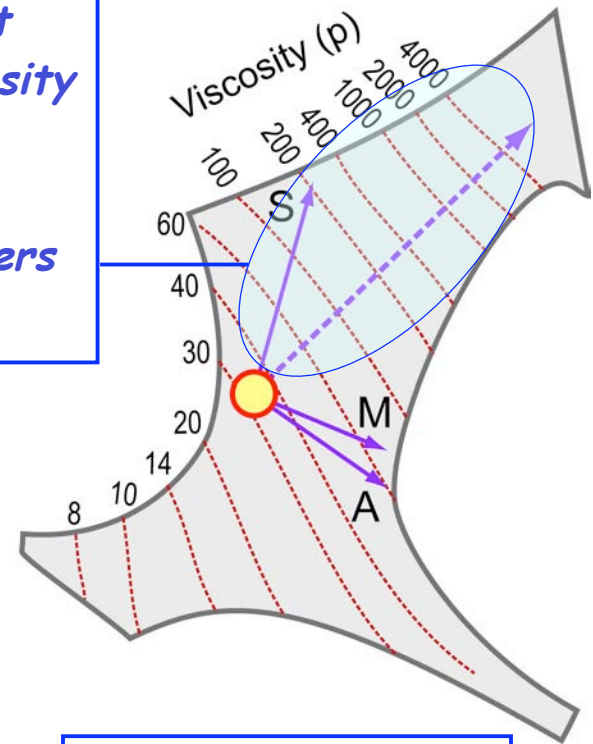
Earlier thoughts on Mitigation Strategies

1400°C
Isothermal
Section
and Isokoms

CS = PseudoWollastonite
C₃S₂ = Rankinite
CAS₂ = Anorthite
C₂AS = Gehlenite

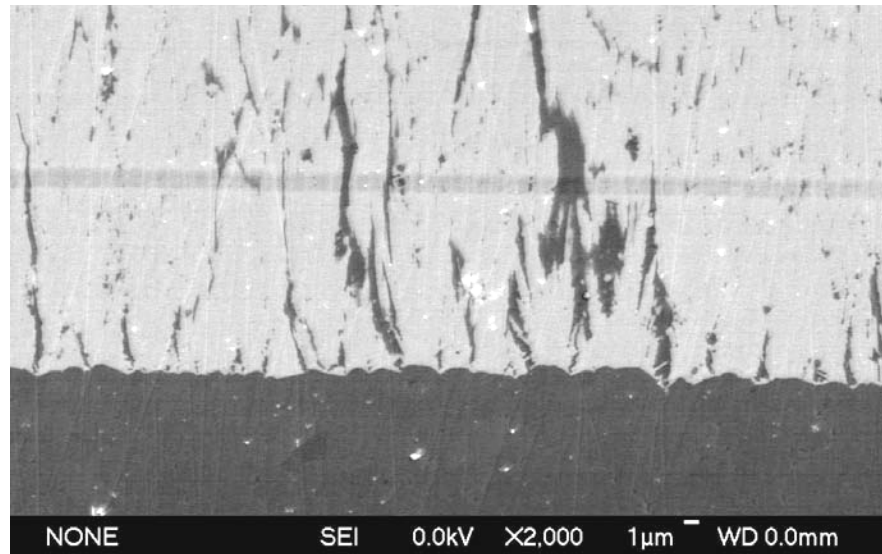
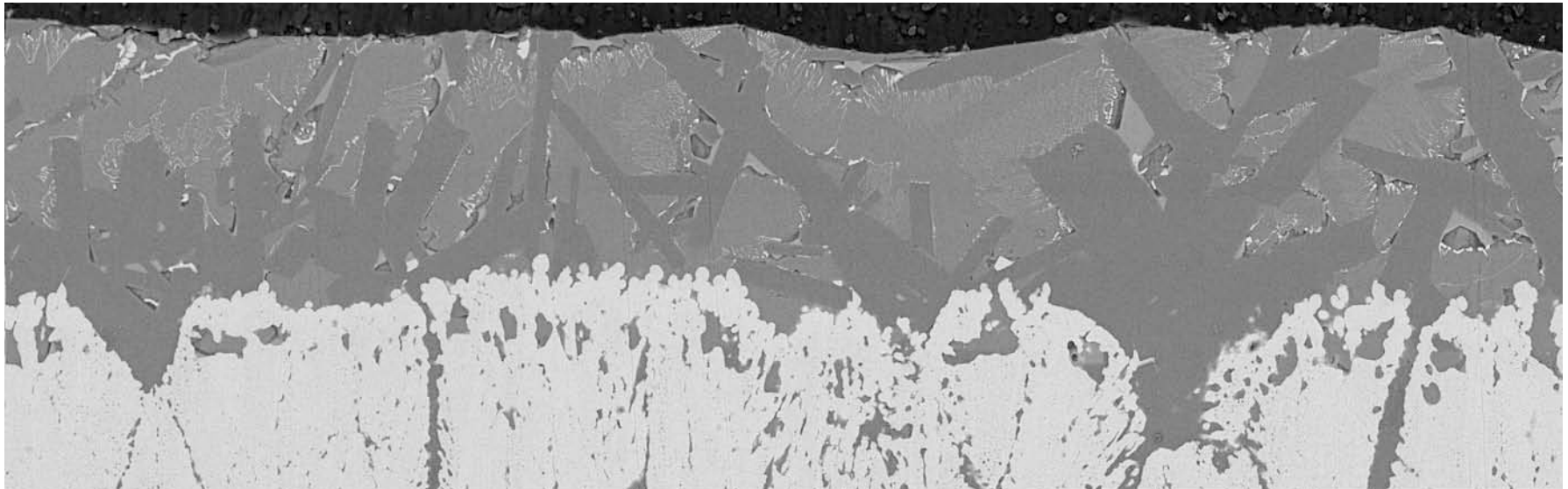


• Additives that increase viscosity by increasing proportion of network formers to modifiers



• Additives that promote crystallization (alumina, mullite)

CMAS on TBC pre-treated with Al_2O_3

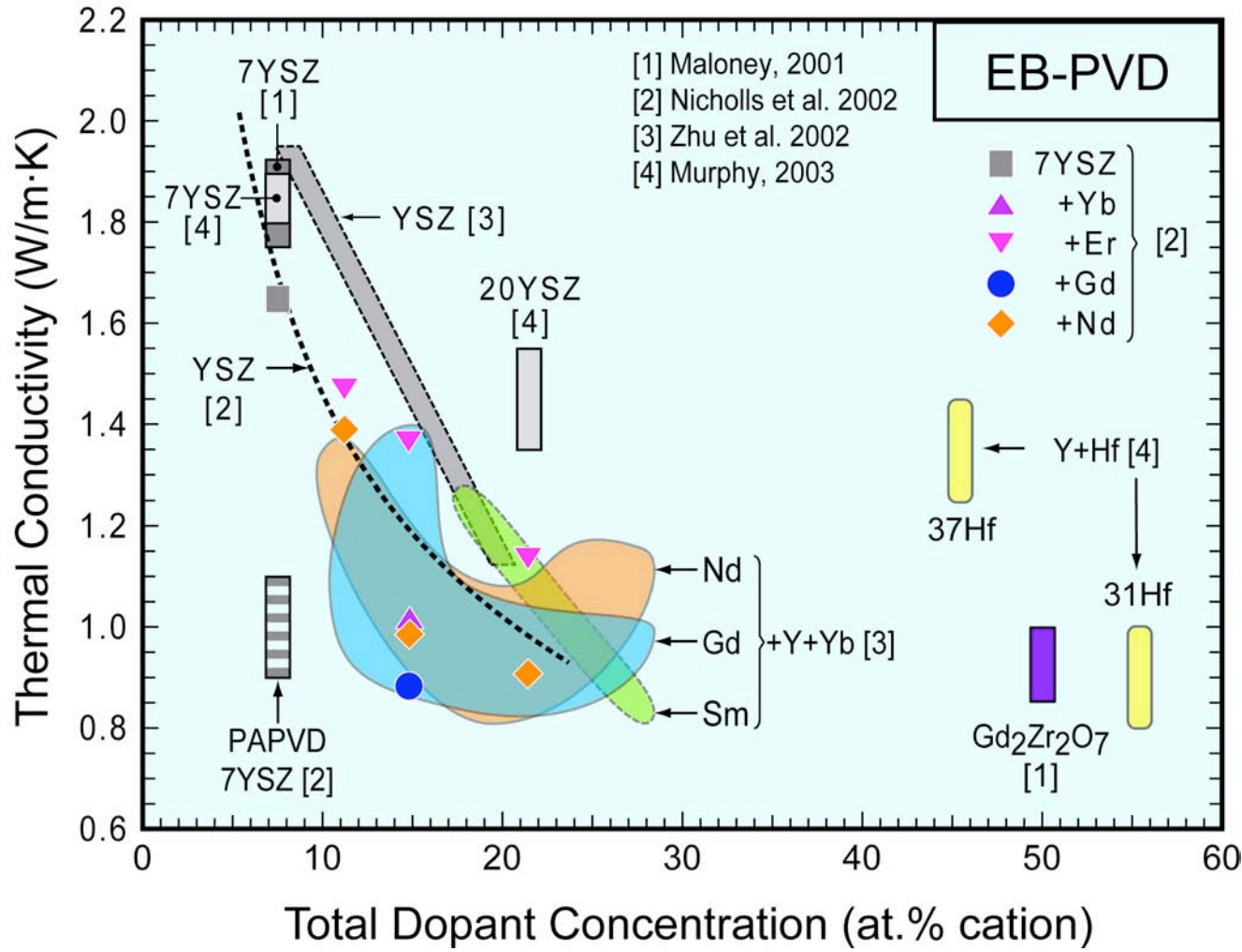


- *Pre-impregnation with Al_2O_3 does promote extensive crystallization (anorthite + spinel).*
- *Crystallization kinetics is not sufficiently rapid to compete with infiltration, presumably because of the isothermal condition and high treatment temperature.*

NONE SEI 0.0kV X2,000 1 μm WD 0.0mm

*Advanced low-k TBCs:
Gd Zirconate*

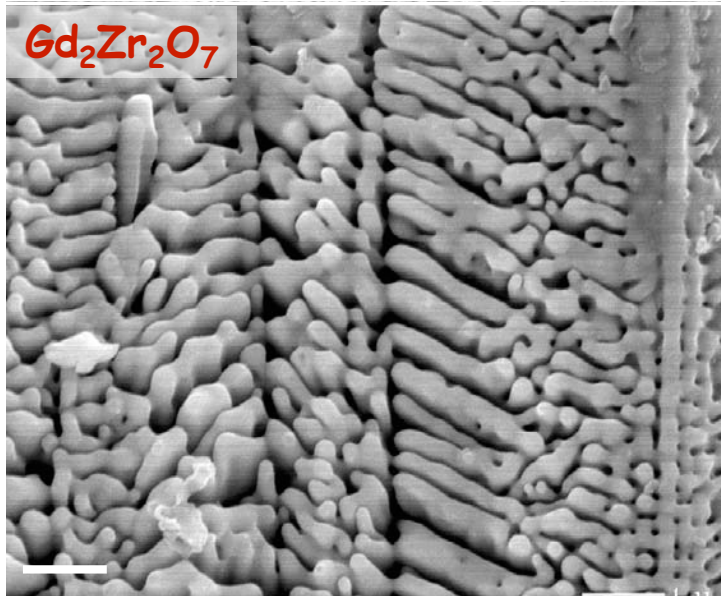
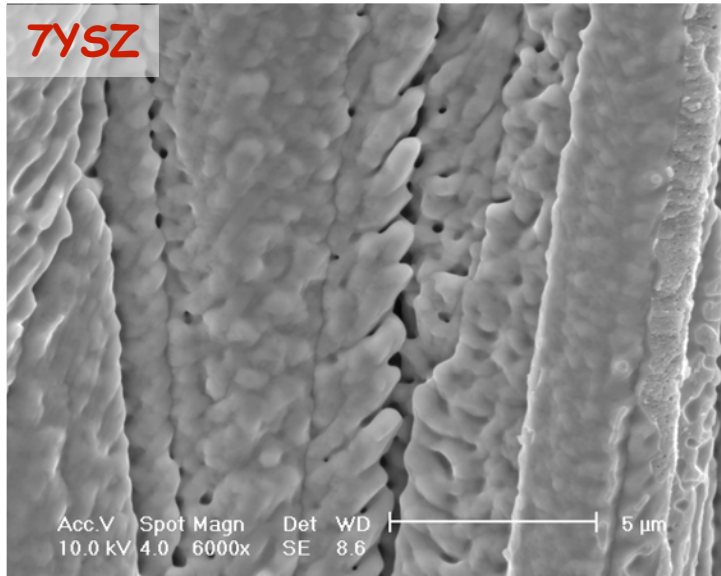
Thermal Conductivity of Some Emerging TBCs



• A large variety of alternate compositions, mostly based on rare earth additions to ZrO₂ or YSZ, offer improved thermal insulation efficiency over 7YSZ. But...

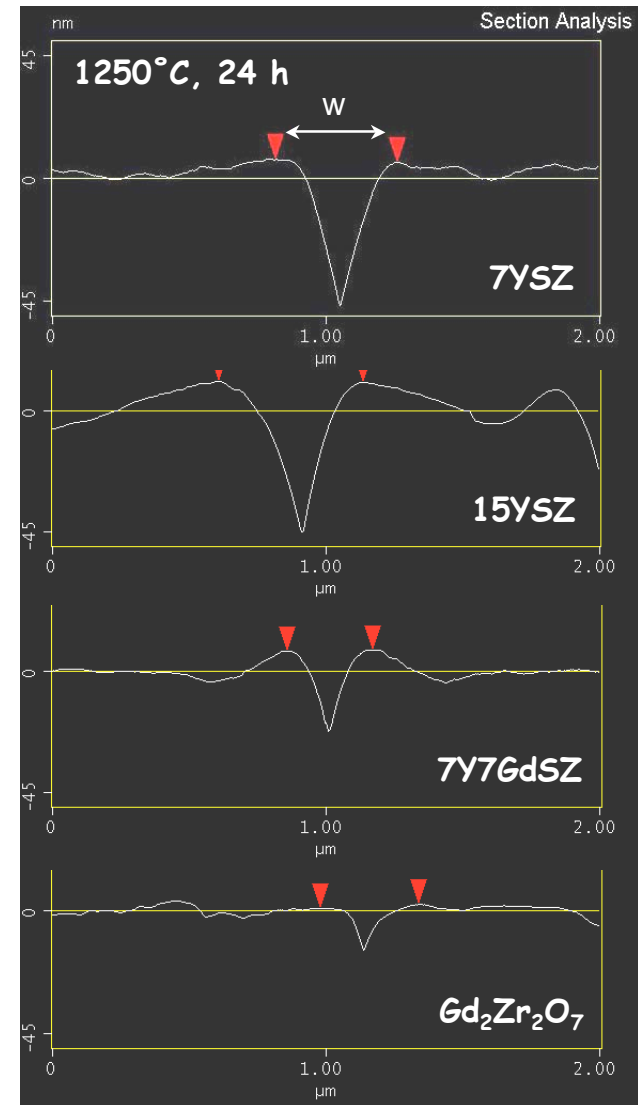
Leckie, Yang

Chemical Effects on Surface Diffusion

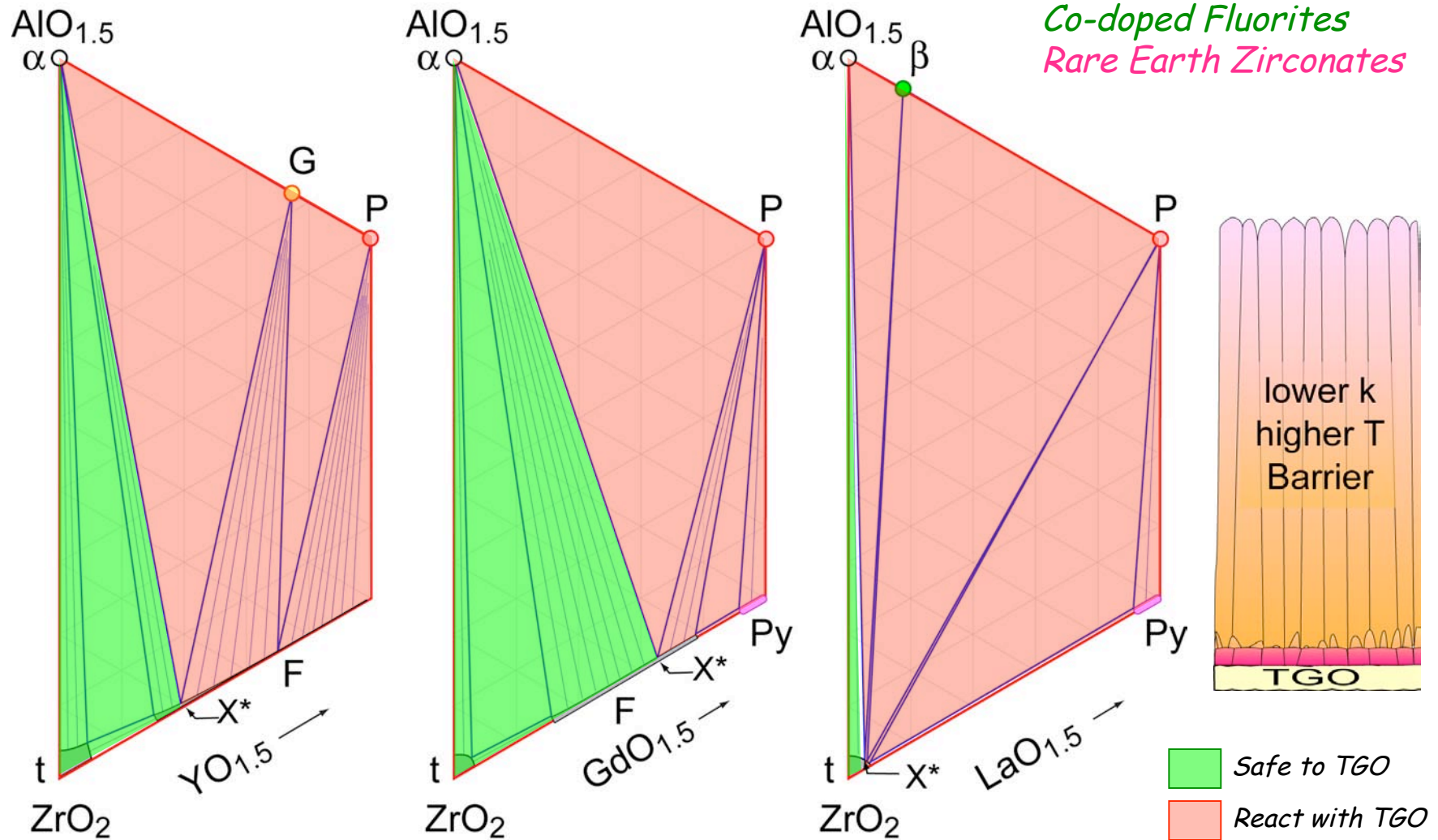


After 100h at 1200°C

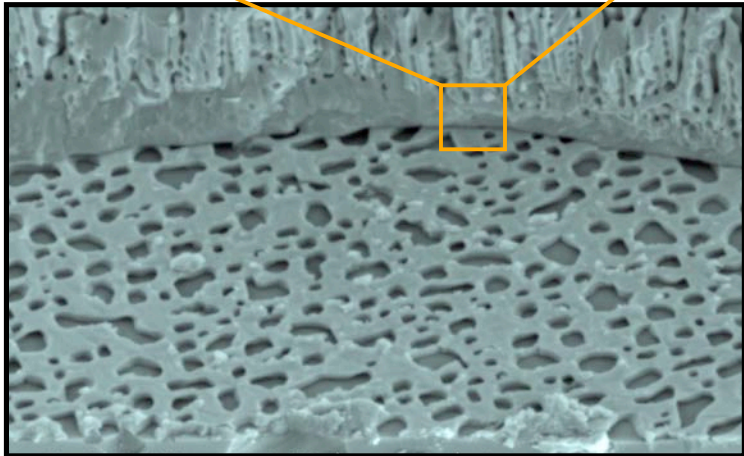
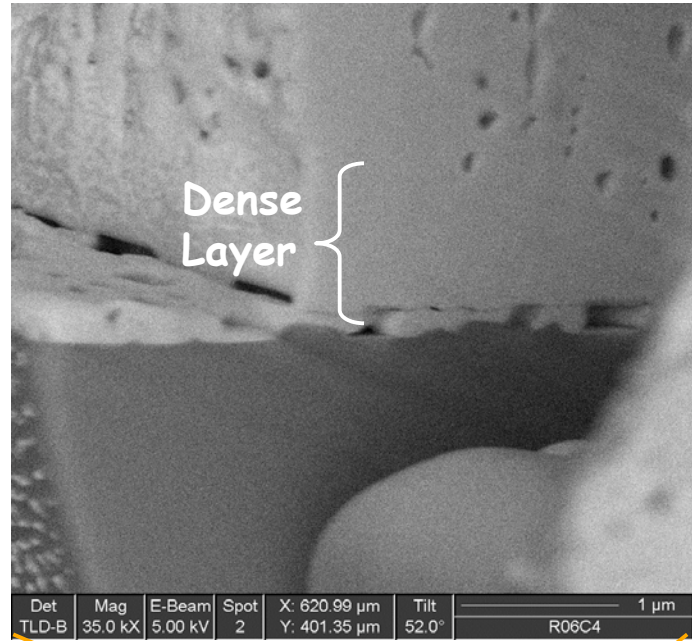
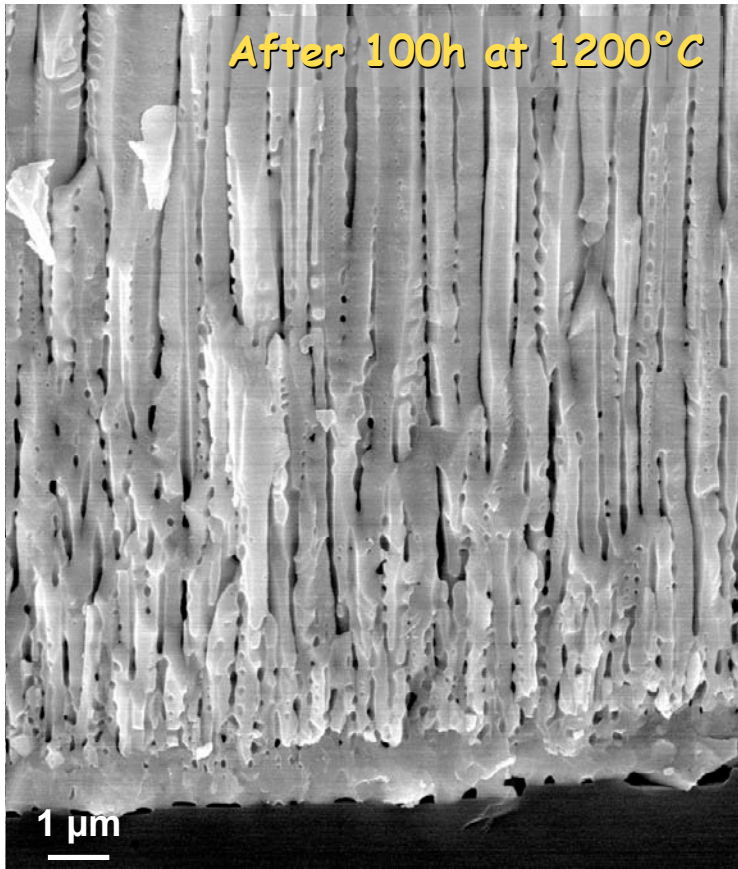
Significant benefits of Gd addition (and likely of other RE's) on improving the stability of the pore architecture, with concomitant benefits to the preservation of low k and strain tolerance.

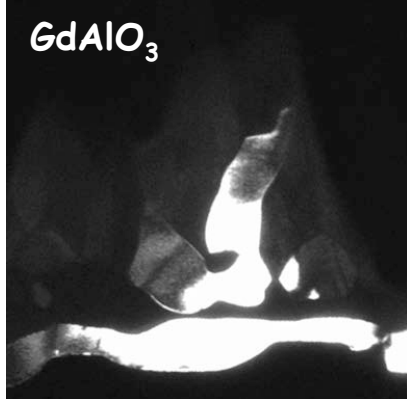
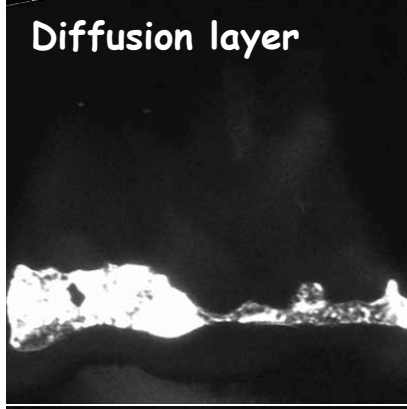
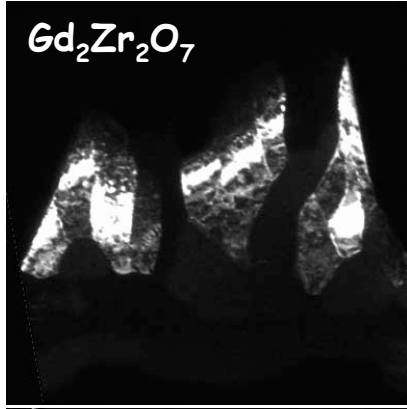


Thermochemical Compatibility Limits

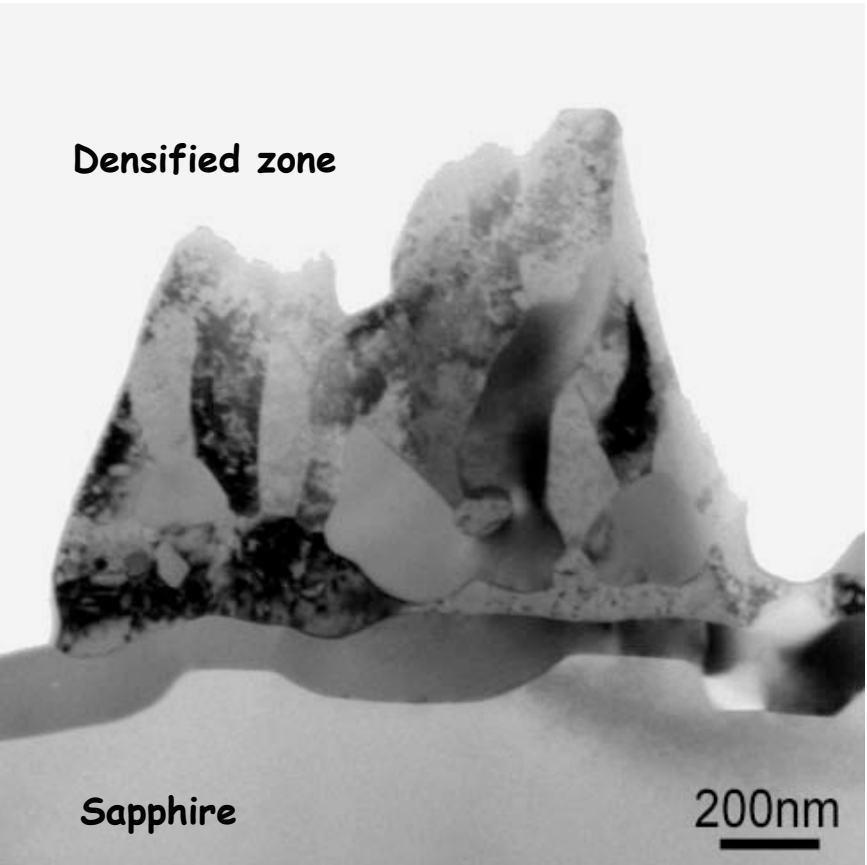


Gd₂Zr₂O₇/Alumina Interface Interaction

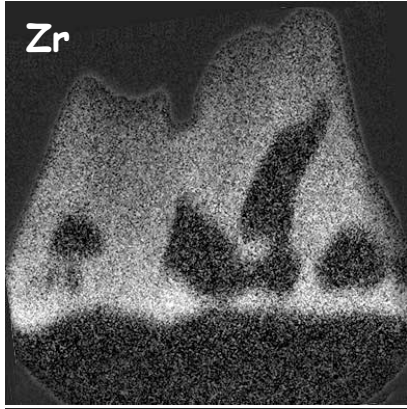




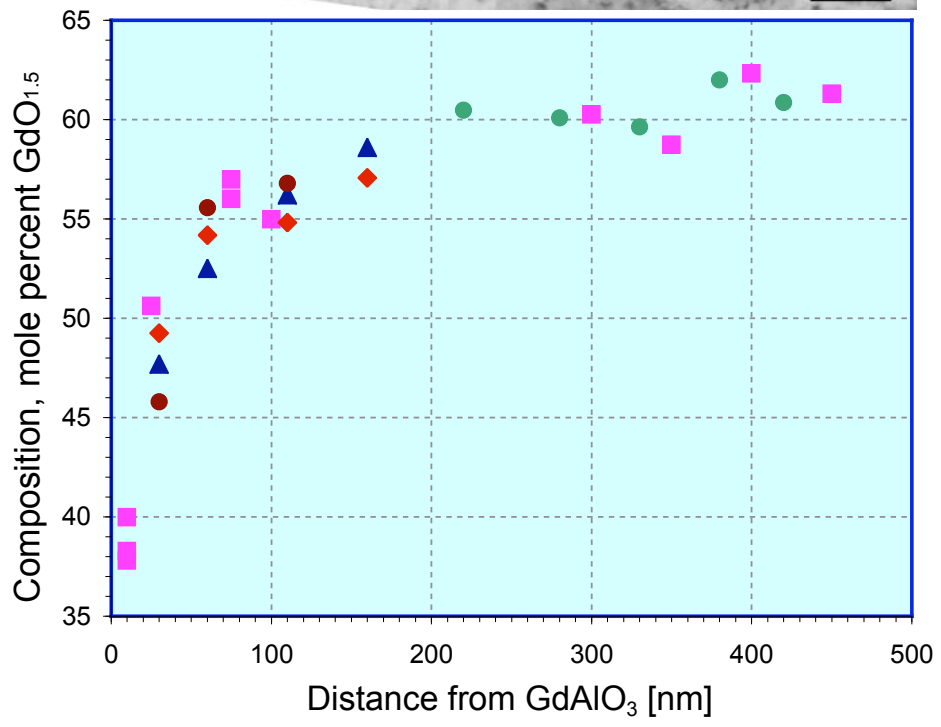
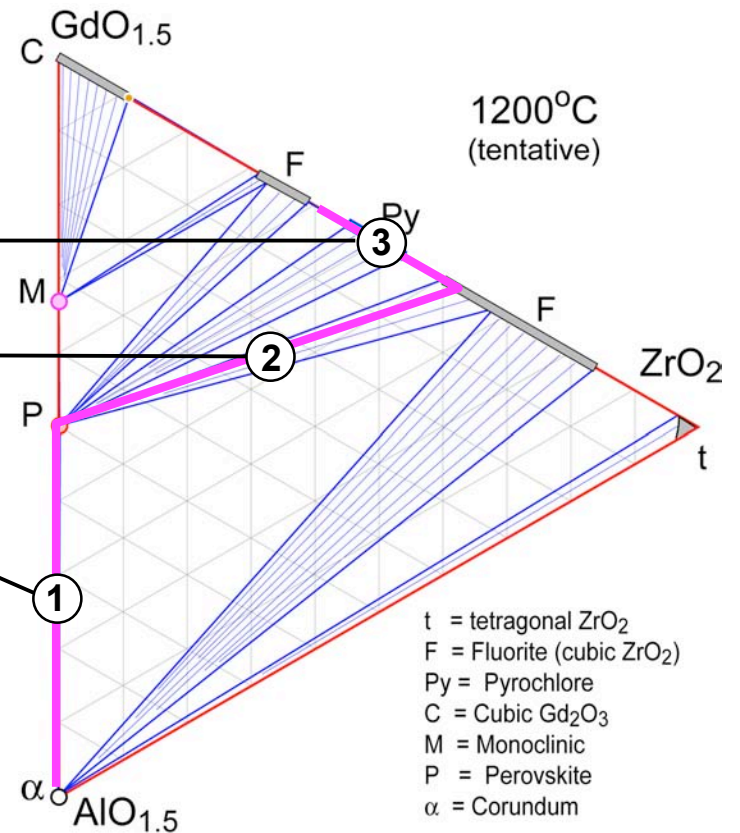
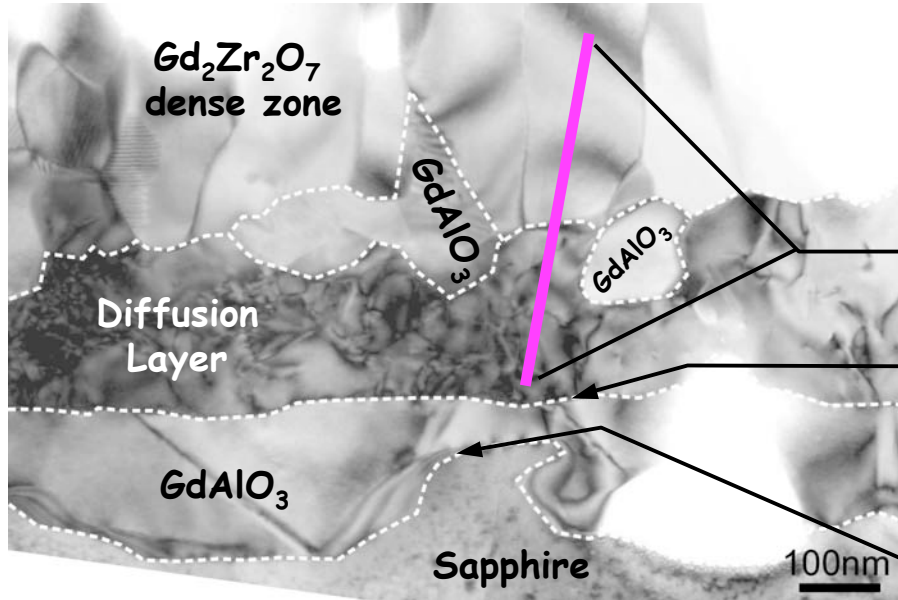
$Gd_2Zr_2O_7$ /Sapphire Interaction Zone



EB-PVD Film, 1200°C/100h



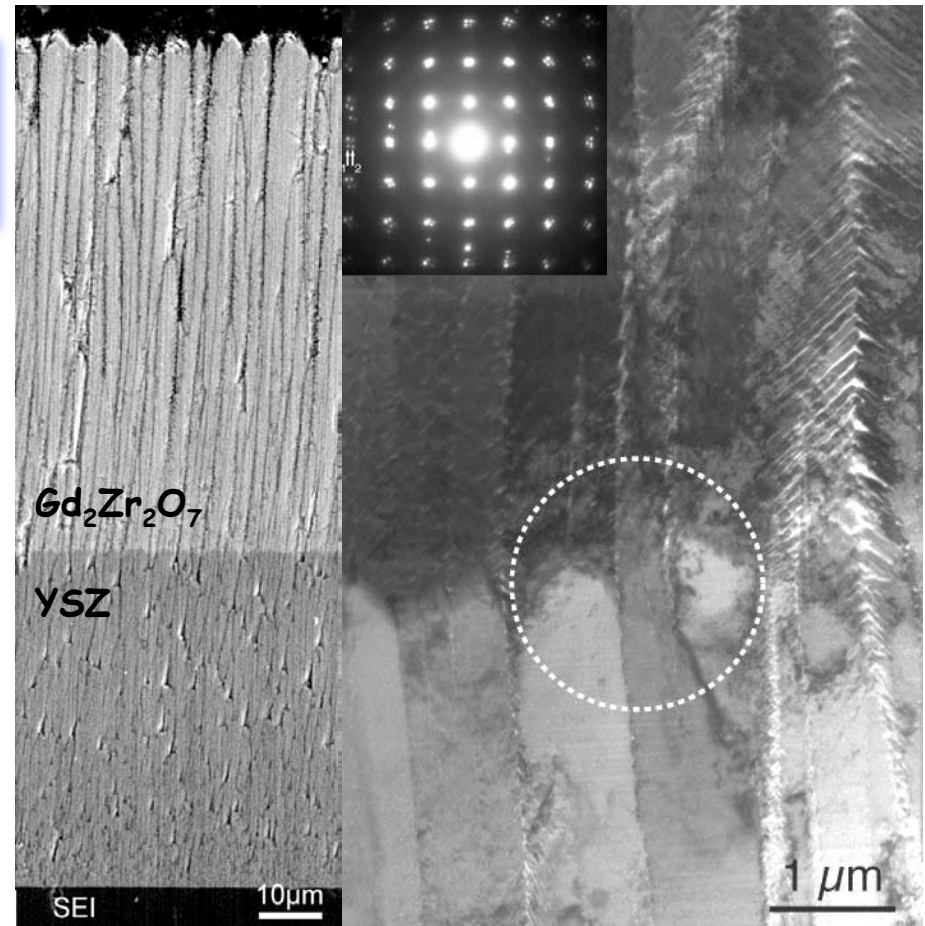
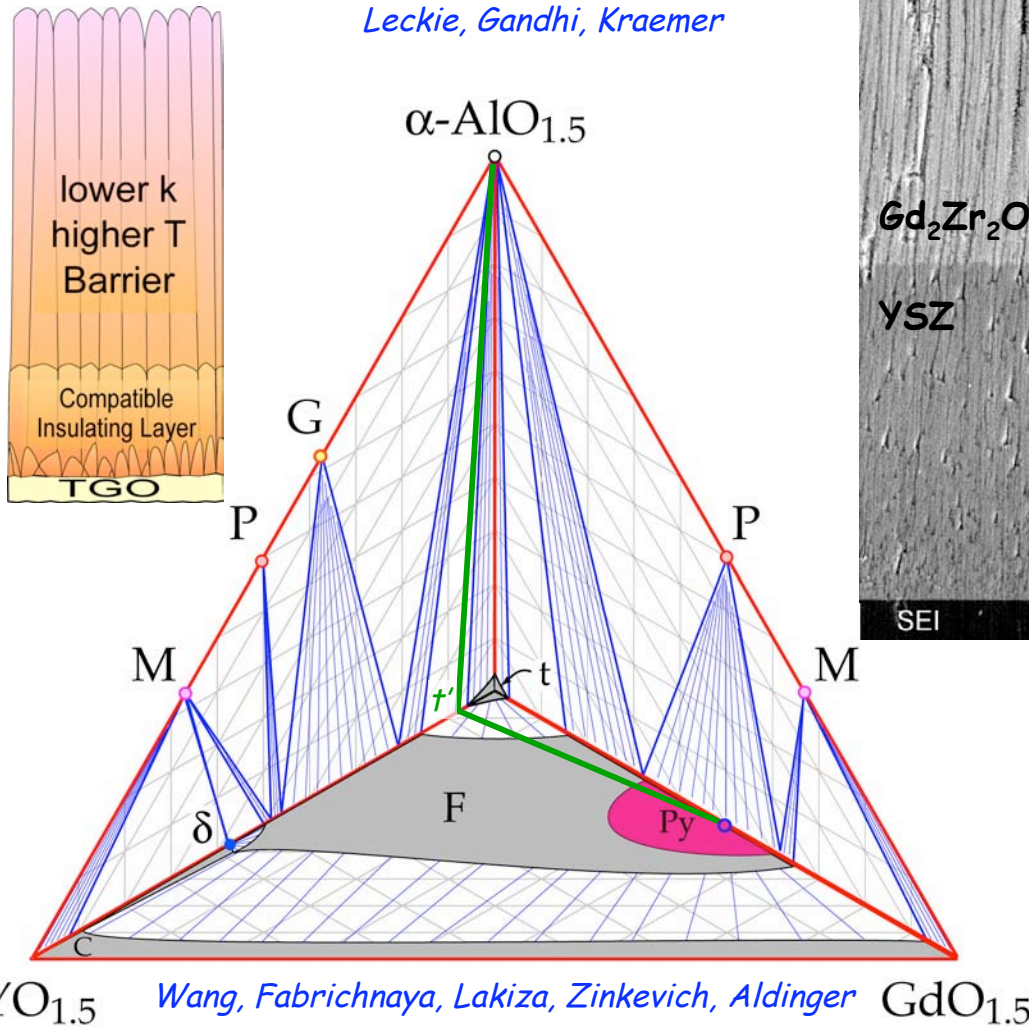
Krämer and Rühle



Diffusion Path

7YSZ Interlayer for Chemical Compatibility

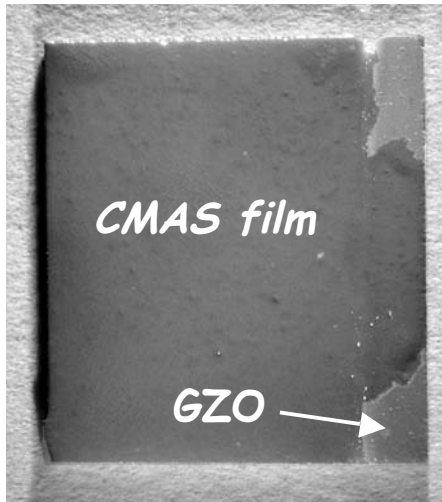
Leckie, Gandhi, Kraemer



- YSZ is an effective barrier to minimize interaction between TGO and Gd₂Zr₂O₇.
- Epitaxial growth favors integrity of the interface.

CMAS Interaction: $Gd_2Zr_2O_7$ v. *TYSZ*

Substantial difference in spreading behavior and reaction layer morphology



(4h/1300°C, Isothermal)

